

Copyright  
by  
Kwabena Oduro Asante  
2000

# **Approaches to Continental Scale River Flow Routing**

**by**

**Kwabena Oduro Asante, B.S., M.S.**

## **Dissertation**

Presented to the Faculty of the Graduate School of

The University of Texas at Austin

in Partial Fulfillment

of the Requirements

for the Degree of

**Doctor of Philosophy**

**The University of Texas at Austin**

**May, 2000**

## **Approaches to Continental Scale River Flow Routing**

**Approved by  
Dissertation Committee:**

---

David R. Maidment, Supervisor

---

James S. Famiglietti, Cosupervisor

---

Francisco Olivera

---

Randall J. Charbeneau

---

Daene McKinney

## **Acknowledgements**

To my parents, Kofi and Akua, and siblings, Akosua, Kwaku and Afua  
for their love and support through the many years of school,

To Dr David R. Maidment, my supervisor, for the interest he took  
in developing me as a person, a hydrologist and a teacher  
and for his infectious enthusiasm,

To Dr James S. Famiglietti, my cosupervisor, for his global perspective  
and his flexibility in allowing me to pursue my goals,

To Dr Francisco Olivera, my teacher and friend, for his patient instruction  
and his insistence that equations remain a part of every modeling decision,

To Dr Randall Charbeneau and Dr Daene McKinney  
for their service as members of my dissertation committee,

To Dr Seann Reed, Dr Zichuan Ye, Ferdinand Hellweger and the other GIS  
Hydro researchers whose prior work laid the foundation for mine,

To Cai Ximing, Mary Lear, Ty Lehman, Kathy Rose, the staff of CRWR  
and the many fine people I met in Texas,

I am truly grateful and give thanks.

I would also like to acknowledge the following institutions for the use of their data and hydrologic models

- US Geological Survey EROS Data Center, Sioux Falls, SD
- National Center for Atmospheric Research, Boulder, CO
- Hydrologic Engineering Center of the US Army Corp of Engineers
- Center for Research in Water Resources, Univ. of Texas at Austin

## **Approaches to Continental Scale River Flow Routing**

Publication No. \_\_\_\_\_

Kwabena Oduro Asante, PhD

The University of Texas at Austin, 2000

Supervisor: David R. Maidment

Cosupervisor: James S. Famiglietti

Recent concerns about global climate change and a series of large-scale hydrologic events such as the Mid-West flood of 1993 and the El Nino of 1997 have focused attention on the need to track the flow of water through the entire hydrologic cycle. On the land surface, databases of routing parameters and routing models are required to describe the movement of runoff generated by Global Circulation Models (GCMs) and other soil water balance models over the earth's surface. In this study, a terrain analysis is performed using 30 arcsecond Digital Elevation Model (DEM) data to develop a global database of terrain derived routing parameters. A computationally efficient grid based routing model, called a source to sink (STS) model, is implemented in this study. It routes flow directly from the point of generation to the desired observation point. The STS model also allows for easy interaction with models of other phases of the

hydrologic cycle by incorporating the boundaries of their modeling units into the definition of its own modeling units. A continental scale STS model is created and parameterized for each continent using datasets derived from the terrain analysis. A process is defined for determining additional velocity and dispersion parameters from observed flow data. Another continental scale routing model is developed using the watershed based approach of the Hydrologic Modeling System (HMS). Hydrologic elements and routing parameters for the HMS model are derived from the same terrain data used in parameterizing the STS model. Basin responses from the two models are compared for various spatial and temporal resolutions and parameter distributions to determine the implications of their respective conceptual models. These comparisons show that basin responses in the STS model are relatively independent of spatial and temporal scale while the HMS model is scale dependent with regard to both spatial and temporal resolution. Basin responses for a fine resolution HMS models were successfully duplicated in a STS model for both the uniform and non-uniformly distributed velocity and dispersion parameter case.

## Table of Contents

<b>LIST OF TABLES</b>	<b>XII</b>
<b>LIST OF FIGURES</b>	<b>XIII</b>
<b>CHAPTER 1</b>	<b>1</b>
Introduction .....	1
1.1 Problem Statement.....	1
1.2 Objectives .....	4
1.3 Research Outline.....	5
<b>CHAPTER 2</b>	<b>7</b>
Literature Review .....	7
2.1 Conceptual Models of a River Basin .....	7
2.1.1 The Watershed Based Approach .....	8
2.1.2 The Cell to Cell Routing Approach.....	9
2.1.3 The Source to Sink Routing Approach.....	10
2.2 Methods of Characterizing Flow .....	10
2.2.1 Translation With Incidental Dispersion.....	11
2.2.2 Translation With An Approximate Dispersion Process .....	12
2.2.3 Translation With Fully Described Dispersion .....	13
2.3 Continental Scale Routing Models .....	17
2.4 Scaling Issues in Routing .....	22
2.4.1 Scale Dependence of Routing Methods.....	23
2.4.2 Scale Dependence of Routing Parameters.....	25
<b>CHAPTER 3</b>	<b>27</b>
Data Development .....	27
3.1 Data Sources .....	27
3.2 Terrain Database Development .....	29
3.3 Preprocessing For the Source to Sink Model .....	40



3.4 Preprocessing For the Hydrologic Modeling System.....	55
<b>CHAPTER 4</b>	<b>64</b>
Methodology.....	64
4.1 The Source to Sink Modeling Approach .....	64
4.1.1 STS Model Assumptions .....	64
4.1.2 STS Model Components.....	67
4.1.3 STS Routing Methodology .....	70
4.1.4 Estimating STS Routing Parameters .....	78
4.2 The Hydrologic Modeling System Approach.....	83
4.2.1 HMS Model Assumptions .....	84
4.2.2 HMS Model Components.....	85
4.2.3 HMS Routing Methodology .....	88
4.2.4 Estimating HMS Routing Parameters.....	93
<b>CHAPTER 5</b>	<b>96</b>
Model Applications .....	96
5.1 The application basins .....	96
5.1.1 The Congo Basin .....	97
5.1.2 The Nile Basin .....	100
5.2 Source to sink model runs .....	102
5.2.1 Longitudinal Decomposability of the STS Model.....	103
5.2.2 Effect of Spatial Resolution of the STS Model .....	107
5.2.3 Effect of Spatial Distribution of STS Parameters.....	113
5.2.4 Effect of Temporal Resolution of STS Model.....	122
5.3 Hydrologic Modeling System Model Runs .....	124
5.3.1 Longitudinal Decomposability of the HMS Model.....	127
5.3.2 Effect of Spatial Resolution of the HMS Model .....	132
5.3.3 Effect of Spatial Distribution of HMS Parameters .....	136
5.3.4 Effect of Temporal Resolution of HMS Model.....	141

5.4 Comparison with Observed Flows .....	151
5.4.1 Comparing STS Simulated Flows with Observed Flows .....	152
5.4.2 Comparing HMS Simulated Flows with Observed Flows .....	158
<b>CHAPTER 6</b>	<b>164</b>
Conclusions and Recommendations .....	164
6.1 Conclusions .....	164
6.1.1 Inferences from Global Terrain Analysis .....	166
6.1.2 Inferences from Global STS Model Implementation .....	167
6.1.3 Inferences from HMS Model Development .....	169
6.1.4 Inferences from Comparing STS and HMS Models .....	170
6.2 Recommendations .....	172
<b>APPENDICES</b>	<b>174</b>
Appendix 1: AML Code for Source to Sink Model Preprocessing .....	175
Appendix 2: Parameters of the T42 mesh .....	179
Appendix 3: FORTRAN Code for Source to Sink Routing Model.....	183
Appendix 4: AML Code for Computing Equivalent Muskingum Parameters from a Field of Velocities and Dispersion Coefficients .....	193
Appendix 5: 10 day flows in the Nile basin, 1953-57 .....	195
<b>REFERENCES</b>	<b>197</b>
<b>VITA</b>	<b>204</b>

## List of Tables

Table 3-1: Projection Centers for Various Continents .....	31
Table 3-2: Sample Projection File for Africa .....	31
Table 3-3: Inland Catchments Identified .....	34
Table 5-1: Effect of Spatial Resolution on Lagged and Dispersed Basin Response .....	112
Table 5-2: Flow Routing Parameters used in the Nile Basin .....	118
Table 5-3: Effect of STS Routing Interval on Congo Basin Response .....	123
Table 5-4: Parameters for the Congo Basin Delineation .....	126
Table 5-5: Effect of Muskingum n on River Reach Response .....	130
Table 5-6: Range of Dispersion Coefficients of a Muskingum Routing Reach with 24 hour Routing Interval and Velocity of 0.3m/s.....	131
Table 5-7: Effect of HMS Enforced Minimum Subbasin Lag .....	143
Table 5-8: Effect of Min. Subbasin Lag Rule on Basin response, Lag Routing .	146
Table 5-9: Effect of Subbasin Lag Rule on Basin response, Muskingum Routing .....	148
Table 5-10: Routing Parameters Computed by Method of Moments .....	155

## List of Figures

Figure 3-1: Inland Catchments of the World.....	33
Figure 3-2: Flow Direction Arrows .....	35
Figure 3-3: Flow Direction Grid of Africa .....	36
Figure 3-4 (a): Histogram of Flow Directions for North America .....	37
Figure 3-4 (b): Histogram of Flow Directions for Africa.....	37
Figure 3-5: Flow Accumulation Grid of Africa.....	39
Figure 3-6: Flow Length Grid of Africa.....	40
Figure 3-7: Components of a Source-To-Sink Model .....	42
Figure 3-8: Sink Locations for the Continent of Africa .....	44
Figure 3-9 (a): Drainage Basins of North America .....	46
Figure 3-9 (b): Drainage Basins of Africa.....	46
Figure 3-9 (c): Drainage Basins of South America .....	47
Figure 3-9 (d): Drainage Basins of Australia .....	47
Figure 3-9 (e): Drainage Basins of Europe.....	48
Figure 3-9 (f): Drainage Basins of Asia .....	48
Figure 3-10: Linking Modeling Units for the African Continent.....	50
Figure 3-11 (a): Parameterized Sources of North America.....	52
Figure 3-11 (b): Parameterized Sources of Africa.....	52
Figure 3-11 (c): Parameterized Sources of South America.....	53
Figure 3-11 (d): Parameterized Sources of Australia .....	53
Figure 3-11 (e): Parameterized Sources of Europe .....	54
Figure 3-11 (f): Parameterized Sources in Asia .....	54
Figure 3-12: Delineated Rivers Coverage of Africa.....	58
Figure 3-13: Delineated Watersheds of Africa.....	58
Figure 3-14: Line Diagram of Hydrologic Element Connectivity .....	60
Figure 3-15: HMS Model Representation of Africa.....	61
Figure 4-1: Diagram of STS Model Components .....	68
Figure 4-2: Diagram of HMS Model Components.....	85
Figure 4-3: Elements of an HMS Basin Model .....	86
Figure 4-4: Soil Conservation Service Triangular Hydrograph .....	90
Figure 5-1: The Four Major Basins of Africa.....	97
Figure 5-2: Area Map of the Congo Basin .....	98
Figure 5-3: Major Tributaries and Flow Gages of the Nile Basin.....	100
Figure 5-4: Source to Sink Model of the Congo Basin .....	103
Figure 5-5: Setup for Evaluating Longitudinal Decomposability .....	104
Figure 5-6: Source to Sink versus Cell to Cell Routing .....	105
Figure 5-7: Comparison of Diffusion Type STS and CTC Discharge .....	106
Figure 5-8: Congo Basin STS Models at 30, 10 and 5 arcminute Resolutions ...	108

Figure 5-9(a): Comparison of Congo Basin Responses for 30 and 10 arcminute Resolution STS Model with Pure Lag Routing .....	110
Figure 5-9(b): Comparison of Congo Basin Responses for 10 and 5 arcminute Resolution STS Model with Pure Lag Routing .....	110
Figure 5-10: Effect of Spatial Resolution on Dispersed STS Hydrograph.....	111
Figure 5-11: Nile Basin (a) Parametric Zones and (b) Sources.....	115
Figure 5-12: Effect of Spatial Distribution of Velocity with Uniform Dispersion Coefficient .....	117
Figure 5-13: Effect of Spatial Distribution of Dispersion Coefficient with Uniform Velocity .....	119
Figure 5-14: Effect of Spatial Distribution of Dispersion Coefficient with Non-Uniform Velocity.....	121
Figure 5-15: Effect of STS Routing Interval on Congo Basin Response .....	123
Figure 5-16: Sample HMS Schematic for Congo Basin.....	125
Figure 5-17: HMS Schematic for Longitudinal Decomposability Runs .....	127
Figure 5-18: Changes in River Reach Response with Muskingum n.....	129
Figure 5-19: Effect of Delineation Threshold on Congo Basin Response for HMS Model with Muskingum Routing .....	133
Figure 5-20: Comparison of 1000 Cell Threshold HMS Model Response with the STS Model Responses in the Congo Basin .....	134
Figure 5-21: Comparison of 1000 Cell Threshold HMS Model Response with the STS Model Responses in the Congo Basin .....	135
Figure 5-22: Basin Response for Iterations of Muskingum x and n Parameters.....	139
Figure 5-23: Equivalent HMS and STS Basin Response for Distributed Parameters .....	140
Figure 5-24(a): Effect of Minimum Subbasin Lag for 24hr-Interval Lag Routing .....	145
Figure 5-24(b): Effect of Min. Subbasin Lag for 12hr-Interval Lag Routing .....	145
Figure 5-25(a): Effect of Min. Subbasin Lag for 24hr-Interval Muskingum Routing .....	147
Figure 5-25(b): Effect of Min. Subbasin Lag for 12hr-Interval Muskingum Routing .....	147
Figure 5-26(a): Effect of Routing Interval on Response with Lag Routing.....	149
Figure 5-26(b): Effect of Routing Interval on Response with Muskingum Routing .....	149
Figure 5-27: Inflow and Discharge Hydrographs in the Sudd Marshes .....	153
Figure 5-28: Excess Input and Discharge Runoff after Baseflow Separation for (a) Period 1, (b) Period 2 and (c) Period 3 .....	154
Figure 5-29: Routing Excess Runoff using Computed Velocities and Dispersion Coefficients for (a) Period 1, (b) Period 2 and (c) Period 3 .....	156
Figure 5-30: Effect of Routing Input Flow using Mean Velocity and Dispersion Coefficients.....	157

Figure 5-31: Nile Basin (a) Gauge Locations and (b) HMS Model Components .....	160
Figure 5-32: Observed and HMS Simulated Flows at Malakal.....	161
Figure 5-33: Observed and HMS Simulated Flows at Khartoum .....	162
Figure 5-34: Observed and HMS Simulated Flows at Aswan.....	163

# **CHAPTER 1**

## **Introduction**

### **1.1 PROBLEM STATEMENT**

The desire to understand the movement of water over the earth's surface has long been a fascination. This desire has mainly arisen from the need to evaluate the amount of water available at a particular location to meet local demand as well as the risk of flooding due to excess water. Hydrologists have been called upon to determine the quantity of flow along rivers at various points in time and space. Until recently, the scope of these problems has been limited to individual communities and consequently, most hydrologic studies have focused on small watersheds. Routing methods have been developed based on these small watersheds. Recent concerns about global climate change and a series of large-scale hydrologic events such as the Midwest flood of 1993 and the El Nino of 1997 have focused attention on the need to track the flow of water through the entire global hydrologic cycle. In the climate modeling community, in particular, there is a need for models which route runoff generated by the land surface component of Global Circulation Models to the ocean cells used in the ocean modeling component. Approaches for routing water through large-scale systems are slowly evolving in response to these modeling needs.

One evolving approach for large scale routing involves dividing the earth's surface into a series of cells using a uniform grid. A vertical soil water

balance is performed on each of these cells, and the resulting excess runoff is routed from one cell to the next until it gets to an outlet or sink. Watershed boundaries are not explicitly delineated. Instead, the flow direction assigned to these coarse resolution cells dictates where the watershed divide should lie. The flow length is simply estimated on the basis of the distance between the centers of adjacent cells. This approach is not computationally efficient since routing is performed throughout the watershed even at locations where discharge values are not required. A trade off must be made between routing detail and the number of modeling units. When used at the continental scale, the routing process in grid based models is often reduced to very simple representations in order to increase computational efficiency. A routing model which computes discharge only at required locations allows a more detailed description of the routing process without sacrificing the spatial resolution of the model.

Grid based approaches differ significantly from other hydrologic models which use a watershed as the primary modeling unit. These watershed-based models are built on the fact that water flows on or near the land surface for a while before entering the river system. The land surface is therefore divided into watersheds with river reaches serving to connect the watersheds to each other and to the discharge location at the basin outlet. Therefore, in modeling river basins, different routing methods are defined for the respective watershed and in-stream phases of flow. Models of land-atmosphere interactions are used to generate input runoff for the routing model. Since the atmosphere is a spatially continuous system, it is more convenient to employ the uniform cells used in atmospheric



circulation models. The modeling units in the land-atmosphere interaction models and the watershed-based routing models are hence not coincident. Although there are ways of accounting for this discrepancy, it can be a real impediment when dealing with runoff which is variable in both space and time. There is hence an advantage to performing routing in a gridded environment when working with time-varying input runoff. The ideal situation would be to work in a routing environment which incorporates the boundaries of both the drainage basin and the soil water balance modeling units.

The relationship between the grid based approach and the watershed modeling approach is not clearly understood. The results of the two modeling approaches cannot be compared because the boundaries of the modeling units do not coincide. There is also a discrepancy in the spatial scale at which the two modeling approaches have been applied. Grid based models were developed for continental scale modeling while watershed based approaches have traditionally been used for local and regional scale modeling. In order to compare the two modeling approaches, the basin boundaries defined in one model should be duplicated in the other. Applying the respective modeling approaches to basins of comparable spatial scale also helps to bridge the discrepancy in spatial scale between climate and watershed models. Current concerns about global and continental scale hydrologic events provide the impetus for performing such intercomparisons in large river basins.

The development of continental scale routing models requires detailed information about the distribution of geographic features and parameters which

influence flow. Geographical Information Systems (GIS) have recently been used in deriving vector representations of watersheds and rivers for hydrologic modeling. GIS based approaches have also been used for deriving hydrologic modeling parameters from gridded representations of the earth. GIS thus provides an ideal environment for developing and parameterizing continental scale routing models.

In summary, there is a need for cell-based routing models to support continental scale hydrologic modeling. Existing models are limited by their inability to accurately define basin boundaries, by inconsistencies between their modeling units and those of associated models and by their computational intensity. A new routing approach which seeks to resolve these inconsistencies in modeling unit definition while only performing computations at required locations is implemented in this study.

## **1.2 OBJECTIVES**

A global database of hydrologic parameters is required to support surface water routing around the earth. Such a database allows the modeler to derive routing parameters for any modeling units defined in a study area. The first objective of this study is to develop a GIS database to support large-scale surface water routing globally.

The second objective is to implement a modeling framework which incorporates basin boundaries in a grid based model while maintaining computational efficiency by only performing routing at desired locations. The

efficacy of the source to sink modeling framework is demonstrated by using it to route runoff generated by the land surface component of a Global Climate Model at the continental scale.

A variety of topographic and climatic conditions are encountered when routing is performed at the continental scale. The third objective of this study is to examine of the robustness of the source to sink approach as compared to the watershed based approach in continental scale applications.

### **1.3 RESEARCH OUTLINE**

In meeting the first objective, existing datasets which could be used in deriving hydrologic parameters globally were identified. These datasets were processed to develop a database of routing parameters.

In meeting the second objective, a continental scale routing model using the source to sink approach was developed for all the continents except Antarctica which has no rivers. The model was used to route 10 years of daily runoff data from a Global Climate Model to receiving ocean cells.

In meeting the third objective, routing models were developed for selected drainage basins using the watershed based and grid based approaches. The models were parameterized from the global database of hydrologic parameters thus producing two independent and yet consistent hydrologic representations of the same drainage basins. Various simulations were performed to determine differences and similarities in the response of the modeling approaches to changes in modeling parameters. To verify its suitability for continental scale routing, the

watershed based model was used to route flow in a large drainage basin, and the results were compared with actual flows in the basin.

The remainder of this dissertation is divided as follows. Chapter 2 describes the various conceptual models and methods used in routing. It also provides a review of prior developments in continental scale routing. In Chapter 3, sources of input data and the development of the global database of hydrologic parameters are described. The procedure for developing the each of the continental scale routing models is also outlined. The theoretical basis of the two continental scale modeling approaches are discussed in Chapter 4 along with methods of determining the required model parameters. This is followed in Chapter 5 by the presentation of results of model runs, and the discussion of the results in Chapter 6. In Chapter 7, the findings of the study are summarized with recommendations for further study.

## **CHAPTER 2**

### **Literature Review**

#### **2.1 CONCEPTUAL MODELS OF A RIVER BASIN**

In developing models of hydrologic systems, it is recognized that processes that occur in nature cannot be reproduced exactly. Even if such a representation of natural processes were possible, the resulting model would be so complex that it would be impossible to solve mathematically. Some simplifying assumptions are consequently made to reduce the complex system to a set of simple descriptive processes (Dooge, 1973, pp.148). Only those processes considered critical to the functioning of the system are described. In this chapter, the conceptual models and methods used in routing are discussed. Existing large-scale routing models are reviewed along with their limitations. Problems of scale dependence affecting routing models are also discussed. To begin with, the hydrologic system is reduced to a simple conceptual model. The control volume proposed by Chow et al (1988, pp.7) provides a conceptual model that is applicable to hydrologic systems in general. They define a hydrologic system as

*“a structure or volume in space, surrounded by a boundary, that accepts water and other inputs, operates on them internally, and produces them as outputs”.*

Hydrologists develop models by trying to relate the input into the control volume with the output using a system response or transformation. The first task in modeling must therefore be the definition of the control volume. There are several approaches to defining a control volume for routing applications. The most common of these can be grouped into three classes as described in sections 2.1.1 to 2.1.3 below.

### **2.1.1 The Watershed Based Approach**

Hydrologists have for a long time envisaged the land surface component of the hydrologic cycle as being made up of river reaches with associated drainage areas. Reaches are defined as stretches of river with no major tributaries in between, and the portion of land draining directly into each river reach is defined as its associated watershed. River junctions are defined wherever two or more river reaches meet, and diversions are defined wherever two or more reaches form downstream of a single reach. Other natural features such as lakes and springs and manmade features such as dams, reservoirs and canals may also be included in the definition of the hydrologic system. In the systems approach, each of these features is regarded as a control volume, and a separate system response is defined to transform the inputs in each control volume into discharge at its downstream end. Sequential links are established among the control volumes such that flow can be passed from one control volume to the next until it arrives at a terminal point such as the continental margin or an inland water body with no outlet. The Hydrologic Modeling System (HMS) developed by the Hydrologic

Engineering Center of the US Army Corps of Engineers (Peters, 1998) and the MIKE BASIN modeling system developed by the Danish Hydraulic Institute (Storm and Kjelds, 1999) are examples of models built on this concept.

### **2.1.2 The Cell to Cell Routing Approach**

A second approach to modeling flow over the land surface involves discretizing the land surface into smaller segments, and routing flow from one segment to the next until it arrives at a terminal point. The underlying assumption in this approach is that the land surface within each of these segments is homogenous. It is therefore not necessary to distinguish between overland and in-stream flow processes. For convenience and computational efficiency, the land segments used are often equaled sized cells and hence the name cell to cell routing. The approach can however be used with other irregularly shaped land segments. The control volume in a cell to cell routing approach is the land segment. Inputs to each segment are transferred to the next downstream segment using a unique response function. The response function is expected to capture the essence of the various flow processes occurring within the control volume. Its growing usage in surface flow modeling has been spurred by the need to couple land surface models with models of the atmospheric and subsurface flow phases of the hydrologic cycle. Watershed boundaries defined in the watershed modeling approach (see section 2.1.1) are of little relevance in these other phases. Examples of surface water routing models using this approach include those developed by Vörösmarty et al (1989), Miller et al (1994), Sausen et al (1994) and Coe (1997).

### **2.1.3 The Source to Sink Routing Approach**

The final approach to characterizing surface flow involves subdividing the land surface into smaller segments and routing the flow from each segment directly to a discharge location such as the continental margin or an inland depression. In this approach, the control volume is drawn around the flow path linking the segment to the discharge location. The system transformation describes the change in distribution of the input when it arrives at the discharge location, allowing for losses within the control volume. The flow path may be composed of different flow regimes such as overland flow and in-stream flow. Water may flow at different speeds through these various flow regimes. The response function defined for each land segment is in effect a summary of all the transformations that occurs along the flow path between the source of input and the discharge location (also called the sink). The name source to sink routing is used by Olivera et al (2000) to describe all models of this kind. Examples of source to sink models include the Clark unit graph method (Clark, 1945), the modified Clark method (Kull, 1998), the methods of Naden (1992,1993) and Olivera and Maidment (1999).

## **2.2 METHODS OF CHARACTERIZING FLOW**

After reviewing control volume definitions used in river basin modeling, the next step is to define the flow routing processes and the nature of the system transformations used to characterize these processes. As mentioned in section 2.1 of this dissertation, the task in hydrologic modeling is to discern the essential



characteristics of flow. With regard to transformation of flow through a control volume, these may be summarized as translation, redistribution and translational losses. Translation refers to the simple movement of water from the input location to the discharge location. During translation, the shape of the input pulse or impulse is altered, mainly as a result of three mechanisms. The shape may change due to shearing forces between the flowing water and the channel surface with which it comes in contact (Maidment, 1993, pp.14.14). The shape may also change due to the damping effect of off-stream storage created by the constant variation in channel dimensions, and by passage through wide water bodies such as lakes and reservoirs (Henderson, 1966, p.355). These first two mechanisms are usually combined into a single mechanism known as flow redistribution. The third mechanism by which the shape of the input pulse may change is by loss of flow through seepage and evaporation. This third mechanism, referred to as translational loss, is usually treated separately since it implies changes in the mass balance.

### **2.2.1 Translation With Incidental Dispersion**

The simplest form of routing involves describing the movement of water through a control volume using the continuity equation along with a mathematical relationship between discharge and control volume storage. In these methods, there is no parameter for explicitly controlling dispersion. Redistribution is achieved as an incidental by-product of the routing process. These methods are jointly referred to as level pool routing (Maidment, 1993, pp.10.6). The most

commonly used level pool routing method is the linear reservoir method (Zoch, 1934) in which discharge from the control volume is assumed to be directly proportional to storage. Another common approach to level pool routing involves the use of approximate numerical methods such as the Runge Kutta to determine discharge from the control volume (Maidment, 1993, pp.10.6). In this method, water is routed sequentially through several discontinuous segments of a river reach. The Puls and Modified Puls methods (Peters, 1998) in which a relationship is established between the storage and discharge from a river reach based on observed data are also examples of level pool routing.

### **2.2.2 Translation With An Approximate Dispersion Process**

The second class of routing methods are those that contain a parameter which, though not descriptive of the dispersion process, can be used to control the magnitude of dispersion experienced by an input passing through the control volume. The two most common examples of this class of methods are the Cascade of Linear Reservoirs attributed by Montes (1998) to Kalinin and Milyukov (1958) and the Muskingum method developed by the US Army Corp of Engineers (Henderson, 1966, p.362).

The Cascade of Linear Reservoirs approach takes advantage of the scale dependence of linear reservoir models by routing input flow through a series of linear reservoirs as it passes through the control volume. While the output of a single linear reservoir is an exponential distribution, subsequent convolutions of this distribution yield gamma distributions (Olivera, 1996). The response of a

cascade of reservoirs containing more than one reservoir is consequently a gamma distribution and the number of reservoirs in the cascade can be used to modify the magnitude of dispersion experienced by an input passing through the control volume.

The Muskingum method approximates the storage effects in a river reach with a trapezoidal control volume consisting of a prism with an overlying wedge. The flow through the prism is assumed to be dependent on discharge only while flow through the wedge is dependent on the difference between the inflow and discharge (Henderson, 1966, p.362). A factor, the Muskingum  $x$ , is applied to the wedge storage to account for the rate of attenuation of flow as it passes through the control volume. The assumption made in applying the Muskingum factor is that in cases where the rate of attenuation is low, the area of the wedge storage will approximate that of a triangle, and thus  $x$  will assume a value of 0.5. In all other cases, the area of the wedge is a concave parabola, and  $x$  will assume a value between 0 and 0.5. The Muskingum  $x$  can thus be used to determine the amount of dispersion experienced by flow passing through the control volume.

### **2.2.3 Translation With Fully Described Dispersion**

The third class of routing methods trace the movement of flow through the control volume with transformations which fully describe both the translation and dispersion processes. These methods generally rely on the momentum equation for unsteady, non-uniform flow (Chow et al, 1988, p.31) shown as Equation 2-1.

Equation 2-1 
$$\frac{\partial V}{\partial t} + \frac{V\partial V}{\partial x} + g\left(\frac{\partial h}{\partial x} + S_f\right) = 0$$

where  $A$  is the cross sectional area of the channel

$V$  is the flow velocity

$S_f$  is the friction slope

$\frac{\partial h}{\partial x}$  is the slope of piezometric head

$g$  is the gravitational constant

$x$  is the distance along the longitudinal axis of the channel

$t$  is time

The momentum equation describes the change of form of an input subjected to the forces of friction and gravity. Since these are the same forces responsible for the deformation of the input as it travels through the control volume, this equation in effect provides a full description of the dispersion process. The momentum equation and the continuity equation (given as Equation 2-2 below) for flow routing are together referred to as the St. Venant equations after the 19<sup>th</sup> century French mathematician who derived them in 1871.

Equation 2-2 
$$\frac{\partial(AV)}{\partial x} + \frac{\partial A}{\partial t} - q = 0$$

where  $\frac{\partial(AV)}{\partial x}$  is the rate of change of flow rate with distance

$\frac{\partial A}{\partial t}$  is the rate of change of area of flow with time

$q$  is lateral inflow or outflow along the channel

There is no analytic solution to these equations in their complete form. Some simplifying assumptions are therefore made to enable the equations to be solved. These solutions are therefore limited in applicability to conditions under which the simplifying assumptions can be shown to hold true. The assumptions and their resulting solutions can be classified into three categories, namely dynamic, kinematic and diffusion wave solutions.

In dynamic wave routing, the full St. Venant equations are used but assumptions are made about the condition of flow at the boundaries. These boundary flow assumptions provide a starting point for computations which then proceed using one of several numerical integration techniques. The most common of these techniques are described by Montes (1998, pp.470). They include the method of characteristics (Massau, 1889, Richardson, 1910 and Lin, 1952), explicit methods (Stoker, 1953) and implicit methods (Preissmann, 1961, Cunge, 1961, 1966, Lai, 1966). Many of these numerical integration methods can only be applied over small space and time steps over which the magnitude of error introduced by the approximation of the integral is small compared to the magnitude of the flow. These numerical stability limitations have been explored in the works of Von Neumann (1950) and Courant and Freidriechs (1948). Dynamic wave routing is generally unsuitable for continental scale applications because the numerical stability limitations make the methods too computationally intensive to be practicable at that scale.

Kinematic and diffusion wave routing methods on the other hand make some assumptions about the condition of the flow parameters. These assumptions allow one or more of the terms in the momentum equation to be dropped thus making it possible to find an exact analytical solution to the St. Venant equations. The development of the kinematic wave approach is attributed by Montes (1998, p.547) to the works of Kleitz (1877), Graeff (1875), Forchheimer (1930), and Lighthill and Whitham (1954). It assumes that within the control volume, velocity is constant in time and space, and the water surface is parallel to the channel bed (Chow et al, 1988, p.281). The momentum equation is consequently reduced to two terms expressing the equality of bed slope and friction slope. The kinematic wave approach cannot be used, on its own, for routing flows at the continental scale because the assumption of a constant water depth does not allow the flood wave to attenuate as it travels through the control volume. Peak attenuation is considered to be an important property in continental scale routing. Kinematic wave routing has however found numerous applications in characterizing overland flow (Iwagaki, 1995, Henderson and Wooding, 1964, Woolhiser and Liggett, 1967).

The diffusion wave routing approach differs from the kinematic wave approach in that it does not make the assumption of a constant water depth within the control volume. The main parametric assumptions made in this approach are the spatial and temporal invariance of flow velocity. The method was first proposed by Hayami (1951) who demonstrated that by making this simplification, an exact solution of the St. Venant equations could be obtained. Hayami

subdivided the input into a series of impulses to which the diffusion wave impulse response function could be applied. The discharge due to each of these impulses was then aggregated at the outlet.

The assumption of time invariant parameters (velocity and dispersion coefficient) within the control volume is one obvious limitation of the diffusion wave method. In real river systems, large flows are translated faster than smaller flows. A solution to this problem was provided by the multiple linearization technique of McQuiver and Keefer (1974) in which the input is further subdivided vertically with different response functions being applied to different magnitudes of flow. Subsequent researchers have also addressed the problem of spatial invariance of parameters by defining ways to estimate a single flow path parameter for a path consisting of several segments each with its own parameters (Olivera, 1996). The flow path parameters thus computed result in a discharge distribution with properties similar to that resulting from sequential routing through multiple segments.

## **2.3 CONTINENTAL SCALE ROUTING MODELS**

Vörösmarty et al (1989) developed a coupled water balance and water transport model for continental scale routing in South America. In their model, the land surface is divided into a 0.5 by 0.5 degree grid, and flow is routed horizontally from cell to cell. Flow through the system is modeled using the continuity equation and a linear reservoir storage function. However, the model attempts to subdivide the storage into separate flood plain and in-stream

components. This introduces a non-linearity in the model which cannot be resolved analytically. A Runge-Kutta integration technique is used to solve for the two storage components. Flow velocity in this model is computed using the mean annual discharge and the empirical velocity functions proposed by Leopold (1953). The main limitation of this model is that it contains several empirical relationships, the validity of which cannot be verified.

Miller et al (1994) proposed to allow for spatially varying storage characteristics of the cell to cell model by making the transfer coefficient in the Vörösmarty model a function of excess storage instead of total storage. In essence, this model implies that in-cell storage is caused by the inability of the cell to transfer water to its downstream neighbor. A sill depth is defined for each cell as the depth of the river channel, and this depth is used to determine a minimum cell storage which must be met before flow is transmitted from a cell to a neighboring cell. Flow in excess of this minimum storage is transmitted to the next downstream cell by a linear storage function as in the Vörösmarty model. The model routes flow globally at a resolution of 2.0 by 2.5 degrees. The flow direction for cells in this model is determined by visual inspection. Flow velocity is determined by an empirical function relating slope within each grid cell to a reference slope and a reference velocity. Again, there is no physical basis for the storage and velocity relationships. The definition of a minimum cell storage is inconsistent with the mechanisms of storage in river systems defined in section 2.2 of this dissertation. Besides, no method is suggested for computing the depth of river channels in each grid cell globally.



Coe (1997) proposed to improve Miller's (1994) cell to cell approach by using lakes and other natural depressions in the land surface to determine the cell storage. In this model, a 2 by 2 degree grid is used to divide the land surface into routing cells. As in Miller's model, discharge is assumed to occur only when the minimum cell storage is exceeded. Consequently, the discharge rate is a function of the difference between the amount of water in the cell and its minimum storage requirements. The minimum storage of each 2 by 2 degree cell is determined by filling the sinks in a finer resolution grid, in this case a 5 by 5 minute grid. Using this approach, regions with no internal drainage are assigned a minimum storage of zero. Sinks in DEMs may result from natural depressions or from errors in the DEM. The raw DEM cannot therefore be used for determining storage without eliminating the erroneous pits. No method is suggested for distinguishing between erroneous pits and true natural depressions in this application. It is consequently unclear whether the cell storage determined from the 5 by 5 minute grids in this application are representative of actual storage capacities in the land surface.

An alternative method of determining discharge in the cell to cell environment is proposed by Sausen et al (1994). In this model, cells on the land surface are assumed to have no storage. All the water available in each cell is allowed to flow in any one of four orthogonal directions. The quantity of water flowing in each direction is determined by an empirical function involving a translation velocity and the land surface slope. As with other empirical functions, there is no physical basis for its use. The validity of the relationship is further thrown into question by the generation of negative discharges during the study.

Kite et al (1994) used a spatially distributed version of the SLURP (Simple Lumped Reservoir Parametric) model to route runoff generated by a GCM. In this approach, watersheds are divided into grouped response units (GRU) using a 10 km by 10 km sized mesh. Within each GRU, flow is routed to an outlet using a velocity calculated for each land use category. The velocity is determined from Manning's equation by assuming a hydraulic radius of 1. This assumption is meant to imply that the width of the river is much larger than its depth. However, a review of the equation for hydraulic radius would indicate that as the width of a channel increases the hydraulic radius does in fact tend towards the depth of flow, not 1. Manning's roughness coefficient,  $n$ , is assigned to each cell based on its land cover category allowing velocity to be computed. The velocity is then used to compute isochrones of travel time as in the Clark hydrograph method (Clark, 1945). Flow at the watershed outlet is determined by aggregating flows from the different isochrones. Flow is routed from GRU to GRU until it arrives at a sink. For this routing a nonlinear, empirical storage function is used to compute storage and outflow. As with other empirical functions, there is no physical basis for its use, and its associated parameters must be determined by calibration.

A more physically based solution is proposed by Naden (1992,1993) who applied a network response function to the Severn and Thames river basins. The response function is derived by convolving the linear solution of the diffusion wave model with the network width function. A network width function is analogous to an area distance diagram and is defined as the number of river

channels within a given distance of the basin outlet divided by the total number of channels in the basin. In this study, the basins are divided into grids cell (40 by 40 kilometers wide) which only serve to define areas of uniform runoff generation. Flow routing is performed through the stream network. The main difficulty with this approach is that it is not easy to discern the relationship between the network width function and the distance-time diagram created by the diffusion equation. The latter is a response function describing the longitudinal distribution of input runoff when it is subjected to both an advective and a dispersive process. The network width function on the other hand is a measure of the distribution of flow channels within a basin. No mathematical or physical justification is given for the convolution. In addition, it is difficult to justify the use of a network width function when distance area diagrams and spatially distributed flow length grids can be computed using Geographic Information Systems.

Lohmann et al (1996, 1998) also used a diffusion wave model coupled with a land surface parameterization scheme to route GCM runoff. In this model, the land surface is seen conceptually as consisting of watersheds and streams, each of which has a response function. Hence even when the land surface is subdivided with a grid, each cell must still be assigned two response functions to account for the respective watershed and stream segments of flow within the grid cell. The main limitation of this model lies in the conceptual model. The grid cell response function accounts for the transmission of flow from within the grid cell to the outlet of the cell. To use the same response to account for flow entering the cell from a neighboring cell would not be accurate since such flow enters the river

system without entering the watershed. The response function for routing flows generated within the grid cell is determined by deconvolution from observed flow data. Even if flow data were available to define grid cell response functions globally, it would still be difficult to justify the assumption of a grid cell as consisting of rectangular watersheds which fit exactly into the cell.

Hagemann and Dumenil (1998) apply a cascade of linear reservoirs to flow routing a cell to cell model. In their model, a grid cell is viewed as being equivalent to a watershed of equal resolution. Flow processes observed in a 2500 km<sup>2</sup> watershed are consequently applied to 0.5 degree resolution grid cell. Within each cell, three separate flow paths are defined. Runoff generated within the grid cell may be routed as overland flow using a cascade of linear reservoir routing or as baseflow using a linear reservoir. In addition, flow entering the cell from upstream cell is routed using another cascade of linear reservoirs. Flows from these three routing processes are aggregated at the outlet of the cell and passed on to the next cell. The main limitations of this model are that the number of reservoirs in a cascade is not a physically based parameter and can only be obtained by calibration. Given that there are three different responses, three different velocities must also be defined for each grid cell. The conceptual model of a grid cell being equivalent to a watershed is also difficult to justify.

## **2.4 SCALING ISSUES IN ROUTING**

The field of hydrologic engineering evolved out of the need to address local flooding problems. Most hydrologic methods were thus developed with

local scale analysis in mind. Today, the scale of hydrologic analysis is shifting to larger scale problems and concerns. The applicability of methods of analysis developed at the local scale to large-scale problems must consequently be addressed. Problems of scale dependence also arise when measurements made at a point are extrapolated to another scale. In section 2.4.1, the problem of scale dependence of routing methods is addressed. This is followed in section 2.4.2 by a brief discussion of current research in scale dependence of hydrologic parameters.

#### **2.4.1 Scale Dependence of Routing Methods**

Routing methods are transformations which are used in conjunction with conceptual models to represent flow processes. If the routing methods are scale independent, then routing parameters determined for a given model at one resolution should be applicable at different resolutions. Methods can become scale dependent if assumptions about the state of parameters become invalid or the solution of the transformation equations becomes numerically unstable.

An example of scale dependence due to assumptions about the state of routing parameters is found in storage routing methods in which linear relationships are used to link control volume storage to inflow and outflow is assumed. These relationships imply that within the control volume, velocity is spatially and temporally invariant (Montes, 1998, pp.582). A similar assumption is made in the simplification of the momentum equation in kinematic wave routing. Over certain routing intervals, the magnitudes of the first two terms of the momentum equation are small even for the variable velocity case (Miller and

Cunge, 1975). The magnitude of these terms may however become significant as the routing interval and reach length increases, making the methods scale dependent. Another illustration of this type of scale dependence is found in the linear reservoir method. Inflows to the control volume are instantaneously distributed throughout the reach thus ensuring uniform storage throughout the reach. Discharge from the reach is then computed on the basis of the control volume storage. At an hourly time interval, it is easy to envisage a 200m long reservoir in which all input is instantaneously distributed throughout the reservoir. It is not as realistic to envisage input being distributed instantaneously over a 1000 km reservoir in one hour simply because such a time period is too short for such a redistribution to take place. A linear reservoir model is thus made scale dependent by the underlying assumption of instantaneous inflow redistribution.

Scale dependence in routing may also be brought about by a numerically unstable solution. Simplifying assumptions are made in solving the mathematical equations describing flow. These assumptions result in a deviation of the estimate from the real value. A solution is said to be numerically unstable one when the magnitude of the deviation of the estimate from the real value is significant compared with the magnitude of the real value itself. In the Muskingum method for example, discharge from a control volume is predicted on the basis of discharge during the preceding time period, inflow in the preceding time period and inflow in the current time period. The simple integration technique used in arriving at the solution was shown by Cunge to result in the elimination of second order derivatives thus introducing an error in the solution (Montes, 1998, pp.572).

This error (similar in form to the diffusion term in the diffusion wave equation) is responsible for the observed attenuation of the hydrograph when the Muskingum method is used for routing flow. The magnitude of this error varies in proportion to the square of the length of the reach. Applying the method sequentially over a reach will therefore not result in the same discharge as a single application across the entire reach. In effect, the Muskingum method is scale dependent because the approximation made in deriving the method results in an error whose magnitude is a function of length. As shown in the work of Cunge (1969) and Koussis (1978), the magnitude of this error can in fact be computed and taken into account. However, unless this correction is made, the Muskingum equation results in a scale dependent model.

In continental scale routing, the use of scale independent methods allows parameters determined from finer resolutions models to be incorporated into coarser resolution models. Scale independent methods also serve to minimize the propagation of systematic errors when routing is performed over large distances.

#### **2.4.2 Scale Dependence of Routing Parameters**

Another approach to the problem of scale dependence involves the use of statistical methods to translate parameters measured at one location to another. This approach, commonly known as scaling theory, has produced numerous relationships many of which are discussed in Gupta et al (1986) and Sposito (1999). The approach is based on the premise that there is an intrinsic relationship between hydrologic parameters and the topographic conditions at the point of

measurement. Statistical methods are used to deduce this relationship from measurements of the parameter and a corresponding topographic index. The relationship is then expanded to cover all similar areas irrespective of spatial resolution. The applicability of scaling theory is not addressed in this research because the range of possible solutions is infinite when an intrinsic relationship is deduced from two sets of data. The presence of measurement errors in limits the reliability of the solution to the data set from which it is deduced. The addition of more data sets simply increases the degrees of freedom in the solution.



## **CHAPTER 3**

### **Data Development**

#### **3.1 DATA SOURCES**

The Digital Chart of the World distributed by Environmental Systems Research Institute (ESRI, 1993) includes digital maps of the world's rivers. The database was derived from operational navigation charts of Australia, Canada, the United Kingdom and the United States. The rivers in this database were digitized from 1:1,000,000 scale maps. The DCW represents the most complete coverage of the rivers of the world currently available in digital format. A coarser resolution coverage is also available in the Arc World dataset (ESRI, 1992) also compiled and distributed by ESRI. The river coverage was digitized from 1:3,000,000 scale maps. Neither of these river coverages incorporates network connectivity.

The River Nile in North-Eastern Africa is one of the most studied rivers in the world. Flow gauge dating as far back as 620 AD have been collected in the basin (Hurst and Phillips, 1938). A major effort to systematize and publish these datasets was undertaken by a team led by Hurst. The results of these efforts are published in a series of volumes entitled 'The Nile Basin' (Hurst and Phillips, 1931-). Flow data from these volumes as well as those reported in Shahin (1985) are used in deriving flow parameters in this study.

30 arc-second Digital Elevation Models (DEM) produced by the EROS Data Center of the US Geological Survey (USGS, 1996) are used to derive hydrologic characteristics for both the source-to-sink and the HMS models. The DEMs which were developed as part of the GTOPO30 mapping project are currently the finest resolution global terrain representation available. The DEMs can be downloaded from the USGS site, over the Internet at

“<http://edcdaac.usgs.gov/gtopo30/gtopo30.html>”

Runoff generated from a Global Circulation Model (GCM) is also available. The Community Climate Model (CCM3) created by the National Center for Atmospheric Research (NCAR) (Kiehl et al, 1996) was used to simulate daily runoff generation for a period of 10 years (Branstetter and Famiglietti, 1998). Runoff was generated over T42 grid cells with a resolution of approximately 2.8 by 2.8 degrees. While the resulting data may not be representative of actual values on the ground surface, they provide spatially varying input that can be used for modeling. The use of GCM runoff also allows routing to be performed in an environment similar to that encountered by global climatologists and other users of continental scale routing models.

River discharge data is required for the calibration and verification of the routing models. The Global River Discharge Database contains monthly flow time-series from 949 runoff stations around the world (Vörösmarty et al, 1996). The database was assembled by reviewing discharge of rivers from published data

sources. These data provide a basis for determining flow routing parameters such as velocity and dispersion coefficient. The data are available over the Internet at “<http://www.rivdis.sr.unh.edu/>”

### **3.2 TERRAIN DATABASE DEVELOPMENT**

As stated in the section 1.2 of this dissertation, the development of a database to support routing at the global scale is of prime importance. The utility of a modeling system is determined not only by its ability to represent a hydrologic system but also the ease with which such a representation can be attained. At the global scale, data availability and computational efficiency determine the ease of representation of a hydrologic system. A terrain analysis is undertaken to develop a global database of terrain-derived parameters required for continental scale hydrologic modeling. The database is used to parameterize two continental scale routing models as described in sections 3.4 and 3.5 of this dissertation. Drainage basins and modeling units are delineated from Digital Elevation Models (DEMs) in accordance with the conceptual models defined in those applications. DEMs are the most detailed description of surface topography available in digital form. They are gridded representations of the land surface with the ground surface elevation of each corresponding piece of land stored in a grid cell. The determination of hydrologic modeling parameters from DEMs relies on the simple premise that water flows downhill, and in the direction of steepest descent. The parameters that influence the response of an area of land to input runoff can hence be determined from surface elevation.

The first objective in GTOPO30 DEM processing is to ensure that all land surface elevations are referenced to a single horizontal datum. In meeting this objective, ocean cells and other water bodies are first removed from the DEM. The USGS sets a datum of 65536 m for all cell located within water bodies and for land surface cells with elevations below sea level (USGS, 1996). In addition, ocean cells are assigned dummy elevation values of -9999. The GTOPO30 DEM was prepared for analysis by assigning null values to the ocean cells. Land surface cells with elevation values greater than 32768 were restored to their true negative elevations by resetting their datum to zero. The resulting land surface grid was raised by 1000m to ensure a positive land surface elevation everywhere. Next, a map projection was used to transform the land surface grid from the World Geodetic Survey ellipsoid of 1984 (WGS84) used to represent the earth in the original DEM onto a flat surface. The map projection selected for this study is the Lambert Azimuthal Equal-Area projection used by the USGS in a similar delineation (USGS, 1997). In this projection, different central longitudes and latitudes are defined for each continent. All other projection parameters are kept constant. A projection center which lies close to the centroid of each continent is chosen in order to minimize areal distortion. The projection centers for the various continents are given in Table 3-1 below.

Table 3-1: Projection Centers for Various Continents

Continent	Central Longitude	Central Latitude
Africa	20 0 0	5 0 0
Asia	100 0 0	45 0 0
Australia	135 0 0	-15 0 0
Europe	20 0 0	55 0 0
North America	-100 0 0	45 0 0
South America	-60 0 0	-15 0 0

A sample projection file is also shown in Table 3-2 below. The parameters of the output projection include the radius of the sphere of reference (6378137m), the longitude of the center of the projection (20.0°), the latitude of the center of the projection (5.0°), the false easting (0.0) and the false northing (0.0).

Table 3-2: Sample Projection File for Africa

```

INPUT
PROJECTION GEOGRAPHIC
UNITS DD
PARAMETERS
OUTPUT
PROJECTION LAMBERT_AZIMUTH
UNITS METERS
PARAMETERS
6378137.00000
20 0 0
5 0 0
0.0
0.0
END

```

The second objective in DEM processing involves correcting erroneous cell values to allow for the derivation of hydrologically correct flow paths. In DEM processing, a pit is a cell or group of cells completely surrounded by higher elevation cells. The delineation programs used in the analysis of these data cannot define flow direction for the cells at the bottom of such pits. While naturally occurring pits exist on the earth's surface, many of the pits in the DEM are the byproduct of the DEM production process. Such artificial pits were located and filled while retaining natural ones. This was done by first filling all pits in the DEM. The filled areas were then isolated by subtracting the elevations of cells in the unfilled DEM from those of the filled one. Natural sinks were identified by comparing the shape of the filled area with those of naturally occurring lakes and depression identified by visual inspection of areas maps. Sources of maps used include the Times Atlas of the World (Bartholomew et al., 1975), the UNESCO Atlas of the World Water Balance (Korzoun et al, 1978), Watersheds of the World (Revenga et al, 1998) and the Perry-Castañeda Library (PCL) Map Collection, available over the Internet at ["http://www.lib.utexas.edu/Libs/PCL/Map\\_collection/Map\\_collection.html"](http://www.lib.utexas.edu/Libs/PCL/Map_collection/Map_collection.html)

After distinguishing between natural and artificial pits, a single null value cell was placed at the lowest point of the natural pits in the unfilled DEM (Olivera et al, 2000). When the resulting DEM was subsequently filled, natural pits were preserved while artificial ones were eliminated. Cells in the catchment of the unfilled natural pits (called inland catchments) are thus allowed to drain internally

in the direction of the null value cell. All other cells drain towards on the continental margin. Figure 3-1 also shows the locations of the major inland catchments identified around the world.



Figure 3-1: Inland Catchments of the World

Table 3-3 lists the names of the natural depressions identified for each continent along with the location (in geographic coordinates) of the corresponding null value cell. Due to the large spatial extent of many of these features, the geographical locations given in the table are only approximate.

Table 3-3: Inland Catchments Identified

Continent	Inland Catchments	Longitude	Latitude
Africa	Lake Chad	14.45	21.09
	Lake Eyasi	35.13	-3.59
	El Wahat Kharga	31.36	22.87
	Lake Turkana	36.43	2.91
	El Djouf	-5.83	21.09
	Lake Rukwa	32.06	-7.83
	Lake Baringo	36.04	1.75
	Okavango Delta	25.84	-20.82
	Aral Sea	59.84	44.86
	Lake Balkash	76.07	46.69
Asia	Oz Issyk Kul	77.39	42.41
	Lop Nor	90.38	39.95
	Kuruk Gol	92.11	42.70
	Turfan Depression	89.30	42.68
	Lake Eyre	140.04	-28.55
Australia	Lake Frome	140.24	-29.47
	Caspian Sea	50.11	43.02
Europe	Dead Sea	37.45	31.33
	The Great Salt Lake	-118.02	39.80
North America	Salton Sea	-115.83	33.31
	Saline Valley	-112.54	41.11
	Death Valley	-117.83	36.70
	Lake Poopo	-67.49	-17.87
South America	Salar de Arizaro	-67.69	-24.85
	Salar de Atacama	-68.27	-23.53
	Salina del Antofelia	-68.03	-26.25
	La Carachi Pampa	-67.45	-26.54



The resulting DEMs were then used in the determination of flow direction and other hydrologic parameters of interest. The GIS software used in this analysis, Arc Info, defines a single flow direction for each cell based on the direction of steepest descent from a given cell to one of the eight neighboring cells. The underlying assumption in this analysis is that each grid cell discharges all its flow to a single neighboring cell. Flow direction is denoted by a value assigned to each grid cell. Figure 3-2 shows the cell values assigned for the respective directions of flow.

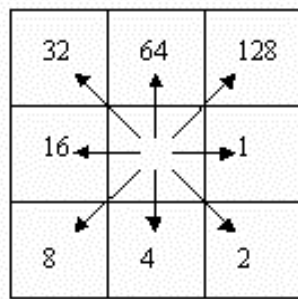


Figure 3-2: Flow Direction Arrows

The flow direction grid is an important component of the database because it is a required input for the derivation of other database components such as watershed coverages, river networks and flow length grids. It must consequently be checked for errors. One simple test performed for this data is the computation of histograms of cell values. The presence of cell values other than those shown in Figure 3-2 denotes the presence of sinks which must be removed by running the Fill function on the corrected DEM again. Figure 3-3 shows the flow direction grid derived for the continent of Africa.

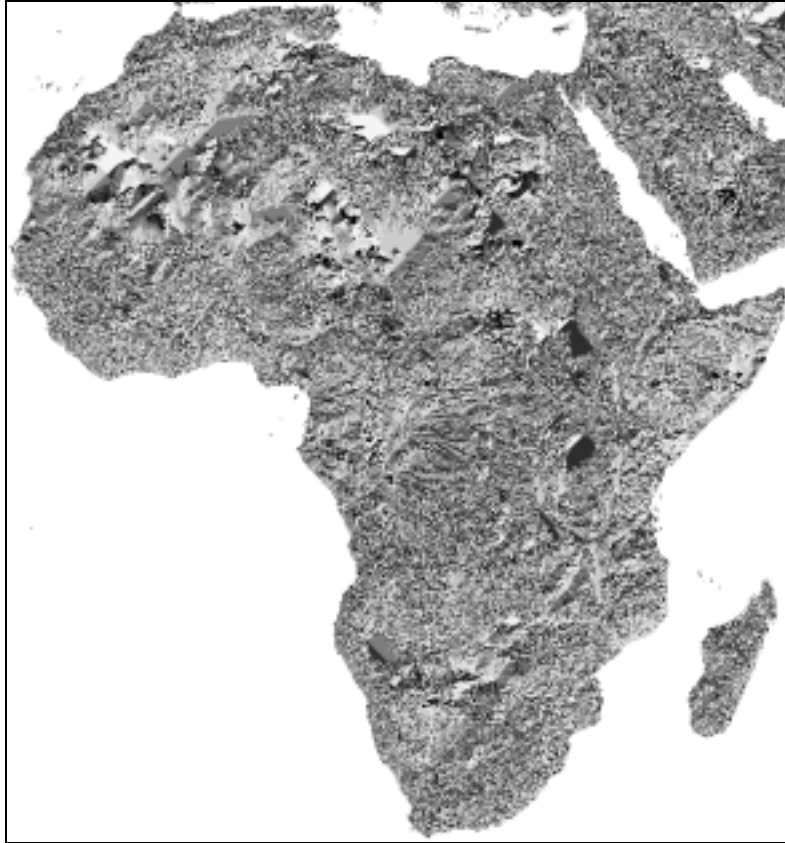


Figure 3-3: Flow Direction Grid of Africa

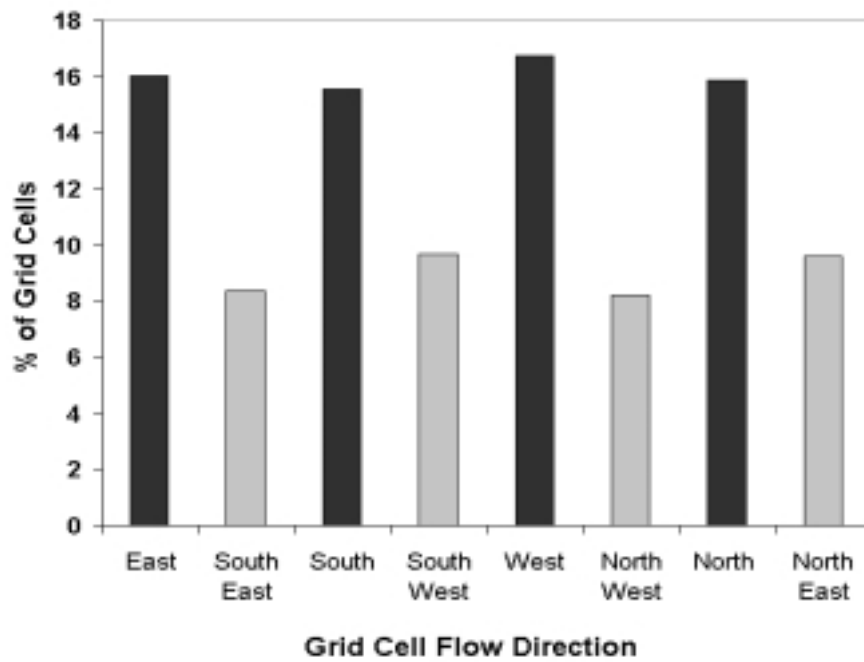


Figure 3-4 (a): Histogram of Flow Directions for North America

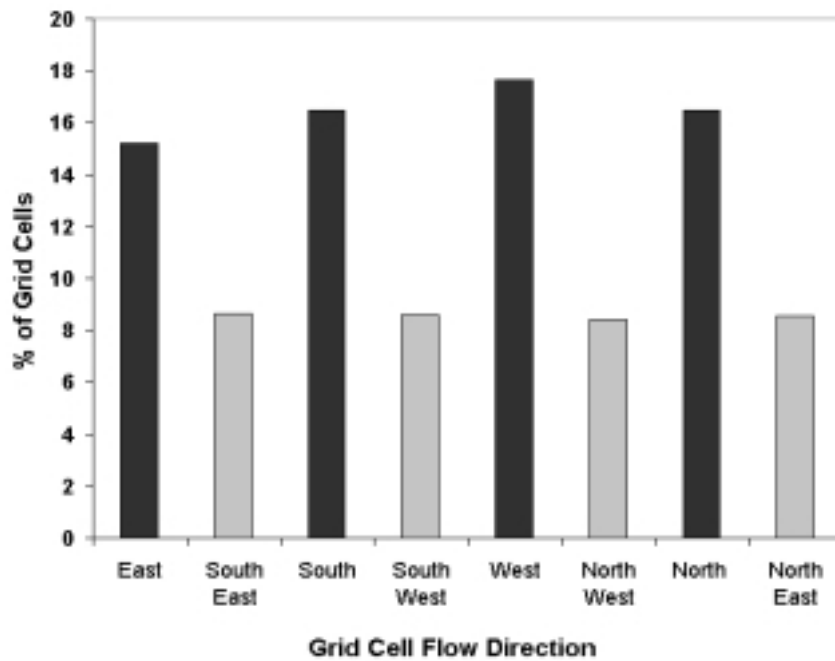


Figure 3-4 (b): Histogram of Flow Directions for Africa

Figures 3-4 (a) and (b) show the histograms of the flow direction grid of North America and Africa. The histograms indicate that the flow direction algorithm tends to favor the cardinal directions (north, south, east and west) over the diagonal directions (northeast, northwest, southeast and southwest). For the entire dataset (of the whole world) 65.8% of grids cells had flow in a cardinal direction as compared to 34.2% diagonals. This indicates that the flow direction algorithm used in the model is biased in favor of flow through the cardinal directions. No cell values other than those corresponding to the respective flow directions in the eight direction pour point model shown in Figure 3-2 were identified in the histograms of the various continents. This indicates that the flow direction grids computed for the respective continents do not contain any sinks.

A flow accumulation grid is another basic database component derived from the flow direction grid. Flow accumulation is measure of the number of upstream cells that drain into a given grid cell. Since each cell in a flow direction grid represents an equal area of land, the value of flow accumulation in any cell can be converted to upstream drainage area by multiplying by the area of the cell. If a weight grid containing a spatially distributed variable such as runoff is supplied, performing flow accumulation results in a grid of the total quantity of the variable upstream of each cell, a quantity that can be used for steady state analysis. Figure 3-5 shows the flow accumulation grid of Africa derived in this study. The darker areas in the figure are areas of high flow accumulation.

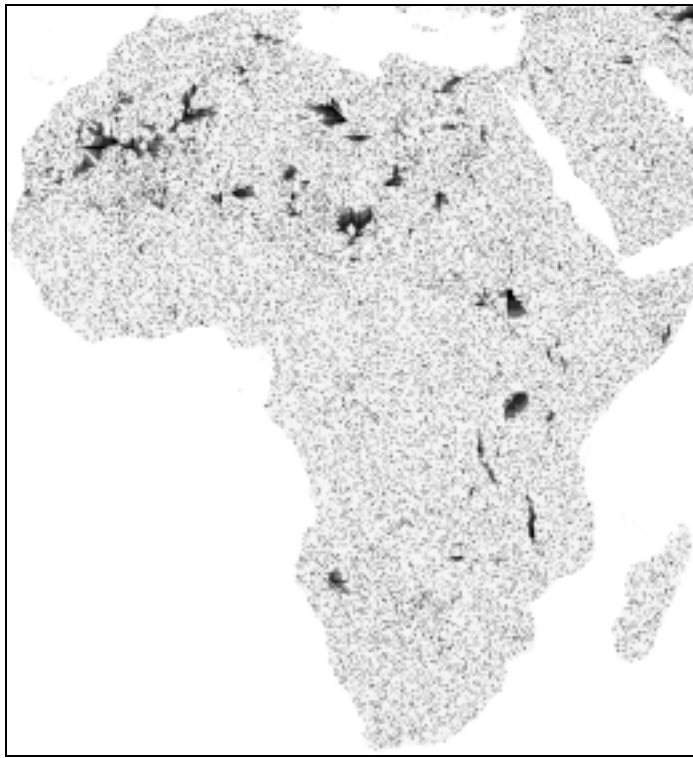


Figure 3-5: Flow Accumulation Grid of Africa

A key determinant of the response of a river basin is the relative distance of various parts of basin from the basin outlet. This distance, often referred to as the flow length, can also be determined from the flow direction grid. Arc Info contains a function for determining flow length from a given cell to its most upstream or downstream cell. The flow length function also includes a weight option which can be used for aggregating quantities along the flow path to or from a given cell. Figure 3-6 shows the flow length grid derived for Africa.

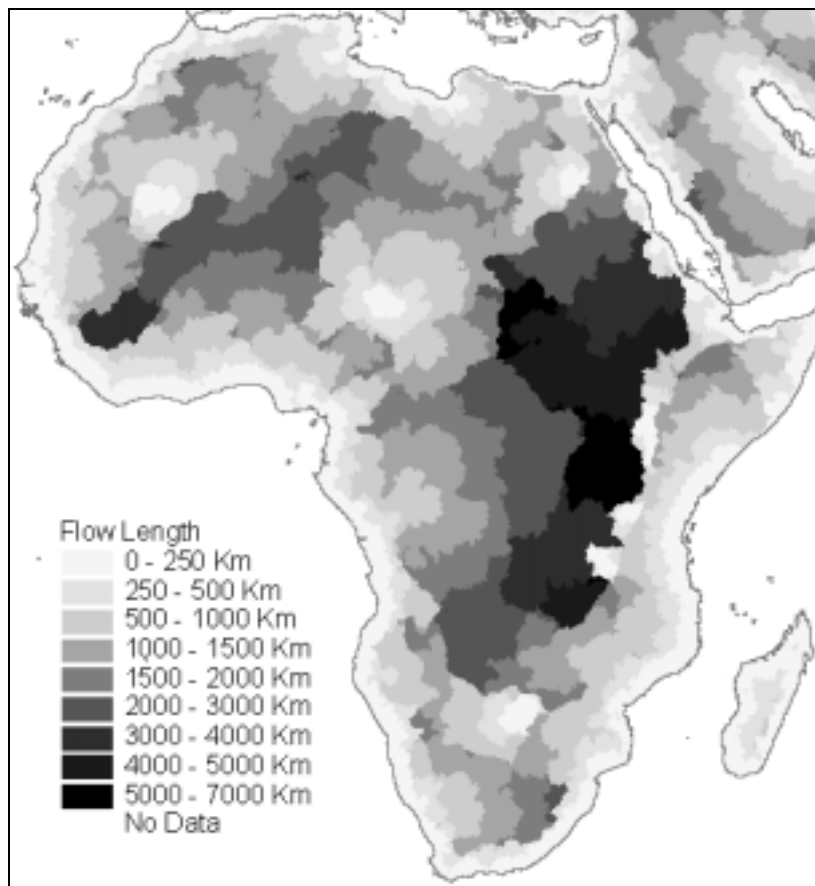


Figure 3-6: Flow Length Grid of Africa

### 3.3 PREPROCESSING FOR THE SOURCE TO SINK MODEL

The development of the database of hydrologic parameters was motivated in part by need to route runoff generated by the land surface component of Global Circulation Models to the ocean cells used in the ocean modeling component. In this section, a preprocessing procedure which allows a surface water routing model to interact with both a soil water balance model and an ocean model is

described. The procedure was applied to each of the earth's continents to justify its label as a continental scale model. The Land Surface Model, LSM (Bonan, 1996) of the Climate Community Model, CCM3 (Kiehl et al, 1998), developed by the National Center for Atmospheric Research was used for runoff generation. The ocean modeling component of CCM3 was not used directly in this study but discharge outlets were defined in a manner consistent with the modeling units used in that component. The goal in this analysis was to demonstrate a procedure for implementing continental scale routing. Hence the parameters and inflows used in this section were not expected to match any observed flows. The routing procedure adopted in the study is described in chapter 4, and a copy of the routine code is included in appendix 3 of this dissertation. Testing of the routing model with various scenarios of routing parameters is described in chapters 5. The procedure defined in this study can be used with other continental scale runoff generation and discharge receiving models after minor adjustments for input data format.

In this application, the source to sink approach (described in section 2.1.3) is preferable to the watershed and cell to cell approaches (described in sections 2.1.1 and 2.1.2 respectively) because of its ability to route flow directly to required locations. Continental scale source to sink models were consequently developed for each continent excluding Antarctica which has no rivers. The processing required to create these models is described in this section. Preprocessing programs developed (by the present author and Francisco Olivera)

in the Arc Macro Language (AML) of the GIS software, Arc Info, are included in Appendix 1 of this dissertation.

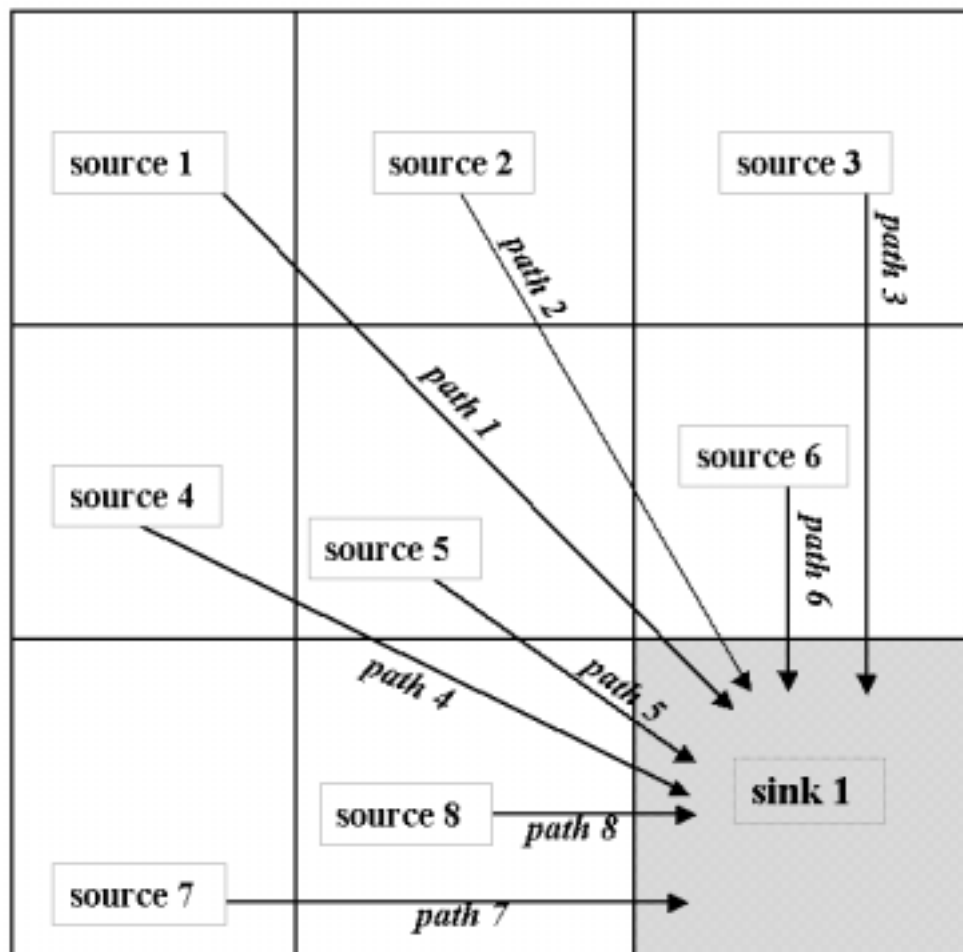


Figure 3-7: Components of a Source-To-Sink Model

The conceptual model for source to sink routing consists of three components namely a source which receives input, a sink which serves as a discharge location and a flow path which links the source to the sink. Figure 3-7 shows a source to sink model consisting of 8 sources linked to a single sink by



flow paths. In this study, sources, sinks and flow paths are defined to allow for easy interaction with the modeling units defined in the respective land surface and ocean modeling components of the CCM3. Each source is linked to a single LSM modeling unit from which it receives input runoff and to a single Ocean model unit to which it discharges its flow. In other words, there must be a one to one relation between sources and sinks and between sources and runoff generating units. The process of establishing these one to one relations is described below.

A line coverage consisting of the continental margin and the outline of inland catchments was first created from filled DEM (described in section 3.2). The coverage was created by identifying all grid cells attached to at least one null value cell, putting them into a separate grid and vectorizing them. A second coverage was created by generating a vector mesh of comparable resolution to the Ocean Model units. For this study, a 3 x 3 degree mesh was used to represent the ocean modeling units. The two coverages were intersected to break up the continental margin into a series of small segments each wholly contained within a single ocean modeling unit. The individual segments were then converted back into raster format using their unique segment numbers as value fields. The grid cells thus created were used as sinks for the division of the land surface into drainage basins. Figure 3-8 shows the sinks defined for the continent of Africa. Each mesh spacing corresponds to an ocean modeling unit. The gray boxes along the continental margin are ocean modeling units which receive their inflow directly from the surface water routing model. The sections of the continental

margin within each receiving unit serve as sinks. Inland catchments are similarly represented by gray boxes located inside the continental margin. All other land surfaces are represented by a light shade of gray.

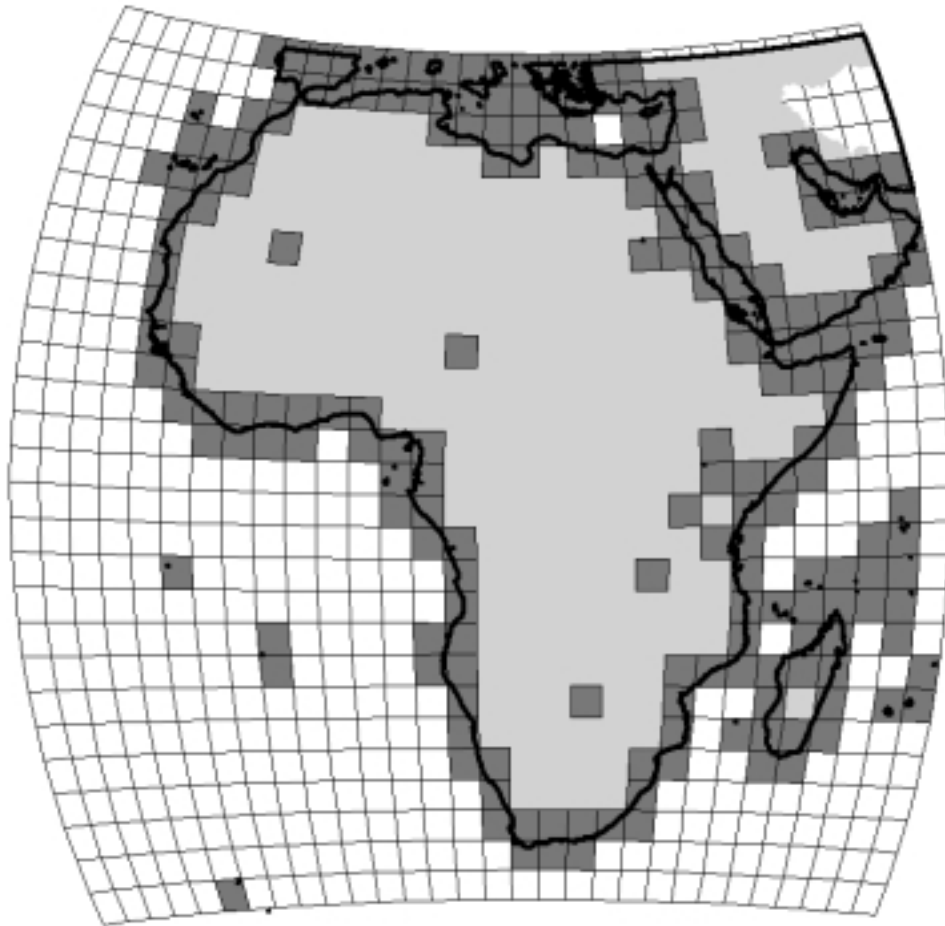


Figure 3-8: Sink Locations for the Continent of Africa

The boundaries of the drainage basins serve to demarcate areas within which sources associated with a particular sink can be defined. In this study, grid

cells identified as sinks were in conjunction with the 1 by 1 kilometer flow direction grids (described in section 3.2) to delineate the drainage basins. The resulting drainage basins delineated for the various continents are shown in Figures 3-9 (a) to (f). Each of the resulting basins bears the id-number of the ocean or inland sink to which its drainage flows. All discharges generated within it can hence be linked to the correct ocean modeling unit. The continental divide between Europe and Asia was established by delineating all basins draining into the inland catchment formed by the Caspian Sea as part of Europe. All basins to the east of this were delineated as part of Asia. This results in the definition of Europe that is much larger than dictated by the political boundaries. It however reduces the computer requirements for modeling the Asian continent which is the world's largest with an area of over 50 million km<sup>2</sup>. This is far more surface area than that of any other continent and would have strained the processing capacity of the computers available for this study. By assigning the Caspian Sea drainage basin to Europe, the model of Asia was reduced to a more manageable size with approximately 38 million grid cells.

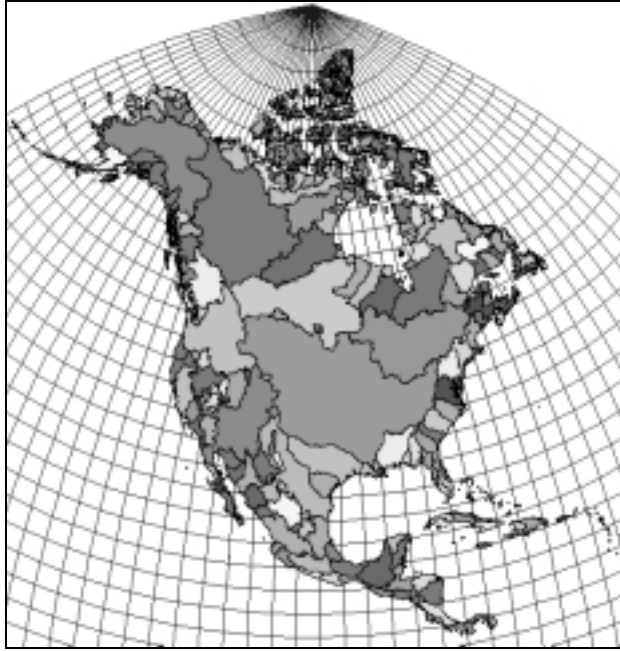


Figure 3-9 (a): Drainage Basins of North America

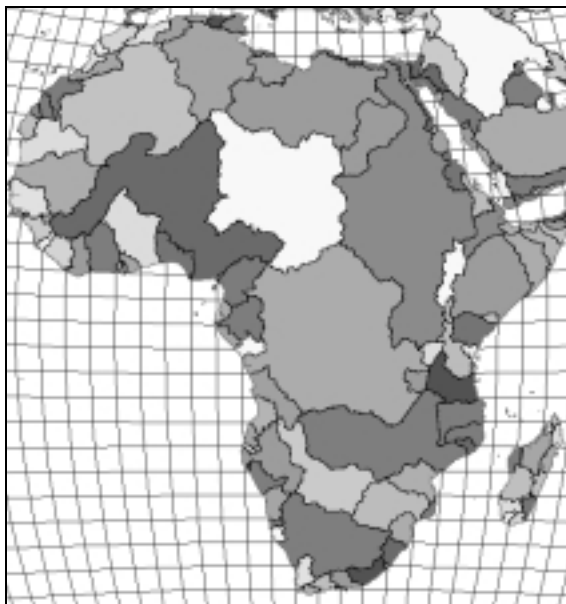


Figure 3-9 (b): Drainage Basins of Africa



Figure 3-9 (c): Drainage Basins of South America

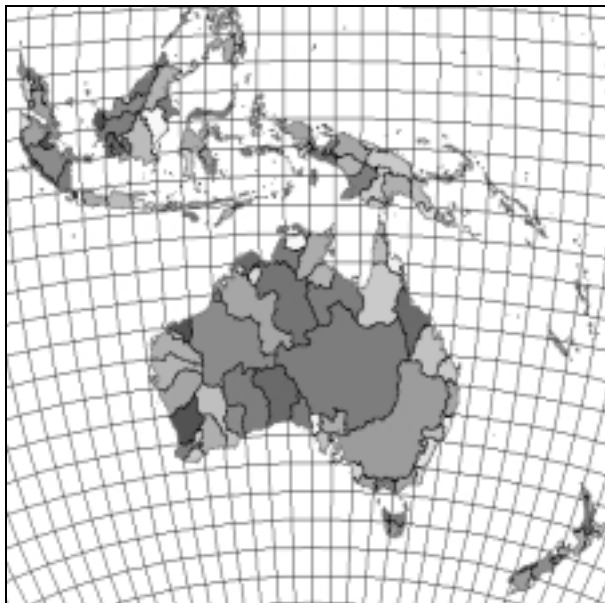


Figure 3-9 (d): Drainage Basins of Australia

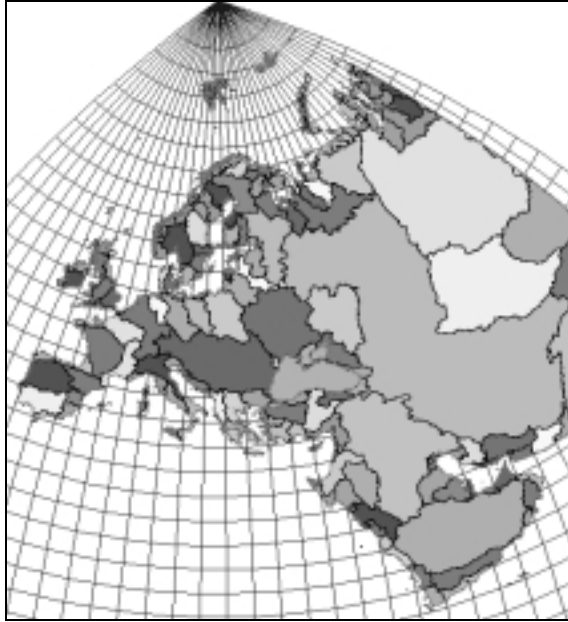


Figure 3-9 (e): Drainage Basins of Europe

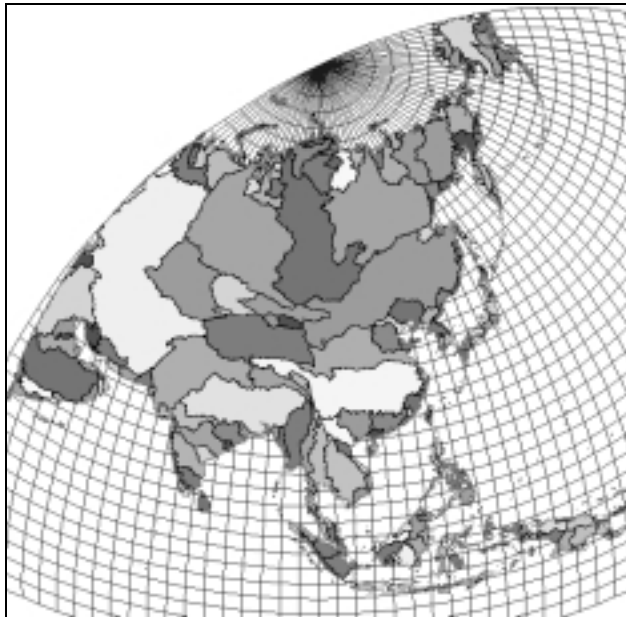


Figure 3-9 (f): Drainage Basins of Asia

With the link between the drainage basins and ocean models established, the next step in preprocessing involves the establishment of a one to one relation between the land surface and the LSM modeling in which runoff is generated. For this purpose, the drainage basins must be divided into smaller areas such that each small area fits exactly into a single LSM modeling unit. Runoff in the LSM can be generated at various resolutions. The runoff used in this particular study was generated on a Gaussian grid with a horizontal resolution of T42 (approximate 2.8 by 2.8 degrees of latitude and longitude). T42 stands for spectral (spherical harmonic basis functions) triangulation 42. It is a mesh defined in geographic coordinates with uniform mesh spacing (in degrees) along the longitudinal direction but slightly non-uniform mesh spacing in the latitudinal direction (Hortal, 1991). The non-uniformity in the latitudinal direction is to account for differences between the spherical or geocentric coordinate system used in atmospheric modeling and the ellipsoidal or geodetic coordinate system used in land surface modeling. Reed and Maidment (1995) describe the differences between the two coordinate systems and outline a procedure for accounting for these differences in hydrologic modeling. The slightly non-uniform T42 mesh translates to a uniform mesh in spherical coordinates thus ensuring a one to one relation between the land surface and atmospheric modeling units. The parameters of the T42 mesh are provided in Appendix 2 of this dissertation. During each routing time step, the LSM generates a single value of runoff in (mm/s) for each

T42 unit. The drainage basin coverage of each continent was intersected with the T42 mesh to create a new polygon coverage. Each polygon in the new coverage is associated with a single LSM modeling unit from which it receives its input runoff and a single ocean model unit to which it discharges its output flow. Figure 3-10 shows the distribution of these polygons on the Africa continent. The intersection of LSM modeling units (represented by a white mesh on the land surface) and the drainage basin boundaries (represented by a thick black line) results in a model with a few sources defined in each drainage basin.

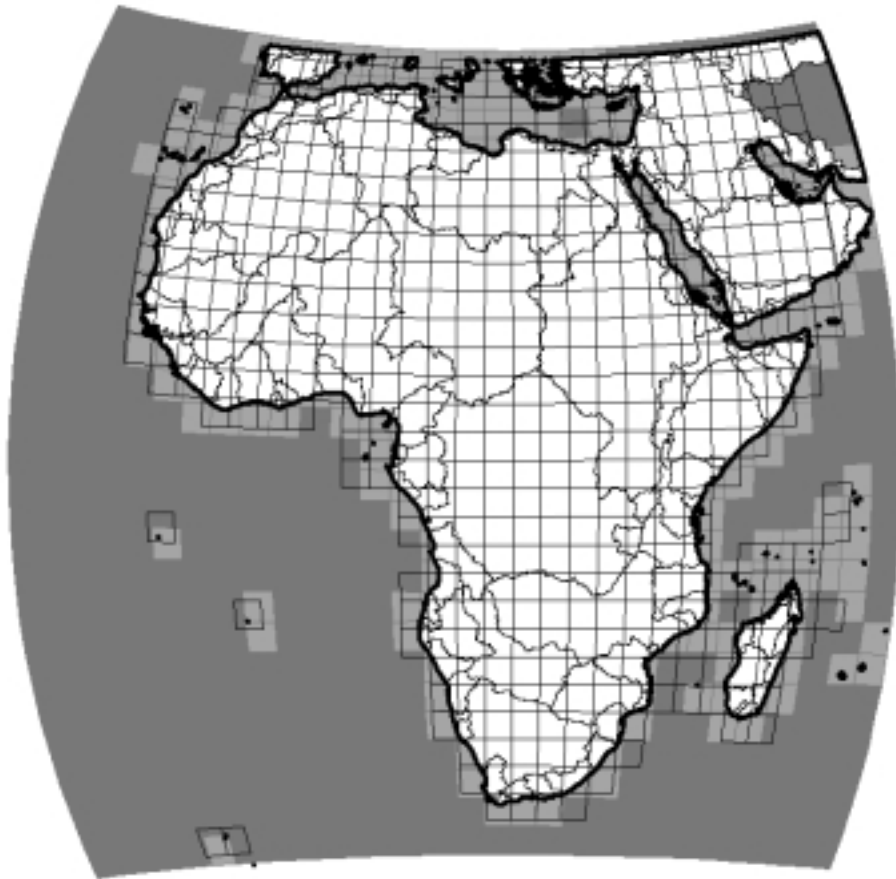


Figure 3-10: Linking Modeling Units for the African Continent



A response function can be defined to describe the transportation of the runoff from each of the sources in Figure 3-10 to its associated ocean cell. Such a response would imply that flows from all areas within each source travel through a single flow path and arrive at the basin outlet at the same time. A single one of these sources covers an area of about 98000 km<sup>2</sup>. This is equivalent to an area roughly 310 km wide and 310 km long. The assumption of a single flow path for the entire polygon is consequently not realistic, and the resulting model would not capture the features of the discharge hydrograph effectively. Smaller source areas are required to allow for better representation of the spatial variability of flow length. A 0.5 by 0.5 degree mesh was intersected with the polygon coverage formed by the intersection of the T42 mesh and the basin coverage to create smaller sources for the source to sink model. The use of a 0.5-degree mesh ensured a maximum source area of approximately 3600 km<sup>2</sup> which corresponds to an area about 60 by 60 km wide at the equator. While this choice of resolution was made in line with the expected resolution of future GCMs, a finer or coarser resolution could just as easily have been selected. The implications of the choice of spatial resolution are explored in section 5.2.2 of this dissertation. The sources defined for each of the continents are shown in Figures 3-11 (a) to (f) below.

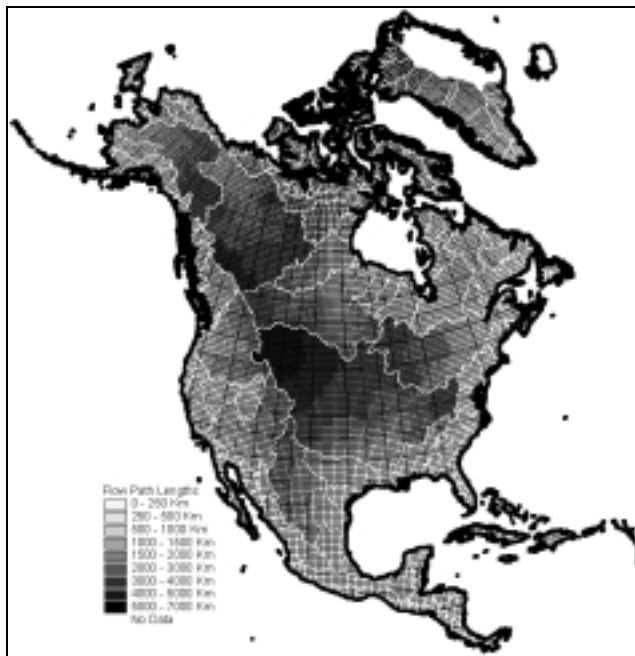


Figure 3-11 (a): Parameterized Sources of North America

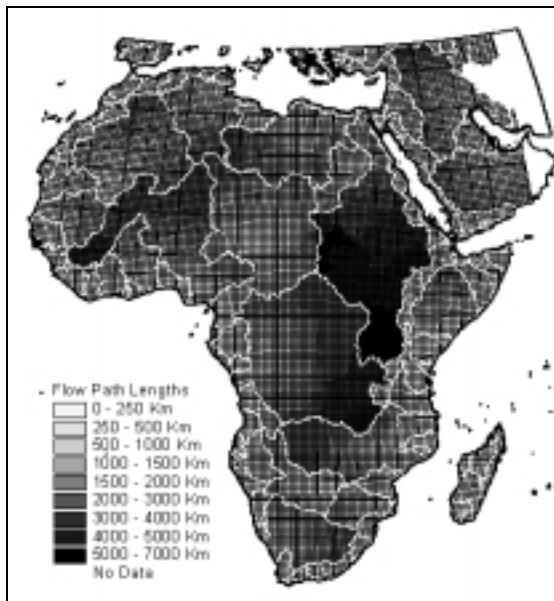


Figure 3-11 (b): Parameterized Sources of Africa

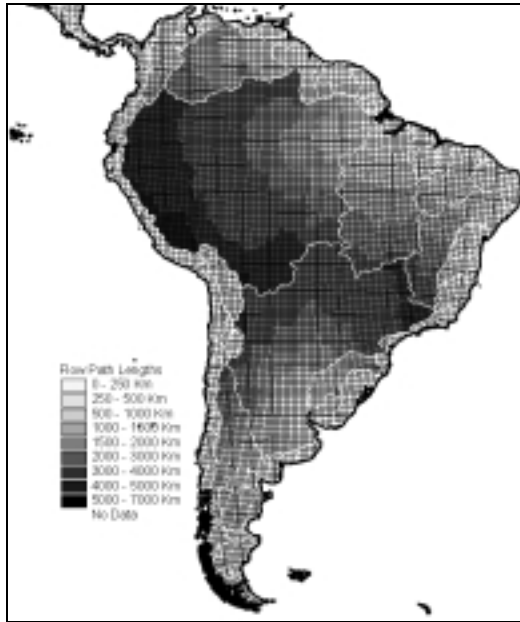


Figure 3-11 (c): Parameterized Sources of South America

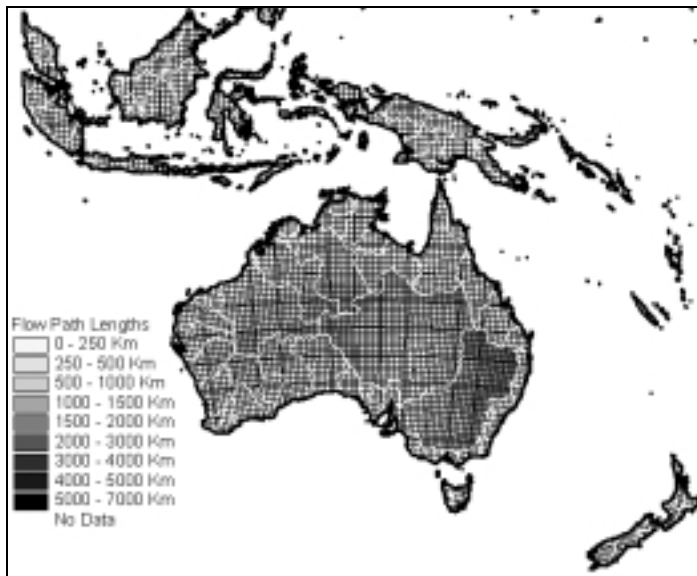


Figure 3-11 (d): Parameterized Sources of Australia

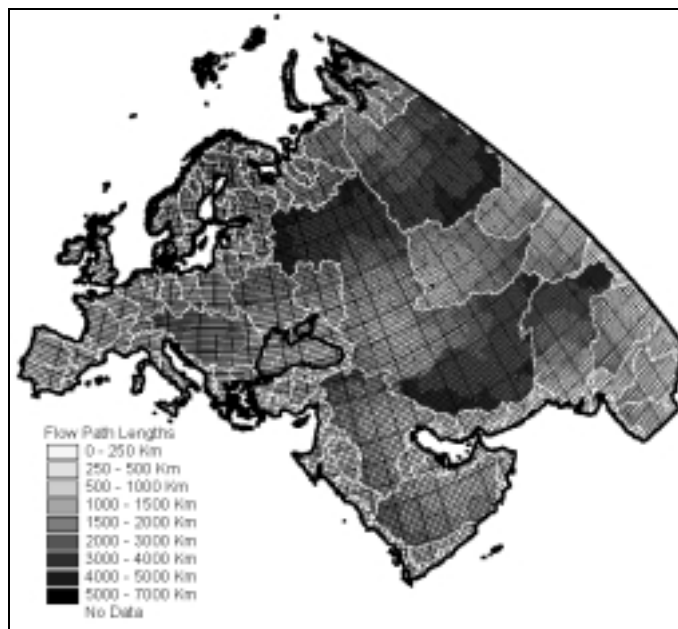


Figure 3-11 (e): Parameterized Sources of Europe

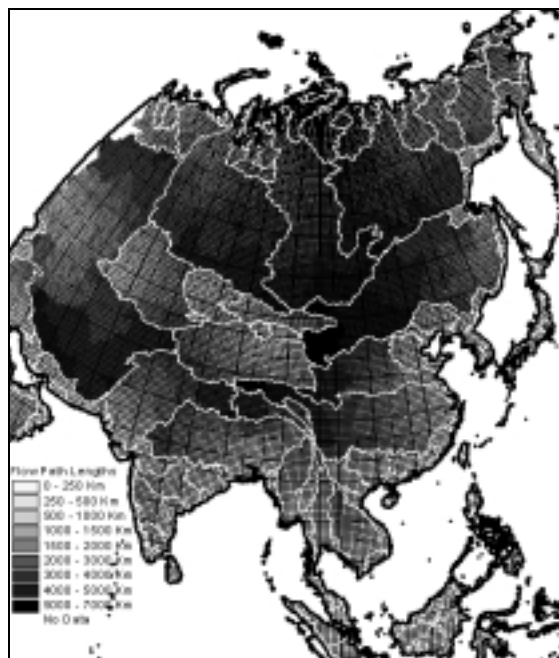


Figure 3-11 (f): Parameterized Sources in Asia

### **3.4 PREPROCESSING FOR THE HYDROLOGIC MODELING SYSTEM**

An important aspect of this research is the validation of the routing process. The typical approach to model validation is to run the model with a set of input runoff values for which there is a corresponding set of observed discharges. The discharges produced by the model can then be compared with the observed values. This approach would not be suitable for validating a routing model which is only concerned with the horizontal transport component of the hydrologic cycle. It would be impossible to determine which errors to attribute to the runoff generation scheme used to produce input data and which to attribute to the routing scheme. A more representative approach would be to compare the discharges from the routing model to those predicted by another routing model given the same input data and corresponding routing parameters. The choice of the second routing model is obviously an important factor in such a comparison since it serves as a baseline. For this study, the Hydrologic Modeling System (HMS) model (Peters, 1998) developed by the Hydrologic Engineering Center of the US Army was selected because of its widespread use and acceptance in the engineering community. The HMS model has the additional advantage that it takes into account spatially distributed parameters which can be derived from the same digital elevation models (DEMs). Since both the HMS and the STS model can be parameterized from the same DEM, a true comparison can be made of their respective routing methods.

As with the STS model, an HMS model of the continental of Africa was developed to justify its label as a continental scale model. The preprocessing required to define hydrologic elements and the element connectivity in HMS is described below. The GIS preprocessor (Olivera and Maidment, 1999) developed at the Center for Research in Water Resources of the University of Texas at Austin, CRWR-Prepro, is used in the delineation. The filled DEM, flow direction and flow accumulation grids described in section 3.2 of this research were used in the delineation. The first objective in the HMS delineation was the definition of all the natural hydrologic elements namely streams, outlets and watersheds. Streams can be derived from DEMs by specifying a minimum drainage area required to constitute a stream. From previous experience working with 30 arc-second DEMs, a threshold area of 1000 km<sup>2</sup> or higher results in a reasonable representation of the river networks. A 10000 km<sup>2</sup> threshold was selected for the continental scale model runs. A finer threshold of 1000 km<sup>2</sup> was however specified for a secondary model of the Congo basin created for more detailed analysis. For the 30 arc-second DEMs, the threshold value also translates to the value of flow accumulation since each cell has an area of 1 km<sup>2</sup>. Hence all cells with flow accumulation values of 10000 or higher were labeled as being stream cells.

The stream cells were then grouped into reaches or links and each link was assigned a unique label to differentiate it from other links. 1791 links were identified in the Congo basin during this delineation. From the definition of flow accumulation, the outlet cell in each link is also the cell with the highest flow

accumulation. CRWR-Prepro contains a function which identifies the outlet cell for each link based on the flow accumulation value of all stream cells. The preprocessor also contains an option which allows the user to specify additional outlets though this option was not exercised in this delineation.

Outlets serve an important role in delineation because they provide convenient starting points for watersheds. By dividing a drainage area into watersheds an HMS modeler can determine over which areas to apply runoff transformation approaches for the overland portion of flow and where to commence in-stream routing approaches such as the Muskingum method. A watershed grid was delineated from the outlet points and flow direction grid, and a vector representation of the entire basin was obtained by converting the respective watershed and stream grids to vector coverages. In vectorizing the streams, a minimum stream length of 710 m was specified to prevent the occurrence of single-cell streams. This value was determined as the approximate length of a single 1 km by 1 km cell with flow through one of its corners. A higher threshold may be specified as long as it is understood that the removal of a given length of stream is justifiable only if routing flow over the specified length does not result in any significant difference between the input and output. The vectorized stream and watershed coverages delineated in Africa at a 10,000 km<sup>2</sup> threshold are shown in Figures 3-12 and 3-13, respectively.



Figure 3-12: Delineated Rivers Coverage of Africa



Figure 3-13: Delineated Watersheds of Africa



The next step in the preprocessing is the calculation of hydrologic parameters. In this step, CRWR-Prepro uses the previously derived flow accumulation grids, as well as flow length grids and other routing parameters to compute the numerical characteristic of each hydrologic element. For watershed runoff transformation, the initial and constant losses were set at zero for all the watersheds, and a single lag time was used to translate flow generated within the watershed to its outlet. The routing interval was specified as one day in line with the frequency of runoff generation, and a flow velocity of 0.3 m/s was used. These specifications imply that when input runoff is applied to the watershed, an initial portion of the input (expressed in mm) is lost through evaporation and infiltration. The remainder of the runoff is transported to the outlet by pure translation with a constant loss rate in mm/hr. The travel time to the outlet is determined as the larger of 0.6 times the lag time along the longest flow path in the watershed and 3.5 days. The lag time along the longest flow path is in turn determined by finding the cell with the longest downstream flow length, calculating the distance from that cell to the outlet and dividing the result by the watershed velocity.

Stream routing parameters were also determined for the Congo river reaches. For this determination, the Muskingum method was specified with a Muskingum  $x$  of 0.3 and an in-stream flow velocity of 0.3 m/s. This specification results in reaches with a lag time greater than the routing interval are routed using the Muskingum method while the rest were routed by pure translation. The Muskingum  $K$  and  $n$  parameters for each element are computed based on the flow

velocity and Muskingum  $x$  provided by the user. A full discussion of the equations and routing methods used in the preprocessing and flow routing processes is given in section 4.2.3. They are only mentioned here to highlight the capabilities of the preprocessor in calculating routing parameters for each model element. The HMS model created of Africa consists of 1551 watersheds, 701 river reaches, 197 sinks and 693 junctions. Figure 3-14 shows the line diagram of hydrologic elements derived for Africa using CRWR-Prepro.



Figure 3-14: Line Diagram of Hydrologic Element Connectivity

The final step in preprocessing involves the writing of a basin file which can be interpreted by HMS. CRWR-Prepro performs this transcription by

converting the parameterized watershed and river network coverages into a line diagram with the connectivity between the elements outlined (Hellweger and Maidment, 1996). It then creates a text file listing each hydrologic element, its attributes and the element to which it is connected at its downstream end. The resulting file was imported into HMS and used to generate a basin model such as the one shown in Figure 3-15 below.



Figure 3-15: HMS Model Representation of Africa

A number of mistakes were encountered when the basin file was first imported into HMS. These mistakes manifested themselves either during the

import stage or when the imported basin model is used to perform a simulation. The type of errors encountered most frequently were those resulting for erroneously created sources, and those resulting from parameters in excess of the permitted range. Erroneous sources arise due to the presence of sliver polygons in the watershed coverage. Sliver polygons are small polygons that are erroneously created when the topology of a coverage is rebuilt. They are often not visible at a glance but they are identified by CRWR-Prepro as sources because they appear to be small closed polygons which are not attached to an outlet. The presence of such sliver polygons is easy to detect when HMS is run because they result in sources with no associated inflow. These sources can be removed by deleting them from the basin file along with the reaches that link them to the next downstream element, usually a junction.

The problem of parameters falling outside their permissible range was also encountered when the HMS basin file was used for flow routing. HMS has a specified maximum Muskingum K value of 150 hours. An error message is generated when HMS encounters a reach with a K value in excess of this value during routing. To correct this error, such reaches were each subdivided into 2 or more equal reaches. The total lag time of the original reach was subdivided among the new reaches, and new values of Muskingum n were also computed for each new reach. Network connectivity was restored by linking the new reaches sequentially to each other and connecting the first and last reaches in the sequence to the original upstream and downstream elements, respectively. To preserve the labeling structure used in the original delineation, new reaches were labeled by

introducing an additional digital after the last digit of the id-number of the old reach. These changes were made by manually editing the basin file.

The creation and parameterization of a HMS model of Africa served to illustrate that a continental scale watershed based routing model could be created and parameterized based on available DEM data. Having previously created a continental scale source to sink model based on the same DEM data, two independent and yet consistent representations of the land surface were obtained. Key features of basin responses computed from the two models can thus be compared. The methods used for computing hydrographs in the respective models are described in chapter 4, and in chapter 5, various simulations are performed to determine the effect of various modeling parameters on the basin responses.

## CHAPTER 4

### Methodology

#### 4.1 THE SOURCE TO SINK MODELING APPROACH

A framework for implementing the source to sink model at the continental scale is described in this section. The assumptions made in the development of the framework, the model components and the routing methodology are described along with methods of estimating routing parameters. In these discussions, the concept of a hydrologic system is adopted to explain the functioning of the framework. A similar description is presented of the watershed based modeling system, HMS, in section 4.2 of this chapter.

##### 4.1.1 STS Model Assumptions

A hydrologic system can be classified by the nature of its transformation as linear or non-linear. The system is said to be linear if the transformation meets the criteria for the application of superpositioning otherwise it is non-linear. Dooge (1973, pp.18) gave the mathematical interpretation of linearity as follows:

*“If a transformation  $X_1(t)$  results in  $Y_1(t)$  and  $X_2(t)$  results in  $Y_2(t)$  then for a linear system,  $X_1(t) + X_2(t)$  results in  $Y_1(t) + Y_2(t)$ ”*

An assumption of linearity is made in the Source to Sink routing model. In other words, a decomposition of the inputs at the source into a series of smaller segments results in an identical output at the sink as would result from a routing the lumped input. Olivera (1996) outlines three major features that characterize linear hydrologic systems. These include longitudinal decomposability which allows rivers to be split into smaller segments and modeled separately, areal decomposability which allows basins to be subdivided and modeled as a series of separate watersheds, and superpositioning of subarea responses which allows the results of simulations in different watersheds to be aggregated

Dooge (1973) presents a rather complete review of linear systems theory and its application in hydrology. In this review, he demonstrates that the assumption of linearity results in some distinct advantages in hydrologic modeling. A linear transformation allows the differential equations describing a hydrologic process to be reduced to a set of algebraic equations which can be solved by serial substitution. The reduction may be achieved using numerical approximations or mathematical transformations. The assumption of a linear system also allows for the modeling of processes that have not been described with mathematical equations. If, for a set of system inputs, a corresponding set of outputs is available, then the mathematical transformation can be derived. The inputs and outputs can be broken down into a series of segments of equal duration. The system transformation can be identified by matrix operations or optimization techniques as the transformation that maps the inputs onto the outputs. This type of transformation identification is only possible if all elements

of a system are linear. The introduction into a river network of a controlled reservoir, for example, would render the whole network non-linear, making the application of linear systems invalid.

The assumption of linearity has been widely used in hydrology and it underlies many routing methods such as the unit hydrograph, the Muskingum method and the linear solutions of the St. Venant equations. However, not all routing methods used in hydrology assume linearity. The form of the dynamic wave equation used in overland flow routing for example is non-linear. Also, the use of a storage function in which storage is a function of inflow or outflow raised to a power other than one results in a non-linear system. Hence linearity must be a stated assumption if superpositioning is to be applied in the source-to-sink routing method.

The second important assumption made in the source-to-sink approach is that transformation parameters relating system input to output are time invariant. In other words, a given system input would result in the same output irrespective of the time of application of the input. For a source to sink model, this implies that the physical location of the flow path linking a source to a sink does not vary with time. In addition, the parameters at each location along that flow path remain constant throughout the routing period. According to Dooze (1973, pp.18), time invariance can be expressed mathematically as follows:

*“If a transformation  $X(t)$  results in  $Y(t)$  then  
for a time invariant system,  $X(t+r)$  results in  $Y(t+r)$   
where  $t$  and  $t+r$  are points in time”*



This assumption is essential to the definition of a system transformation or instantaneous unit hydrograph which can be applied for subsequent events. If a system transformation changes with time then the outputs due to two events occurring within a few minutes of each other cannot be superimposed because they undergo different transformations. Hydrologic systems rely on the time invariance of parameters to predict the output of future events. If a system transformation is time variant then no relationships can be deduced from past events, and consequently, no predictions can be made for the output of future events based on what happened in the past. Implicit and explicit methods used to solve the full St. Venant equations are examples of time variant solutions.

#### **4.1.2 STS Model Components**

In source-to-sink modeling, a river basin is viewed as a series of sources each defined and parameterized not in relation to neighboring cells but in relation to an observation point or sink located further downstream. Sources interact with sinks through a response function. The model is not fully spatially distributed in the sense that the location of water is not tracked throughout the system. Rather, water is provided as input at the source and only measured as it flows into the sink. The flow path linking each source to its sink serves to trace the control volume within which flow is routed. If the location of a sink changes, a new response function must be defined for each source since the definition of the flow path is also altered. Figure 4-1 provides an illustration of the major components

defined for the STS model implemented for routing Land Surface Model (LSM) runoff to the continental margin in this study.

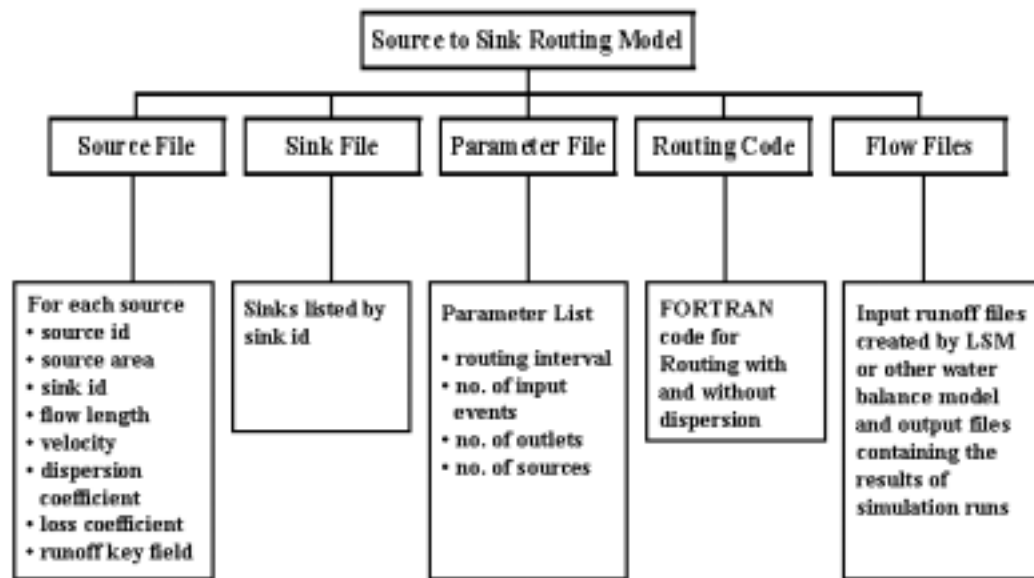


Figure 4-1: Diagram of STS Model Components

The source file contains a listing of all the sources within a study area along with characteristics of their associated flow paths. The parameters listed for each source include a unique identification number (source-id), its area (source area), the identification number of its associated sink (sink-id), the length of flow path from source to sink (flow length), the effective velocity of flow from source to sink (velocity), the effective dispersion coefficient along the flow path (dispersion coefficient), the effective first order loss coefficient along the flow path (loss coefficient) and a key field linking each source to a unique modeling unit in the runoff generation model (runoff key field). The sink file contains a

listing of the all the sinks within the study area by the same sink-id used in the source file. The sinks listed may include both inland catchments and river basin outlets located at the continental margin. The parameter file contains simulation specific information including the routing interval (in seconds), the number of input events, the number of sinks and the number of sources. The routing code for the STS model was developed in the FORTRAN programming language. Separate versions of the routing code are maintained for pure translation and dispersed model runs. The details of the routing process are described in section 4.1.3. The flow files consist of the input runoff files (Branstetter and Famiglietti, 1998) generated by the Land Surface Model (LSM) and the output files containing routed flows generated by the routing code. The LSM runoff is reported for each T42 cell in millimeters per second. A single runoff file is generated during each routing interval. In this study, the runoff files were named in terms of the routing interval during which they were generated so that “h0001.txt”, for example, is the runoff file generated in the first routing interval. For computing basin response, a single runoff file with a uniform runoff input was provided. The output files generated by the routing code in this study include a file containing the routed flow time series (in cubic meters per second) for each sink, a file containing the total input runoff (in cubic meters) for each drainage basin for each time period, and a file containing the response function along the flow path (in terms of fraction of inflow) for each source. The actual routing procedure is described in section 4.1.3 followed by methods of deriving routing parameters in sections 4.1.4.

#### 4.1.3 STS Routing Methodology

Routing is performed in a space first, time second order. Hence given a set of spatially distributed inputs, the Fortran program routes each input for all the sources before going to the next input. The results of routing individual input sets are superimposed at the sinks. The values of discharge at the outlet are not correct until all the sets of inputs have been routed. Input runoff for each routing time step is generated as an ASCII file. The link between records in the file and sources in the basin file of the source to sink model is established through a key field that is transferred from the T42 mesh to the source polygon coverage when the two are intersected during preprocessing as described section 3.3 of this dissertation. For this study, the key field was created from the X and Y coordinate indices (listed in Appendix 2 of this dissertation) using equation <number below>. The origin of coordinate indices (1,1) is defined at the southwestern corner of the T42 mesh at (0°, -87.864°) in geographic coordinates.

Equation 4-1                       $K = 1000Y + (129 - X)$

where K is the value of the key field

Y is the Y coordinate index with values ranging from 1 to 64

X is the X coordinate index with values ranging from 1 to 128

Flow in the STS model is routed directly from a source to its associated sink along a flow path. A response function is defined for each flow path which

describes the shape of the hydrograph at the sink given an instantaneous input at the source. The response function includes a measure of the travel time, storage effects and losses due to evaporation and infiltration along the flow path. No additional flow is allowed to enter the flow path between the source and the sink since a separate source is defined for each geographic location. Even though, in reality, flows from the various sources may pass through the same channel, flows from each source can be treated as separate entities because of the assumption of linearity. Travel time is computed by dividing the downstream flow length by the translational velocity. The term translational velocity is synonymous with wave celerity and is used to differentiate it from flow velocity at a given cross section. If different velocity zones exist, their combined effect along the flow path can be determined by expressing velocity in terms of flow time through each segment and adding up to get the total flow time for the entire reach. Velocities along a flow path cannot be averaged since velocity is a vector quantity without accounting for length and direction of the velocity vector. On the other hand, flow time is a scalar quantity and can be summed up irrespective of direction. Olivera and Maidment (1996, 1999) define a GIS based approach for performing the summation of flow time in a spatially distributed field using a weighted flow length scheme. For a flow path composed of  $n$  segments or grid cells, the total flow time through the flow path is given by

Equation 4-2 
$$t = \sum_{i=1}^n \frac{l_i}{v_i}$$

where  $l_i$  is the length of each flow path segment or grid cell  
 $v_i$  is the flow velocity through the segment or grid cell  
 If a weight grid of  $1/v_i$  is supplied, the weighted flow length function results in a spatially distributed grid of flow time from each cell to the outlet.

Storage effects that describe the deformation of an input pulse as it travels downstream along a channel must similarly be taken into account. The storage effect has been attributed to the shear forces between the sides of the channel and the moving water (Fischer et al, 1979). These forces result in a velocity profile across the stream section such that particles closest to the sides of the channel are transported at a much lower velocity than those closer to the center of the stream. The result is that input water is spread out longitudinally along the river channel as it travels downstream. Additional spreading out results from the damping effect of irregular channel cross sections (Henderson, 1966). Such irregularities result in the storage of water along the banks thus delaying the arrival of some portions of the input at the downstream location. Several approaches for dealing with storage are documented in the literature. Conceptual models such as the linear reservoir and the cascade of linear reservoirs (described in the section 2.2 of this dissertation) have been used for this purpose. Linear reservoir models describe the storage effects between two interconnected elements. In the source-to-sink method, the sink is remote from and usually unconnected to the source. Hence a linear reservoir cannot be applied directly. The Lag and Route method uses pure translation to account for advection to a remote outlet followed by a linear reservoir or cascade of linear reservoirs

(Maidment, 1993, pp.26.10) to account for storage effects. Both the cascade of linear reservoirs and the lag and route methods are classified as advection methods with approximate dispersion parameters as discussed in section 2.2.2 of this dissertation. While these approaches may yield reliable results in large scale routing (Dooze, 1973, pp.257), there is only an approximate physical basis for their use. Methods that derive directly from the St. Venant equations are preferable because they incorporate a full description of the dispersion process.

Maintaining the assumption of linearity and time invariance made earlier, the momentum equation

$$\text{Equation 4-3} \quad \frac{\partial V}{\partial t} + V \frac{\partial V}{\partial x} + g \left( \frac{\partial h}{\partial x} + S_f \right) = 0$$

can be reduced to

$$\text{Equation 4-4} \quad \frac{\partial h}{\partial x} + S_f = 0$$

by assuming a constant velocity.

$$\text{Equation 4-5} \quad \frac{\partial V}{\partial t} = \frac{\partial V}{\partial x} = 0$$

The impulse response function resulting from this simplification was shown by Hayami in 1951 (Montes, 1998) to take the following form

$$\text{Equation 4-6} \quad h(x,t) = \left( \frac{x}{\sqrt{4PDt^3}} \right) \exp \left[ - \left( \frac{(Vt - x)^2}{4Dt} \right) \right]$$

where

$D$  is the dispersion coefficient in  $\text{m}^2/\text{s}$

$V$  is the flow translational velocity in  $\text{m/s}$

$x$  is the distance from the source in meters

$t$  is the time after input in seconds

$P$  is the numerical constant  $\pi = 3.14159$

This equation is referred to as the passage times distribution. It can be convolved with the input runoff at a source to generate flow at the sink. The flow resulting from numerous sources can be superimposed at an associated sink such that for any time,  $t$ , the total discharge,  $Q$ , at the sink is given by

Equation 4-7 
$$Q = \sum_{i=1}^n I_i * h_i(x, t)$$

where  $n$  is the number of sources associated with the sink

$I_i$  is the input runoff in modeling unit  $i$  at time  $t$

$h(x, t)$  is the response of element  $i$  at the sink and

$*$  is the convolution integral

Assuming a first order decay process for translational losses, an additional term can be introduced into the exponent of the response function (Maidment, ed., 1993 , pp.14.18) such that



Equation 4-8

$$h(x,t) = \left( \frac{x}{\sqrt{4PDt^3}} \right) \exp \left[ - \left( \frac{(Vt-x)^2}{4Dt} \right) - Kt \right]$$

where  $K$  is a positive, first order decay constant with units of  $(\text{second})^{-1}$

The exponential term in the first passage time distribution ensures that the response asymptotically approaches zero without ever touching it. This results in a long time series the latter terms of which are close to but greater than zero. The small terms cannot be ignored because they would result in a mass balance problem which may become significant for long term modeling applications. In order to apply the first passage times distribution in a mass conservative manner, it must be applied over a limited range of time steps with normalized coefficients of the impulse response functions which sum up to one for unit input. Fischer et al (1979) suggests that for simulations involving the first passage times distribution, the significant width of the dispersed cloud can be assumed to be 4 standard deviations. The width of the impulse response function,  $W$ , is consequently given by Equation 4-9 below.

Equation 4-9

$$W = \sqrt{32Dt}$$

where  $D$  is the dispersion coefficient in  $\text{m}^2/\text{s}$

$t$  is the time after input in seconds

In this application, the width of the response function is used to estimate the number of time intervals over which an input is distributed when it arrives at

the outlet. By ensuring that the total area under the response over this width is equal to 1, the first passage times distribution is applied in a mass conservative fashion without taking into account the endless tail that results from the exponential function asymptotically approaching zero.

The assumption of a constant velocity,  $V$ , and dispersion coefficient,  $D$ , used to simplify the momentum equation does not limit the utility of the model in areas where  $D$  and  $V$  are not constant. Olivera (1996, 1999) demonstrates the use of the flow length function in estimating a single dispersion parameter in place of a spatially distributed field of coefficients. In his approach, the dispersion coefficient in the first passage times distribution is replaced with the flow path Peclet number such that the response function becomes:

$$\text{Equation 4-10} \quad u_i(t) = \frac{1}{2t \sqrt{P (t/t_i) / \Pi_i}} \exp \left\{ -\frac{[1 - (t/t_i)]^2}{4 (t/t_i) / \Pi_i} \right\}$$

where  $u_j(t)$  is the response at the outlet of flow path  $i$

$t_i$  is total flow time along flow path  $i$

$P$  is the numerical constant  $\pi = 3.14159$

$\Pi_i$  is the Peclet number along flow path  $i$  with  $j$  segments and is computed as follows:

$$\text{Equation 4-11} \quad \Pi_i = \frac{\left[ \sum_j \left( \frac{1}{v_j} \right) x_j \right]^2}{\sum_j \left( \frac{D_j}{v_j^3} \right) x_j}$$

The use of the Peclet number however introduces another parameter whose magnitude does not lend itself to direct interpretation. From McCuen (1998), the total variance along a flow path can be determined as the sum of variance along the component segments. This property derives from the fact that variance is a scalar quantity. For a given flow path,  $i$ , made up  $n$  segments ( $j = 1$  to  $n$ ), the net variance is given by Equation 4-12.

$$\text{Equation 4-12} \quad \text{variance}_i = 2 \sum_{j=1}^n \left( \frac{D_j}{v_j^3} \right) L_j$$

In this study, a single value of the respective diffusion coefficients and flow velocities are computed for each flow path based on the scalar nature of the parameters. The value of single flow velocity that results in the same travel time as the non-uniform segment velocity along a given flow path  $i$  is computed from Equation 4-13 as follows:

$$\text{Equation 4-13} \quad v_i = L_i / \sum_{j=1}^n \left( \frac{L_j}{v_j} \right)$$

where  $L_i$  is the length of the single reach

This is in effect a division of the flow path length by the total flow time. Similarly, a single value of dispersion coefficient which results in the same flow path variance can be computed for each flow path from Equation 4-14.

$$\text{Equation 4-14} \quad D_i = \sum_{j=1}^n \left( \frac{D_j}{v_j^3} \right) L_j / \left( \frac{L_i}{v_i^3} \right)$$

Computing the flow path parameters in this way allows the first passage times distribution to be used in its original form thus eliminating the need to introduce another parameter such as the Peclet number.

#### **4.1.4 Estimating STS Routing Parameters**

In addition to the distance of the source from the sink, the three main parameters that must be estimated for a source to sink model are the diffusion coefficient,  $D$ , the flow velocity,  $V$ , and the loss coefficient,  $K$ . The physical meaning of these parameters is described in this section. This is followed by a description of the method adopted for estimating the three parameters from observed flow data.

The dispersion coefficient is a measure of the amount of stretching that an input undergoes. In many applications in water quality modeling, the dispersion coefficient is derived from channel properties (Fischer, 1967). The dispersion coefficient used in the derivation of the diffusion wave method is a compound  $D$  which incorporates the effects of both off-stream storage and spreading due to friction between flowing water and channel surface, as shown in Equation 4-15.

Equation 4-15       $D = D_F + D_W$

where  $D$  is the compound dispersion coefficient in  $\text{m}^2/\text{s}$

$D_F$  is the dispersion coefficient due to friction in  $\text{m}^2/\text{s}$

$D_W$  is the dispersion coefficient due to off-stream storage in  $\text{m}^2/\text{s}$

This compound dispersion coefficient cannot therefore be derived from channel section properties measured at a specific location as this would exclude the cumulative effect of off-stream storage (Henderson, 1969). It must therefore be derived from flow measurements. Dispersion coefficients compiled by Fischer et al (1979) and Seo and Cheong (1998) may be used as first estimates. Empirical functions such as Equation 4-16 suggested by Fischer (1967) for computing longitudinal dispersion in natural streams may also be used as a first estimate if river cross section data is available.

Equation 4-16 
$$D_F = \frac{0.01V^2w^2}{d\sqrt{gRS}}$$

where  $D_F$  is the dispersion coefficient due to friction in  $\text{m}^2/\text{s}$

$V$  is the average stream velocity in  $\text{m/s}$

$w$  is the width of the stream in  $\text{m}$

$d$  is the gravitational acceleration in  $\text{m/s}^2$

$R$  is the average depth of the stream in  $\text{m}$

$g$  is the hydraulic radius in  $\text{m}$

$S$  is the friction slope expressed as a decimal

However, these equations require the use of a hydraulic radius which in turn requires the modeler to make an assumption about the quantity of flow. Also, they only take into account the dispersion due to friction.

The diffusion wave method describes the propagation of a flood wave downstream. The flow translation velocity used in the method is thus a measure of wave celerity not in-stream flow velocity at a location. It is a measure of how

quickly a flood wave is propagated through the flow channel. The wave celerity for a wide rectangular channel is 1.5 or 1.667 times as high as in-stream flow velocity depending on whether one adopts Chezy's equation (Henderson, 1969) or Manning's equation (Chow et al, 1988) as a starting point. As with the diffusion coefficient, flow translation velocity cannot be determined from equations which include hydraulic radius as these require an assumption about the quantity of flow. Approaches involving the replacement of the hydraulic radius with a steady parameter such as drainage area (Maidment et al, 1996) hold promise. However, in the opinion of this author, there is insufficient verification of the approach with velocity data to justify their use globally. Empirical functions proposed by Leopold (1953) and Carlston (1969) have been used to determine flow velocity (Vörösmarty et al, 1989). However, these equations were intended to define the variation of flow velocity with river stage at a given location. Their utility in characterizing flow velocity over a general domain is thus brought into question. A method of deriving velocity from observed flow measurements is proposed later on in this section.

As water flows through the landscape, it incurs losses in the form of seepage into the ground and evaporation into the subsurface. As shown in section 4.1.3, a first order loss function can be included in the first passage times distribution. The first order loss coefficient,  $K$ , can be expressed either in terms of fraction lost per unit of travel time or fraction lost per unit of travel distance. The former is sensitive to changes in flow velocity while the latter is not. It is consequently more convenient to adopt the fraction lost per unit of travel distance

approach when performing calibrations since a mass balance performed at the beginning of the calibration remains valid at the end of the run irrespective of changes in velocity. The exponential function associated with first order losses determines the fraction of input flow that makes it through the flow path to the sink. The presence of side flow and spring flow in natural flow systems makes it difficult to define a physical basis for the computation of the loss coefficient. It must be determined from observed flow data.

After reviewing several calibration approaches, the method of moments (Dooge, 1973, pp.254) was adopted. The method is based on the premise that if the application of a given transformation to one time series yields another then the difference between scalar moments of the two time series is equal to the moment of the transformation. The first moment of a flow time series taken about the origin is a scalar quantity, and it corresponds to the flow time. The second moment taken about the mean is a measure of variance, and dispersion coefficient can be calculated from the variance using Equation 4-12. Consequently, given two flow time series from gauging stations located a given distance apart on the same river reach, the flow velocity and dispersion coefficient of the first passage times distribution linking them can be determined from Equations 4-11 and 4-12. Whenever possible two gauge stations with no major tributaries between them are selected. The method can be applied when tributaries are present though the values of the parameters thus obtained are less reliable.

The loss coefficient is used to achieve a mass balance. When time series from two gauging stations are used, the value of the loss coefficient is not a

meaningful quantity. The presence of side flow from adjacent sources and recharge due to springflow in natural systems ensures that losses incurred along the flow path cannot be attributed to the usual mechanisms of evaporation and infiltration. When a soil water balance model is used in conjunction with a routing model, the loss coefficient can be viewed as a calibration factor whose value can be determined analytically from mass balance considerations.

The main advantage of using the method of moments is that it can only yield one correct solution for a given pair of time series. Optimization routines may yield alternative solutions for the same set of data. The value of the resulting parameters may also depend on the type of objective function used to arrive at a solution. In addition, the convolution integral often results in highly non-linear relationships for which conventional non-linear optimization routines such as the Generalized Reduced Gradient (GRG2) algorithm (Lasdon and Waren, 1978) used in the Excel Solver are unsuitable.

The accuracy of parameters determined by this approach is heavily dependent on the temporal resolution of the flow data. There is currently no public domain database of daily flow time series available for global applications. Monthly flows produced by Vörösmarty et al (1996) are the most complete global time series of runoff data available for this study. The effect of inaccuracies arising from using monthly time series may be minimized by using a long time series and by obtaining parameters from as many different pairs of stations as are available for each river basin.



The key conceptual limitation of this method lies in the assumption that peak discharge at the downstream gauging station is associated with the arrival of flow from the upstream gauging station. The assumption may not hold in basins where there is very high rainfall in the drainage area between the two stations. Peak discharge at the downstream discharge station could occur independent of the arrival of flow from the upstream station. Wherever possible two stations with similar quantities of flow are selected. This ensures that the contribution of any additional flow entering the reach between the two stations can only augment or shift slightly the time of occurrence of peak flow at the downstream station. This method of calibrating flow parameters is especially useful because it lends itself to large-scale implementation on a river network.

In conclusion, velocity dispersion coefficient and loss coefficients for the source to sink model must be derived from flow data. Methods for deriving these values have been suggested in this section. The watershed based approach of HMS is similarly discussed in section 4.2 below.

## **4.2 THE HYDROLOGIC MODELING SYSTEM APPROACH**

The modeling approach used by HMS differs from the source-to-sink approach in that the river basin is viewed as a series of hydrologic elements linked to each other in series. HMS performs routing by passing flow from one element to the next until it gets to a terminal point. Any local flow generated within each element is added to flow entering it from upstream elements, and the total flow is passed on to the next downstream element. The assumptions underlying an HMS

model, its component modules and methods as well as a calibration procedure are described in this section.

#### **4.2.1 HMS Model Assumptions**

The assumptions of linearity and time invariance discussed in section 4.1.1 are also made in an HMS model using the Soil Conservation Service method for watershed transformation and the Muskingum method for in-stream routing. These assumptions allow an HMS model to deal with temporal variations within each hydrologic element before moving to the next downstream element. Flows from all upstream elements can subsequently be superimposed in the downstream element. For a non-linear system, the response in each element is a function of the flow.

Another important assumption is made about the sequential nature of the connection between hydrologic elements. Subbasins are assumed to be connected to river reaches via junctions. (The term subbasin is used instead of watershed in HMS and is maintained in discussions about HMS in this dissertation). The sequential connectivity assumption implies that there is no side flow into a routing reach. In reality, river reaches as a whole act as drainage outlets for the subbasin associated with them. Water from the subbasin can enter the river network at any point within the subbasin. The definition of a subbasin connected to the river reach at the subbasin outlet is therefore a simplification of the real life system. The river basin cannot be divided into separate overland and in-stream flow components without allowing for side flow in the river reaches. However, it is a

simplification that allows the river basin to be modeled in a vector (as opposed to a raster) environment. The definition of a subbasin in which flow from each location enters the river network at a particular point in along the reach requires a fully distributed channel routing model. Such a model is computationally intensive and difficult to implement in a vector environment. The partially distributed approach of HMS allows parameters within hydrologic elements to be lumped while defining different responses and parameters for each subbasin and river reach.

#### 4.2.2 HMS Model Components

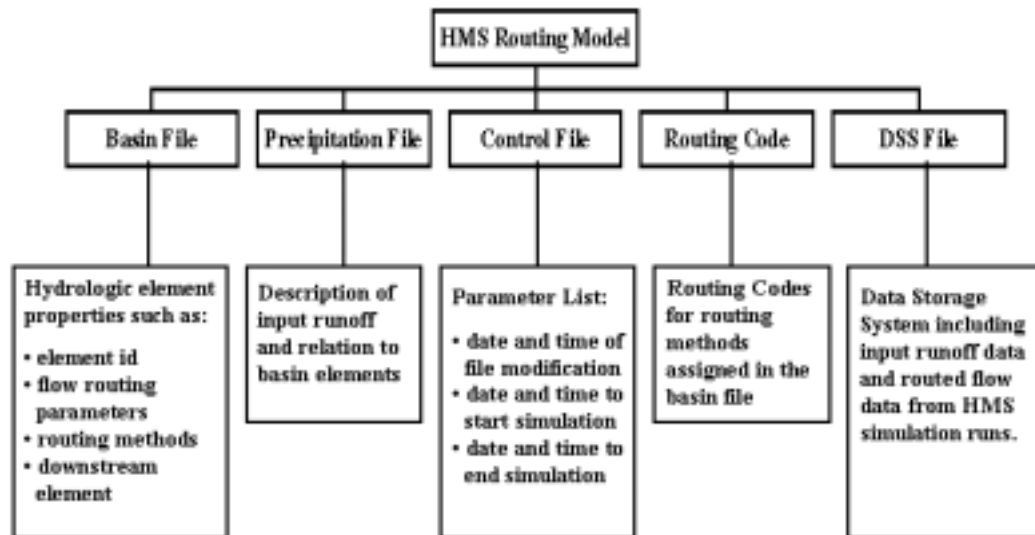


Figure 4-2: Diagram of HMS Model Components

As shown in Figure 4-2, a typical HMS model is made up of three components; a basin model, a precipitation model and a control specification model. The basin model contains information describing the hydrologic elements

in the basin being modeled. It contains a list of the routing parameters and element connectivity as well as the methods for computing losses, transforming runoff and routing flow in each element. The classes of hydrologic elements include subbasins, river reaches, junctions, diversions, reservoirs, sources and sinks. Figure 4-3 shows the symbols used to represent these hydrologic elements in HMS.



Figure 4-3: Elements of an HMS Basin Model

CRWR-Prepro, a preprocessor developed at the Center for Research in Water Resources of the University of Texas at Austin, allows the element connectivity to be derived from Digital Elevation Models (DEMs). This GIS based preprocessing results in the creation of a basin file which can be interpreted by HMS. The preprocessing procedure is described in section 3.4 of this dissertation.

A portion of the precipitation falling on a subbasin is lost through infiltration and evaporation. Methods of computing these losses in HMS include the Soil Conservation Service curve number method, an initial plus constant loss approach, and the Green and Ampt infiltration method. After accounting for these losses, the remaining excess precipitation is transformed to the subbasin outlet where it enters the stream system. HMS allows the user to specify one of several

runoff transformations for each subbasin. These include the Clark unit hydrograph, Snyder's synthetic unit hydrograph and the Soil Conservation Service transformation method. When the runoff enters a river reach, it is routed to the next downstream element using a user defined routing method. The routing options available in HMS include the Muskingum method, the Modified Puls, the Kinematic Wave and the Muskingum-Cunge method. Junctions in HMS serve as control points where flow from multiple reaches or subbasins are aggregated before being passed on to the next downstream element. Sinks on the other hand serve as terminal points where flow is aggregated without being released. The presence of control structures in real river systems is allowed for by the inclusion of diversion points and reservoirs in the HMS basin description. Storage dependent diversions and releases can be specified for the respective diversion and reservoir components. The information contained in the basin model does not vary with the quantity of flow.

The precipitation model on the other hand contains all information describing time varying inputs. In this model, the quantity of precipitation occurring during each time interval is specified. There are several options for providing precipitation data. These include precipitation gages with or without gage weights, gridded precipitation or spatially averaged precipitation with a single value provided for each subbasin. The model also contains standard precipitation events typical of certain geographical areas. However, these data are only available for the United States, east of the Rocky Mountains. Discharge time series for flow gauging stations are also stored in the precipitation module.

The control specification model is used to specify simulation start and end times, and routing intervals. The control model plays an important role in HMS modeling because in addition to defining simulation parameters it serves to tie the routing process to reality. Actual dates and times are used in reporting simulation results allowing for easy interpretation of flow data. The reference framework for these dates is set in the control model. Routing intervals that can be specified in an HMS model include 1, 2, 3, 4, 5, 6, 10, 15, 20 and 30 minutes as well as 1, 2, 3, 4, 6, 8, 12 and 24 hours. No other routing interval can be specified in HMS though flow routed at one of these intervals can subsequently be resampled to another routing interval.

For each HMS simulation, the user is allowed to specify one of each of the component basin, precipitation and control modules. The routing methods used for the simulations in this study are described in section 4.2.3 below.

#### **4.2.3 HMS Routing Methodology**

The routing methods defined for HMS subbasins and river reaches in this study are described in this section along with the justification for their selection. The range of methods available for this study was limited not by the methods available in HMS but rather by the methods available in the preprocessor used in the study. The benefits of using a method not available in the preprocessor would be easily outweighed by the tedious nature of the task of piecing together and parameterizing a hydrologic network of a large basin by hand.

The HMS preprocessor, CRWR-Prepro, currently allows the user to select one of two methods for determining subbasin losses, namely the Initial plus Constant loss approach, and the Soil Conservation Service curve number approach. The Initial plus Constant loss approach was selected for this study because it relies on currently available data while the curve number approach does not. There is currently no global database of curve numbers, and the development of such a database would be beyond the scope of this research. The initial and constant losses can also be set to zero when input runoff is supplied from a soil water balance model, allowing runoff to be transported to the subbasin outlet without losses.

Runoff generated in a subbasin is limped together and routed to the basin outlet using the Soil Conservation Service unit hydrograph method. In this method, the distribution of flow at the subbasin outlet is computed by stretching the SCS curvilinear hydrograph to fit the dimensions of the input. The parameters of the curvilinear hydrograph are stored as a table of values. However, the SCS triangular hydrograph, shown in Figure 4-4 (reproduced from Chow et al, 1988, pp.229), is often used to illustrate its shape. This is because the triangular hydrograph results in the same distribution of area under the rising and falling limbs as the curvilinear hydrograph. The lag time in each subbasin is computed as the larger of 0.6 times the length of the longest flow path divided by the flow path velocity and 3.5 times the routing interval. The lag time thus computed is equated to the time to peak,  $t_p$ , in the figure while the routing interval is equated to the duration of excess rainfall,  $t_r$ . The other parameters, time to peak,  $t_p$ , peak

discharge,  $q_p$ , and duration direct runoff duration,  $t_b$ , can be determined from the other two parameters.

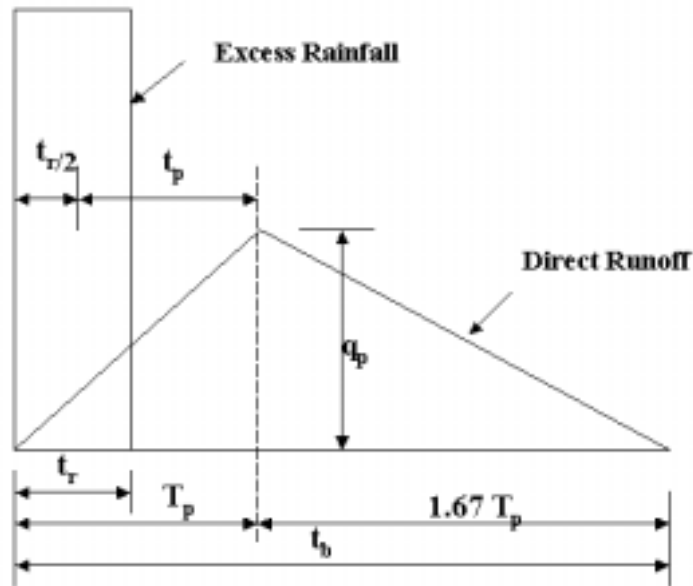


Figure 4-4: Soil Conservation Service Triangular Hydrograph

The preprocessor allows the user to select either the Muskingum or the Lag routing method for in-stream routing. In the Lag method, flow is transported through the river reach by pure translation using a lag time computed by dividing the length of the reach by flow velocity. Muskingum method was selected because of its ability to include a dispersion process in its routing of flow. In HMS, each river reach is subdivided into multiple sub-reaches, and the Muskingum method is applied in sequentially to each sub-reach. The subdivision of a routing reach into sub-reaches ensures that numerical stability considerations are satisfied. If the routing reaches become too long, the magnitude of the error due the approximate numerical integration used in the Muskingum method



becomes significant compared to the magnitude of the flows. On the other hand, if the reaches are too short the routing process tends towards pure translation, and the effect of flow redistribution due to the Muskingum method becomes insignificant. The number of routing sub-reaches,  $n$ , defined for each river reach in CRWR-Prepro is given by Equation 4-17 (Olivera and Maidment, 1999).

$$\text{Equation 4-17} \quad n = \text{int}\left(2x \frac{L_s / V_s}{\Delta t}\right) + 1$$

where  $x$  is the Muskingum  $x$  coefficient

$L_s$  is the length of the reach

$V_s$  is the flow velocity in the reach

$\Delta t$  is the routing interval

The discharge from each characteristic reach is computed using the Muskingum storage function and the continuity equation. The method of coefficients is employed by HMS for this routing as shown in Equation 4-18 to 4-21 below (Maidment, 1993, pp.10.7).

$$\text{Equation 4-18} \quad Q_{j+1} = C_1 I_{j+1} + C_2 I_j + C_3 Q_j$$

$$\text{Equation 4-19} \quad C_1 = \frac{\Delta t - 2Kx}{2K(1-x) + \Delta t}$$

$$\text{Equation 4-20} \quad C_2 = \frac{\Delta t + 2Kx}{2K(1-x) + \Delta t}$$

Equation 4-21 
$$C_3 = \frac{2K(1-x) - \Delta t}{2K(1-x) + \Delta t}$$

where  $I$  is the inflow into the reach

$Q$  is the discharge from the reach

$K$  is the Muskingum  $K$  often interpreted as lag time

$x$  is the Muskingum  $x$  coefficient which controls dispersion

$\Delta t$  is the routing interval

Dooge (1973) points out that solving the Muskingum equation using the method of coefficients is equivalent to applying the response function given in Equation 4-22 below.

Equation 4-22 
$$u(t) = \frac{1}{K(1-x)^2} \exp\left[-\frac{t}{K(1-x)}\right] - \frac{x}{1-x} \delta(t)$$

where  $\delta(t)$  is the Kronecker delta function which assumes a value of 1 at  $t$  equal to zero and a value of zero elsewhere

The parameters that must be supplied by the user include the routing interval, river reach and watershed lengths, flow velocities, and Muskingum  $x$  for river reaches. The choice of routing interval takes into account the temporal resolution of the input runoff and the desired resolution of the output flows. The implication of the choice of interval is discussed in section 5.3.4. The lengths of the routing reaches and watershed are automatically computed from flow length grids by the preprocessor, CRWR-Prepro. Muskingum  $K$  is equated to travel time and is computed by dividing the river reach length by the flow velocity supplied

by the user. The derivation of the user defined flow velocity and Muskingum  $x$  parameters is discussed in section 4.2.4.

In summary, the choice of routing methods in this study was dictated by the availability of data and by the limitations of the HMS preprocessor used. The methods selected required two DEM based parameters (river and watershed flow length) and two additional parameters (flow velocity and Muskingum  $x$ ). Flow losses were not taken into account in this study.

#### **4.2.4 Estimating HMS Routing Parameters**

Dooge (1973, pp.254) proposes a procedure for determining the Muskingum  $x$  parameter based on channel characteristics for uniform channels. The method requires the specification of channel slope, Froude number and a reference discharge which allows the hydraulic radius to be calculated. The approach cannot be used in this study since models requiring an assumption about the quantity of flow were similarly rejected for the STS method in section 4.1.4. The method of moments, applied in the source to sink modeling application, could not be adopted for HMS because of difficulties in determining a single response function for the multiple subreach Muskingum routing method applied in HMS. The method of moments proposed by Dooge (1973, pp.254) corresponds to the single reach case and is not applicable in HMS.

In this study, the Muskingum equation was employed to route the flow observed at an upstream station to a downstream gauging station while using HMS's optimization routine to calibrate the parameters in the reaches in-between.

The optimization routine adjusts the routing parameters until a match is found between the routed and observed flows at the downstream station. A spreadsheet solution similar to this optimization computation is difficult to implement because of the multiple routing subreaches involved. The Muskingum equation impulse response function Equation 4-19 above is for the single routing reach case. From the nature of the equation, it is easy to see that the equation is not linearly decomposable. The presence of the conditional second term ensures that convolving the function with itself will result in at least three terms, and hence multiple convolutions will result in an equation that is not similar in form to the original equation. The impulse response function for the multiple reach routing case is not available in the literature. Consequently, the multiple reach case would have to be solved by manually reconvolving the output of preceding subreaches. An optimization run with multiple reaches quickly becomes too complex to implement in a spreadsheet.

HMS has an inbuilt calibration program in which the values of specified parameters can be calibrated from observed rainfall and corresponding stream flow measurements. In this program, the user can specify the initial values of the parameters, whether a parameter is to be changed or held constant during a particular run, constraints on the values of parameters, the nature of the objective function and the search method to be employed during an optimization run. In addition, the program has inbuilt constraints (listed in Appendix 4 of this dissertation) which limit the range of values a parameter can assume. The user specified parameter constraints are ignored if they fall outside those imposed by

HMS. The method of parameter calibration proposed in the HMS documentation (Peters, 1998) combines the rainfall-runoff transformation process with the routing process in determining the routing parameters. It is therefore not ideal for independent calibration of the routing process.

For independent calibration of in-stream routing parameters, the optimization routine in HMS could be used to calibrate flow between two stations in a manner similar to that described for the Source to Sink model in section 4.1.4. The procedure adopted in this study was to create a separate model using the river reaches located between the two stations. A source with an associated flow gauge was inserted at the upstream station while a sink with an associated flow gauge was inserted at the downstream end. Observed flows at the respective upstream and downstream stations are introduced into the model by editing the gauge data from the edit menu in the project definition window of HMS. An optimization is then run to calibrate first the Muskingum K parameter and then the Muskingum x.

## **CHAPTER 5**

### **Model Applications**

#### **5.1 THE APPLICATION BASINS**

As outlined in section 1.2 of this dissertation, the testing of the source to sink and watershed based routing models under various modeling scenarios is an important aspect of this study. Two drainage basins were selected for this testing based on the three criteria described below. The first criterion was that the basin had to be large enough to justify the application of a continental scale routing model. Effects, such as the spatial variability of parameters, are relatively insignificant in small basins, but take on much more significance in large basins because of their capacity to influence flow. The selection of large basins ensures that such effects can be taken into account. Secondly, the application basins had to have a variety of topographic and climatic regions. Such variety is necessary if the models are to be applied globally. The availability of runoff data for model calibration was the third criterion for selection. The Congo and Nile basins were selected because they fulfilled these requirements and because of their location in Africa, a continent of special interest to the author. The basins are described in sections 5.1.1 and 5.1.2. This is followed in sections 5.2 and 5.3 by a discussion of the results of model runs for the respective STS and HMS models. In section 5.4, STS and HMS routed flows are compared with observed flows in the Nile basin.

### 5.1.1 The Congo Basin

Along with the Nile, the Niger and the Zambesi, the Congo is one of the four major basins of Africa as shown in Figure 5-1.



Figure 5-1: The Four Major Basins of Africa

The Congo basin is located on the Equator in Central Africa and has a drainage basin which extends through 7 countries including the Democratic Republic of Congo, the Republic of Congo, the Central African Republic, Cameroon, Tanzania, Angola and Zambia. From its sources in the East African lakes of Tanganyika, Mweru and Bangweulu, it flows predominantly north for the first half of its course. Near the Congolese city of Kisangani, the river makes a 90-

degree turn and heads westward towards its mouth at the Atlantic Ocean. Figure 5-2 shows a map of the Congo with its main tributaries, Sangha, Kasai, Ubangi and Lualaba highlighted.



Figure 5-2: Area Map of the Congo Basin

The mean annual rainfall in the basin is about 1600 mm, and the mean annual runoff is about 370 mm. With a basin surface area of over 3.8 million square kilometers, this results in a mean annual discharge of approximately 45000 m<sup>3</sup>/s at its mouth in the Atlantic Ocean. The Congo ranks second only to the



Amazon in the quantity of discharge at the mouth. The high rainfall in the region allows flow in the basin to be simulated without having to deal with the problems of runoff generation in arid basins which are best dealt with in soil water balance models.

Its location in the equatorial belt ensures that different parts of the Congo basin receive substantial rainfall throughout the year. The northern and central portions of the basin have two major rainfall seasons which begin in March and October each year (Kazadi, 1996). In the south, the two rainfall seasons gradually merge into a single season beginning in December and lasting for six months each year. These rainfall peaks are associated with the passage of the Inter-Tropical Convergence Zone (ITCZ). This is a large zone of low pressure caused by excessive heating from an overhead sun. During the northern summer, the midday sun is directly overhead in the tropical regions of the Northern Hemisphere. This results in higher temperatures and consequently, lower air pressures at the surface. Moist air flows from the oceans towards these low pressure areas. The moisture is released as rainfall on the land surface when the air is forced to rise on entering the convergence zone or by orographic effects. The ITCZ causes heavy rainfall in the areas it passes over as it moves north and south between the tropics during the respective northern and southern summers. The Congo basin is thus representative of a large river basin in which the spatial distribution of input varies significantly with time.

### 5.1.2 The Nile Basin

Located in the northeastern part of Africa, the Nile basin is another of Africa's large river basins. Figure 5-3 shows the Nile basin with its major tributaries and gage locations highlighted.

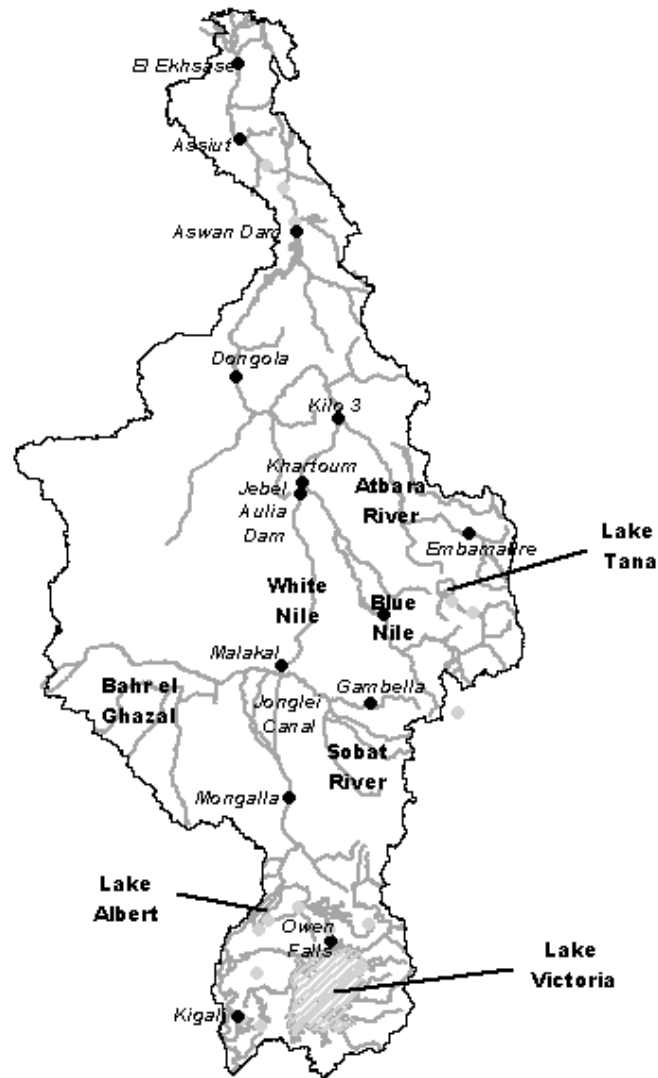


Figure 5-3: Major Tributaries and Flow Gages of the Nile Basin

Its two longest tributaries have their sources in Lake Albert and the Luvironza River in the East African Highlands. The Albert Nile and Victoria Nile as the two tributaries are called emerge together from Lake Albert to form the White Nile which subsequently flows northward through northern Uganda and the Sudan. Near the Sudanese capital of Khartoum, the White Nile is joined by another major tributary, the Blue Nile, which rises out of Lake Tana in the Ethiopian Highlands. The merged Nile then flows northward through Egypt to its mouth at the Mediterranean Sea. From its most distant source to its mouth, the Nile flows a distance of 6680 kilometers, making it the world's longest river. Its drainage basin extends through 8 countries and covers an area of 3.25 million km (Revenga et al, 1998).

Rainfall in the basin varies from 1200 mm per year in the Highland Lake region to almost zero in the desert region near its mouth (Hurst and Phillips, 1938). This rainfall distribution provides a unique setting in which to study the behavior of water as it flows over long distances without significant input from the watersheds closest to its mouth. In addition, there is a wide variety of topography which influences the flow of water in the Nile basin. The Blue Nile basin is characterized by steep slopes on the order of 1m per km between Lake Tana and Khartoum. In the Sudd marshes in southern Sudan, the White Nile flows through a very flat region with slopes on the order of 0.01 m per km or less (Hurst and Phillips, 1938). Flow velocities in these marshes are an order of magnitude lower than in the rest of the basin, and the river loses about half of its flow on its way through the marshes. The East African Highlands are also characterized by

lakes and marshes though the influence of these on stream flow is not as pronounced as those of the Sudd. The Nile is thus representative of a large river basin with several zones of significantly different topography and hydrology.

## **5.2 SOURCE TO SINK MODEL RUNS**

In section 3.3, the development of a global STS model was described. Drainage basins were delineated from stretches of coastline in that description. In the watershed based modeling approaches of HMS, drainage basins are delineated from a single 1 km cell. The boundaries of drainage basins in the two approaches are thus inconsistent and their results cannot be compared. To allow for intercomparison of model results, the drainage basin boundaries used in the STS and HMS models must coincide exactly. The subbasins from the HMS delineation were merged together to form a single drainage basin. Sources for the STS model were defined by intersecting the merged basin with a 0.5 by 0.5 degree mesh. Average travel distance from each of source to the basin outlet was determined as the mean of all flow length grid cells underlying each source. The resulting STS model consists of 1378 sources with flow parameters determined from the same DEM as the HMS model. Figure 5-4 below shows the sources defined in the Congo Basin model used for the model intercomparison runs. The darker areas represent areas of increasing flow length.

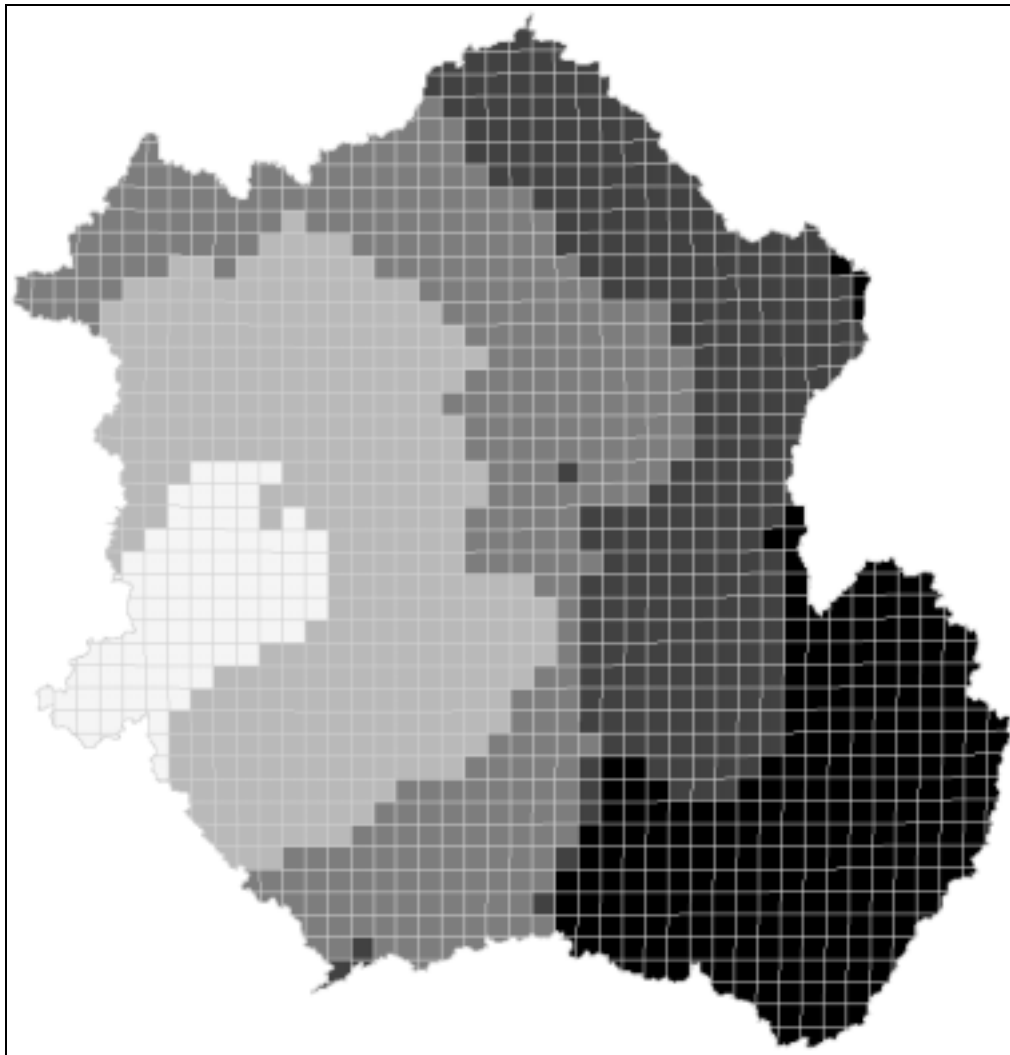


Figure 5-4: Source to Sink Model of the Congo Basin

### 5.2.1 Longitudinal Decomposability of the STS Model

In developing models of hydrologic systems, methods and conceptual models which yield the same value irrespective of the size of the modeling unit selected are more reliable. The control volume in a source to sink model is the flow path. Hence it is important to affirm that a source will yield the same

response at its sink irrespective of the number of subreaches into which its path is divided. Olivera (1996) identifies the property of flow paths or other control volumes to yield the same response irrespective of the number of constituent segments as longitudinal decomposability. Given the longitudinal decomposability of the first passage times distribution (Olivera, 1996), a source to sink model using this equation is expected to be longitudinally decomposable along the flow path from the source to the sink. A set of runs conducted to verify this property is described in this section.

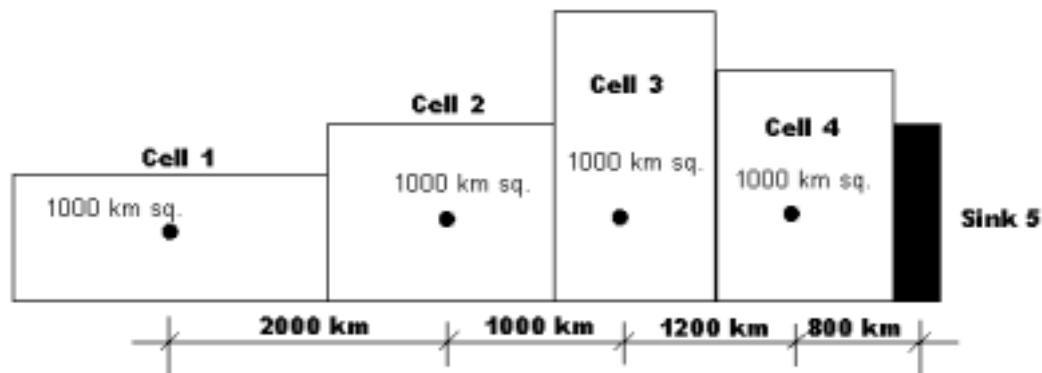


Figure 5-5: Setup for Evaluating Longitudinal Decomposability

The simplest approach to testing the longitudinal decomposability of a flow path is to divide it into a number of subreaches and determine if the resulting flow path response to an impulse is the same as that of the single reach. In a river basin, flows routed directly from the point of runoff generation to a sink could be compared with flows routed sequentially through intermediate flow elements. A source to sink model was setup with a set of four rectangular cells, each with a surface area of 1000 km<sup>2</sup>. As shown in Figure 5-5, the distance between the centroids of adjacent cells varied from 2000 km between cell 1 and 2, to 1000 km

and 1200 km between cells 2 and 3 and cells 3 and 4, respectively. From cell 4, the most downstream, to the outlet, sink 5, a further distance of 800 kilometers was allowed such that cells 1, 2 and 3 are 5000, 3000 and 2000 kilometers away from sink 5, respectively. An instantaneous impulse of 1 millimeter of water was applied simultaneously to all four cells and routed to the sink by two different approaches. In the first approach, source to sink routing, flow is routed directly from the respective cells to the sink. In the second approach, cell to cell routing, the input is routed from each cell to the next downstream cell until it arrives at the sink. The diffusion wave equation is used to route flow in both cases. A flow velocity of 0.3 m/s and a dispersion coefficient of 1500 m<sup>2</sup>/s are assumed throughout the setup. Figure 5-6 below illustrates the difference between the two routing approaches.

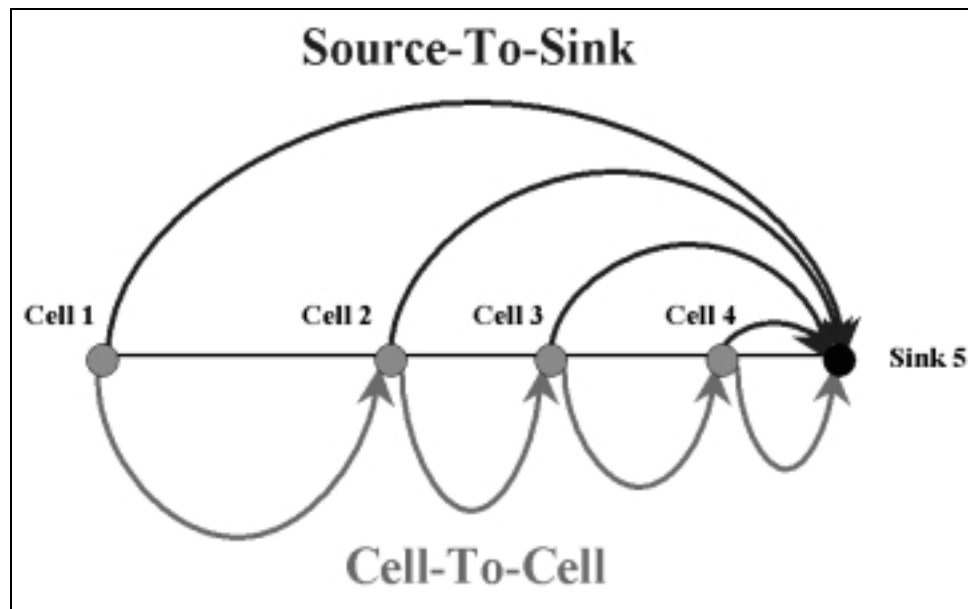


Figure 5-6: Source to Sink versus Cell to Cell Routing

The discharge arriving at the sink from the approaches are shown in the Figure 5-7 below. The discharge hydrographs indicate that for the setup used in this run, the difference between the runs is negligible. The cell to cell model results in a slightly longer tail but the magnitude of this difference is very small compared to the long distance over which flow was routed.

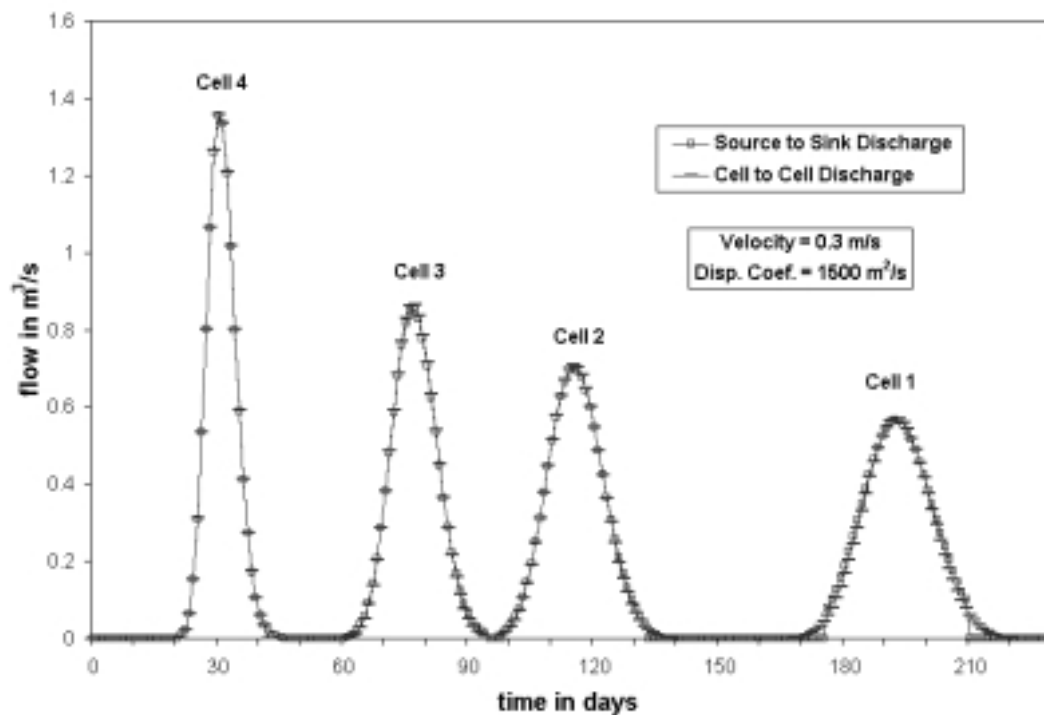


Figure 5-7: Comparison of Diffusion Type STS and CTC Discharge

The first moment of the source to sink model response is approximately 0.36 hours higher than that of the cell to cell model. A comparison of the second moments of the respective responses indicates that the cell to cell model does in fact exhibit more dispersion with a 0.24% increase in second moment. The



magnitude of this difference is very small and could be ignored given uncertainties in the routing parameters.

### **5.2.2 Effect of Spatial Resolution of the STS Model**

Another set of runs were setup to study the effect of spatial resolution on model outputs. In this set of runs, the effect of additional modeling detail achieved through the definition of additional sources on the basin response is examined. A suitable modeling spatial resolution can be defined, for a given modeling time step, by determining the spatial resolution below which no significant change occurs in the basin response. In other words, the task is to determine the coarsest spatial resolution at which a basin can be represented with a STS model without significantly distorting the basin response. If the modeling resolution used is finer than required, the model will generate the same result but at a higher cost of computer resources and processing time. A coarser resolution model on the other hand would begin to exhibit some of the properties of scale dependence present in other models.

The Congo basin was modeled with sources defined at different resolutions. The resolutions used include half a degree, 10 arc-minutes and 5 arc-minutes. At each of these resolutions, the flow length from each source to its corresponding sink was calculated as the mean value of the cells in the underlying 30-arcsecond flow length grid. The total drainage area as well as velocity and dispersion coefficient were kept constant for each of the runs. Figure 5-8 shows the sources defined in the Congo basin at each of the three resolutions.



Figure 5-8: Congo Basin STS Models at 30, 10 and 5 arcminute Resolutions

In response to this question, the STS model was run with the terrain being subdivided into different resolutions. The resolutions used include 30, 10 and 5 minutes. The results of this simulation (shown in Figures 5-9 (a) and (b)) indicated that much of the noise seen in the STS hydrograph is due to the coarseness of the spatial discretization. A relatively smooth curve can be obtained by using a finer discretization of the drainage area. The improved smoothness is however to be differentiated from the change in dispersion characteristics observed with cell to cell models. The definition of finer resolution sources results in less deviation of a given flow value from preceding and subsequent values. It does not however result in changes in the degree of spreading out experienced by inflow as would be the case if the dispersion characteristics of the model were altered. The overall effect of going from a 30 arc-minute to a 10 arc-minute resolution (Figure 5-9 (a)) is much more pronounced than that resulting from the change from a 10 arc-minute to a 5 arc-minute resolution (Figure 5-9 (b)). This implies that as the resolution of sources becomes finer, the basin response becomes better defined though its dispersion characteristics remain unchanged.

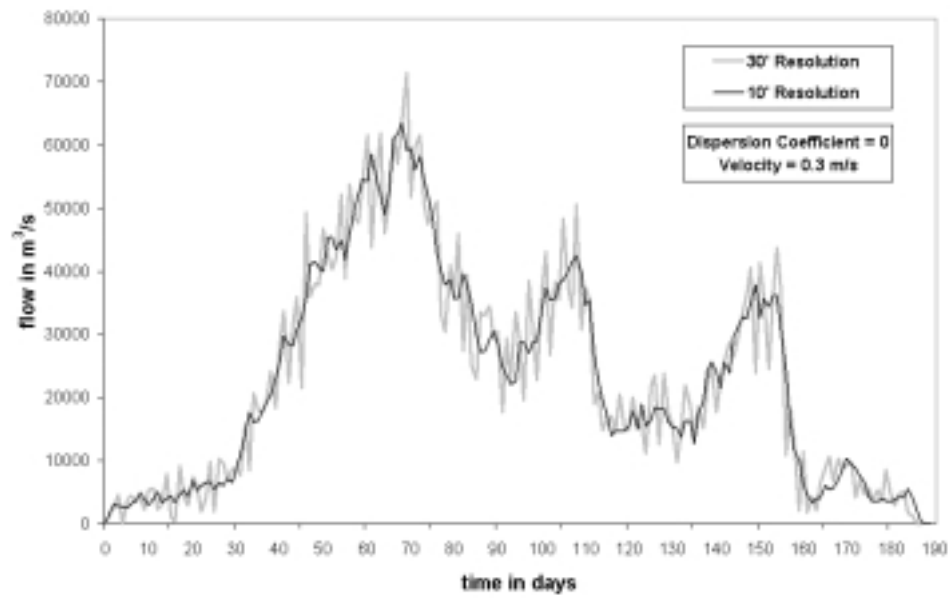


Figure 5-9(a): Comparison of Congo Basin Responses for 30 and 10 arcminute Resolution STS Model with Pure Lag Routing

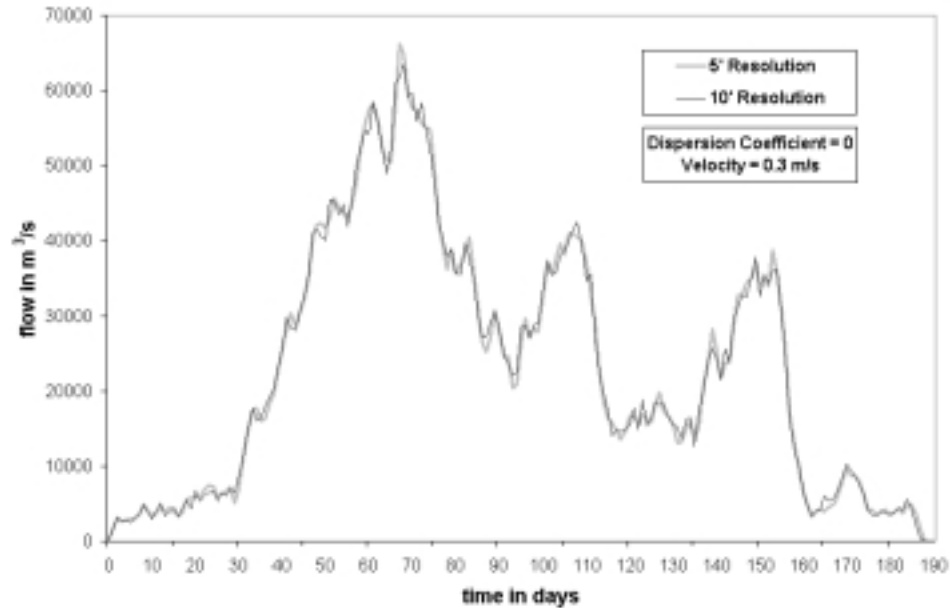


Figure 5-9(b): Comparison of Congo Basin Responses for 10 and 5 arcminute Resolution STS Model with Pure Lag Routing

When the dispersion effect is included in the routing process, the effect of resolution is much less pronounced. While a slight deviation may be observed at the points of inflexion, the basin responses shown in Figure 5-10 indicated that the overall basin is relatively insensitive to the resolution of the sources. The spreading out of inflow along each flow path is sufficient to obscure the effect of spatial discretization.

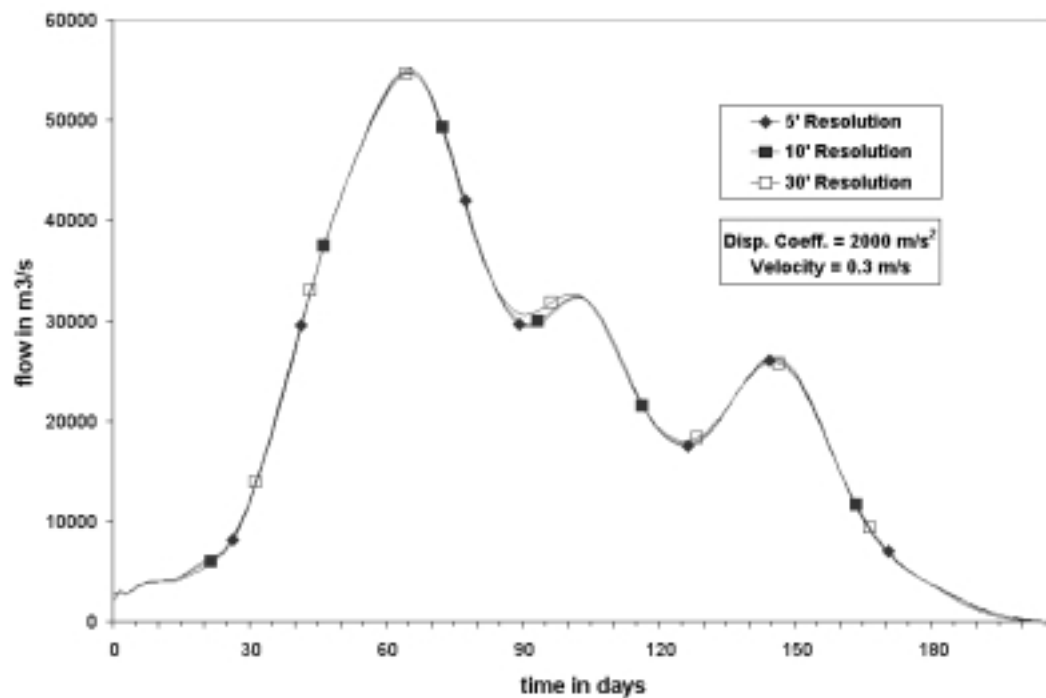


Figure 5-10: Effect of Spatial Resolution on Dispersed STS Hydrograph

In Table 5-1, a comparison of the lag times and variance of the pure lag and dispersed basin response for the three resolutions is presented. For each set of runs (pure lag and dispersed), the 5 arc-minute resolution is used as the

baseline for determining magnitude of change in lag time and standard deviation. The results indicated that for both sets of runs, the magnitude of changes in dispersion characteristics with changes in resolution were small as indicated by the high correlation values. The higher correlation for the dispersed routing case indicates that the inclusion of the dispersion effect makes the basin response much less sensitive to the resolution of the sources. Comparing the first set of runs to the second also reveals that the introduction of the dispersion effect results in a reduction of the overall basin lag time by a full routing interval from 90.2 days to 89.2 days. There is a corresponding increase in standard deviation though of a much smaller magnitude.

Table 5-1: Effect of Spatial Resolution on Lagged and Dispersed Basin Response

Spatial Resolution	First Moment (days)	Second Moment (days <sup>2</sup> )	Correlation	Change in Lag Time (hrs)	Change in Std. Deviation (hrs)
Lagged Basin Response					
30'	90.223	1521.525	0.9533	0.480	3.549
10'	90.244	1528.636	0.9975	0.024	1.364
5'	90.243	1533.083	BASELINE	BASELINE	BASELINE
Dispersed Basin Response					
30'	89.135	1557.380	0.9997	1.272	4.379
10'	89.189	1567.439	0.9999	0.024	1.325
5'	89.188	1571.815	BASELINE	BASELINE	BASELINE

### **5.2.3 Effect of Spatial Distribution of STS Parameters**

In the previous set of runs in section 5.2.2, the effects of varying the spatial resolution of STS model sources were explored. This section describes a series of runs in the Nile basin to examine the effects of spatially varying routing parameters on the basin response. The goal in this section is to determine whether or not the assumption of uniform routing parameters made in several source to sink models (Naden, 1993, Lohmann et al, 1996) results in a significant alteration of the impulse response of a large drainage basin. The routing parameters examined in this study are the velocity, dispersion coefficient and loss coefficient.

Given a field of spatially distributed parameters, a process of determining equivalent uniformly distributed parameters is required. The process adopted depends on whether the spatially distributed parameter is scalar or vector in nature. Scalar quantities can be added together and subtracted from each other because they are linearly decomposable. If the quantities are vector in nature then both the magnitude and direction must be taken into account. Vector quantities are therefore not linearly decomposable. For example, the mean value of velocity in a field of spatially varying velocities is a meaningless quantity since each individual velocity value in the field has a magnitude and a direction. The arithmetic mean value of a field of parameters is hence only meaningful if the parameters in the field are scalar quantities. To determine a representative uniform value for a field of vector quantities, two approaches may be adopted. One approach would be to first resolve all the values in the field into a single

direction and determine the magnitude of the parameter in the resolved direction. The second approach would be to convert the vector parameter into an associated scalar parameter, determine a single value of the scalar quantity by summation or averaging and use the single scalar value to determine a representative value of the vector parameter for the field. For example, a velocity field could be converted into a field of flow time, a scalar quantity. A mean or total value of flow time could be determined from the resulting field and used to derive a single value of velocity for the entire field. By so doing, the total lag time in the basin, the first moment of the basin response, is preserved allowing the effect of spatial variability to be analysed independently.

The spatial variability runs were conducted in the Nile basin because of the availability of flow data throughout the basin (Hurst and Phillips, 1938). Figure 5-11 shows the STS model of the Nile basin with key parameteric zones highlighted. As described in section 5.1, the Blue Nile basin is characterized by high flow velocities and low dispersion while the Sudd marshes are characterized by low velocities and high dispersion. Part (b) of the figure shows the sources defined in the basin with longer flow lengths represented by darker shades. The model consists of 1808 sources attached to a single sink.





Figure 5-11: Nile Basin (a) Parametric Zones and (b) Sources

The STS model was run in several iterations. In the first set of runs, the effect of hydrodynamic dispersion was held constant by applying a dispersion coefficient of  $1500 \text{ m}^2/\text{s}$  for all runs. The model was set up first with a uniform flow velocity and then with spatially variable velocity. For the variable velocity case, three velocity zones were defined. In the Blue Nile basin, water flows from an elevation of 3000 m above sea level in the Ethiopian Highlands to an elevation of 1400 m at its confluence with the White Nile at Khartoum, a distance of about 1700 km. Observed flows published by the Nile Control Department in Egypt (Hurst and Phillips, 1938) indicate that peak discharges take approximately 4 days to travel the 418 kilometers from Wad el Aies to Khartoum. This indicates a flow

velocity of approximately 1.2 m/s. In the Sudd Marshes in the Sudan, the White Nile takes about three months to travel the 711 kilometers between Mongalia and Malakal resulting in a velocity of about 0.1 m/s. Similarly, velocity in the White Nile outside of the marshes is estimated based on a flow length of 794 km and a travel time of 20 days between Malakal and Mogren just south of Khartoum as 0.5 m/s. A 1 km<sup>2</sup> grid of these three velocities was first developed, and a grid containing its inverse was calculated. Flow time from each grid cell to the basin outlet was computed by using Arc Info's weighted flow length function with the flow direction grid and the grid containing the inverse of velocity as inputs. The resulting grid contains cumulative flow time along the flow path from each grid cell to the basin outlet. The flow time for each source was then determined as the mean of all 1 km<sup>2</sup> cells in the flow time grid. The flow time for each source can be used for computing the discharge hydrograph directly from Equation 4-11 as described in section 4.1.3 of this dissertation. It can also be used to compute a new flow path velocity which preserves total flow time along each flow path from source to sink. The latter option was adopted in this study because it allows the diffusion wave equation to be used in its original form without having to introduce additional parameters. The basin response for this run was compared with the response for the equivalent uniform velocity case. The equivalent uniform velocity was calculated by dividing the sum of flow time along all flow paths in the basin by the sum of flow length for the whole basin. The equivalent uniform velocity therefore preserves the average basin lag time, allowing the two simulations to be compared. The basin response for the respective non-uniform

and uniform velocity cases are illustrated in Figure 5-12. The light grey line represents the basin response for the non-uniform velocity case while the darker line represents the uniform velocity case.

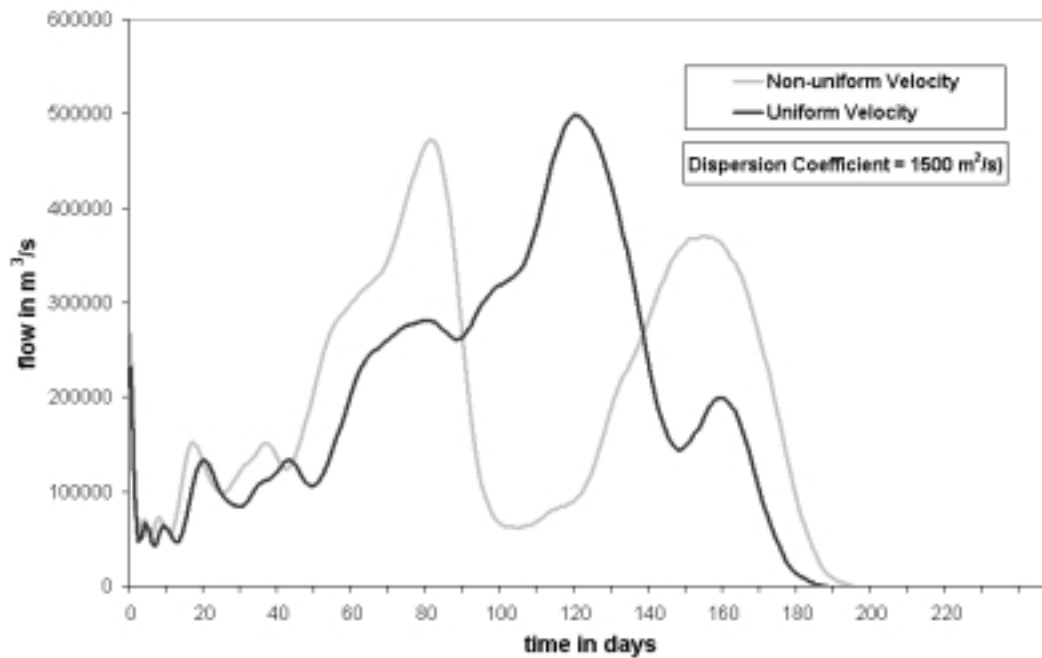


Figure 5-12: Effect of Spatial Distribution of Velocity with Uniform Dispersion Coefficient

For the Nile basin, the difference between using a uniform velocity as opposed to a non-uniform velocity is significant. The basin response is modal for uniform velocity and bimodal for non-uniform velocity. A routing method which could not account for the spatial variability of flow velocity could not possibly represent the hydrology of a basin like the Nile. The run serves to highlight the importance of accounting for spatially variable velocities in large basins.

The next set of runs was conducted to study the effect of spatially distributed dispersion coefficient on the basin response. In this set of runs, the

flow velocity was kept constant while uniform and non-uniform dispersion coefficients were adopted for respective runs. For the non-uniform case, dispersion coefficients of 4500 and 300 m<sup>2</sup>/s were assigned for the Sudd and Blue Nile basins respectively while the rest of the basin was assigned a coefficient of 1500 m<sup>2</sup>/s. These dispersion coefficients were order of magnitude estimates based on the measured values reported in Fischer (1979) and Seo and Cheong (1998). They were not intended to duplicate the actual basin response but rather as estimates to allow the effect of spatial variability to be studied. Table 5-2 summaries the flow routing parameters used in the Nile basin.

Table 5-2: Flow Routing Parameters used in the Nile Basin

Region	Velocity (m/s)	Dispersion Coefficient (m <sup>2</sup> /s)
Blue Nile Basin	1.2	300
Sudd Marshes	0.1	4500
Rest of the Nile Basin	0.5	1500

A 1 km<sup>2</sup> grid containing the dispersion coefficient values was created for the Nile Basin. From Equation 4-10 in section 4.1.3, variance along each flow path can be estimated given flow path velocity and length as well as the local values of dispersion coefficient for all intervening segments. The flow path variance for the flow path from each source to its sink was computed by averaging the flow path variance for all grid cells within each source. A representative dispersion coefficient was then computed for the flow path

associated with each source using Equation 4-12. This coefficient results in the same amount of variance along the flow path from source to sink as would result from routing flow sequentially through the respective dispersion zones. As with the flow path velocity, the dispersion coefficient was inserted into the diffusion wave equation and used in the routing. The results from this run were compared with those from the uniform dispersion coefficient case. A uniform dispersion coefficient which resulted in the same total variance when applied uniformly to all the flow paths was then determined from the sum of flow path variance in the non-uniform case. For the coefficients zones defined in the Nile basin, the equivalent uniform dispersion coefficient was determined as  $907.55 \text{ m}^2/\text{s}$ .

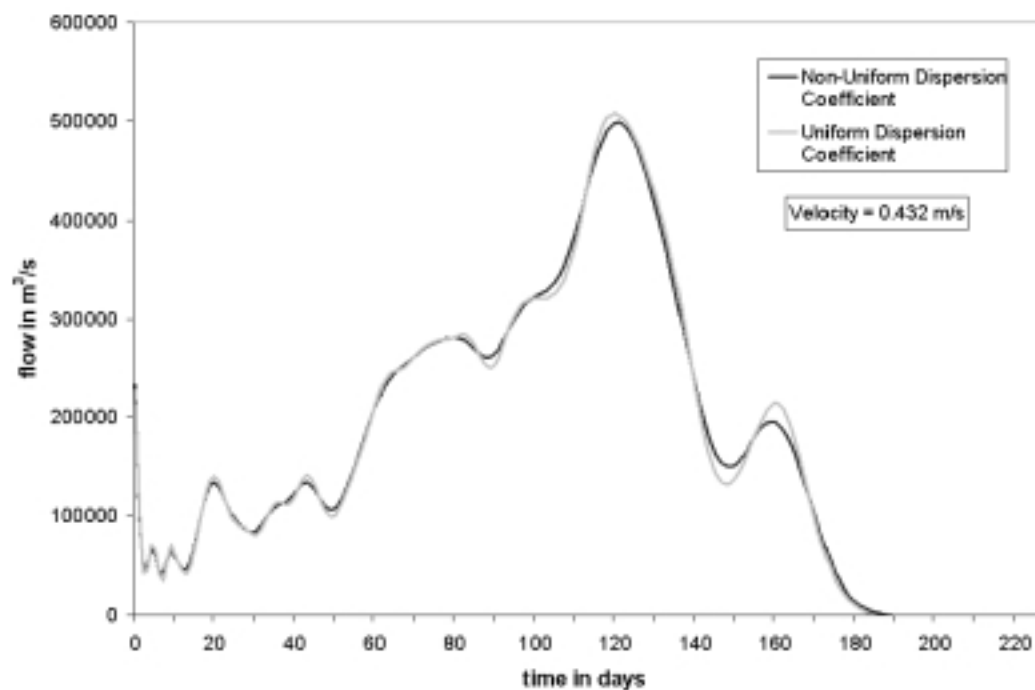


Figure 5-13: Effect of Spatial Distribution of Dispersion Coefficient with Uniform Velocity

The results of the two simulations are shown in Figure 5-13. The lighter gray line represents the basin response with both dispersion coefficient and velocity uniform while the darker line represents the non-uniform dispersion coefficient case. Peaks and troughs are slightly less defined in the non-uniform dispersion case, particularly in the latter part of the hydrograph. This seems to imply that there is more complete dispersion of flow in the non-uniform flow case. However, the difference between the observed values in the two runs is minimal compared to the obvious disparity observed in similar runs with the velocity. This would seem to imply that velocity is a much more significant parameter in determining the response of a basin and that the influence of spatially distributed dispersion coefficients could be ignored without significantly altering the basin response. However, before such an assertion could be made, the combined effect of spatially variable velocity and dispersion coefficient had to be examined. A simulation run was consequently performed with both of the parameters non-uniformly distributed.

Figure 5-14 shows a comparison of the non-uniform velocity, uniform dispersion coefficient case with the case in which both parameters are non-uniform. Non-uniform dispersion coefficient did not have a marked influence on the basin response when applied with uniform velocity. However, when velocity is non-uniform, the effect of a non-uniform dispersion coefficient on the Nile basin response was significant. The second of the two discharge peaks observed in the Nile was substantially attenuated, resulting in a 30% reduction in peak flow. The reason for this difference is that the topographic conditions that result in

low velocities are the same as those associated with high dispersion coefficients. The peak attenuation associated with low velocities is therefore compounded by the high dispersion coefficients in the same region. Areas with higher velocities are likewise more likely to have low dispersion coefficients. Water travels quickly through such areas and the effect of dispersion is not very pronounced.

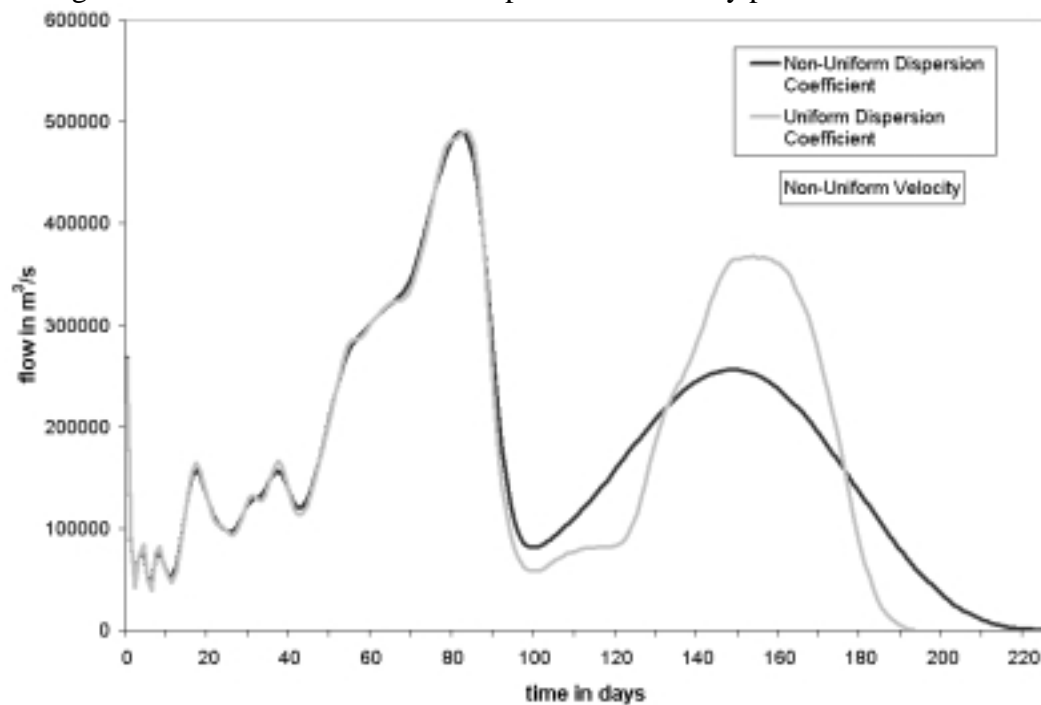


Figure 5-14: Effect of Spatial Distribution of Dispersion Coefficient with Non-Uniform Velocity

The key inference from the runs with spatially variable parameters is that if variable velocity zones exist in a basin then it is important to consider the effect of non-uniform dispersion coefficient as well. On the other hand, a uniform dispersion coefficient can be assumed if the assumption of a uniform velocity can be shown to reasonably represent flow conditions in the basin.

#### **5.2.4 Effect of Temporal Resolution of STS Model**

Having examined the effect of spatial resolution and spatial variability on basin response, another series of runs was conducted to examine the effect of temporal resolution of the routing model on the basin response. The goal in this set of runs was to determine how the choice of a routing time interval impacts the flow time and dispersion characteristic of a drainage basin. This determination is important because it provides useful information on whether or not the source to sink model can be used to establish a global database of velocity and dispersion coefficients. A model that is temporally scale independent will yield the same results for a given set of parameters irrespective of the routing interval. It can hence be used as a standard for the determination of routing parameters for use in other routing models. STS models of the Congo Basin were used to route inflow at routing intervals of 6, 12 and 24 hours respectively using a uniform flow velocity of 0.3m/s and a dispersion coefficient of 1500 m<sup>2</sup>/s. Figure 5-15 shows the resulting time series plotted with a single horizontal time scale.



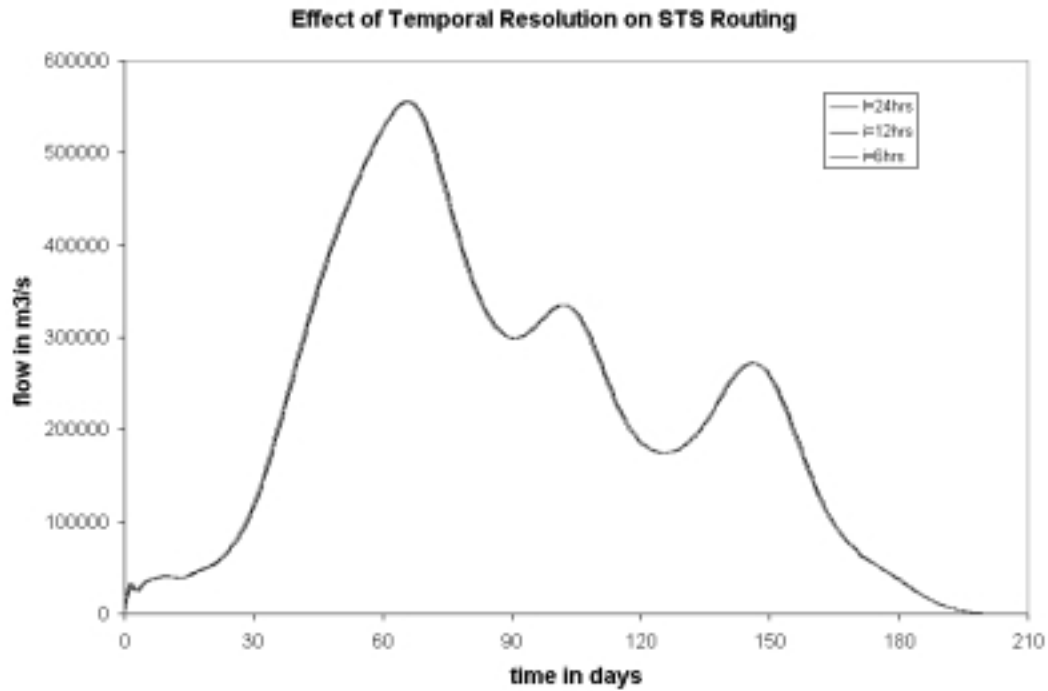


Figure 5-15: Effect of STS Routing Interval on Congo Basin Response

The graphs of the respective routing intervals are indistinguishable from one another. A comparison of their respective first and second moments in Table 5-3 reveals that there is a minimal shift whose magnitude is much smaller than the routing interval.

Table 5-3: Effect of STS Routing Interval on Congo Basin Response

Routing Interval	First Moment (days)	Second Moment (days <sup>2</sup> )	Change in Lag Time (hrs)	Change in Std. Deviation (hrs)
6 hours	89.169	1549.488	0.432	0.431
12 hours	89.174	1549.930	0.312	0.297
24 hours	89.187	1550.903	BASELINE	BASELINE

The results of this simulation indicate that the source to sink model is relatively insensitive to choice of routing time interval. Routing parameters determined at one temporal resolution would therefore be applicable to other temporal resolutions.

### **5.3 HYDROLOGIC MODELING SYSTEM MODEL RUNS**

Having examined the effect of various routing and model parameters on the response of a source to sink model, a similar set of simulations were performed on the watershed based model for comparison. As discussed in section 3.4, validation of the source to sink routing process in this study is performed by comparison with an HMS model of the same basin. A series of simulations performed with the watershed based approach of HMS are described in this section. The change in the response of a sample HMS reach due to longitudinal decomposition is examined in section 5.3.1. The Congo basin response is compared for different models resolutions and routing intervals in sections 5.3.2 and 5.3.4 respectively while the ability of an HMS model to represent spatially distributed parameters in the Nile Basin is examined in section 5.3.3.

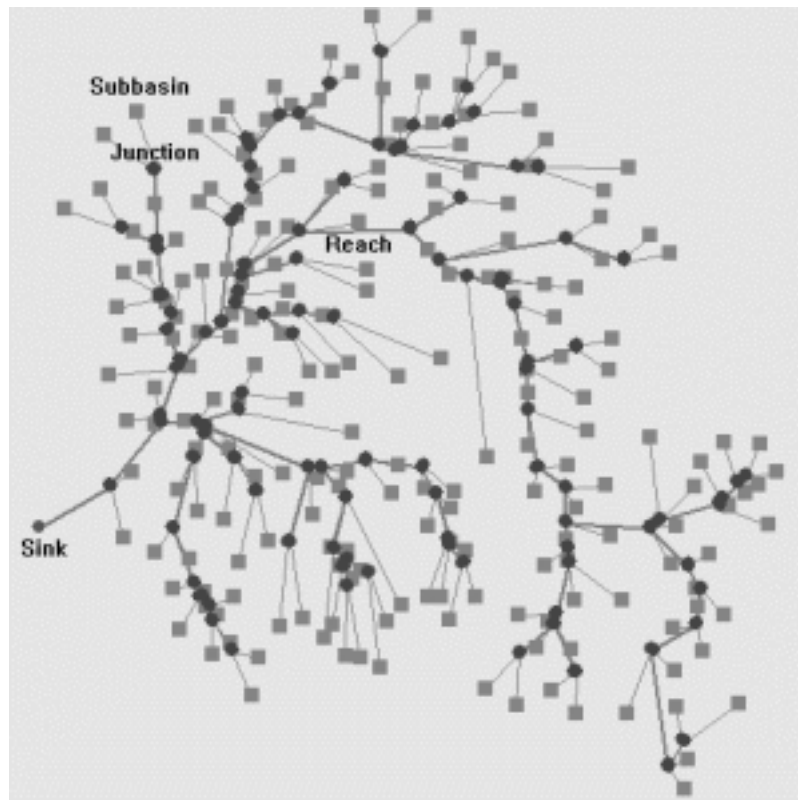


Figure 5-16: Sample HMS Schematic for Congo Basin

Figure 5-16 shows an HMS schematic for the Congo Basin delineated at a 10000-cell threshold. The process of deriving an HMS basin file containing a description of the hydrologic elements and the connectivity among these elements is described in section 3.4 of this dissertation. In that delineation, the threshold for stream delineation was specified as 10000 km<sup>2</sup>. A more detailed model of the Congo basin was created for the model intercomparisons. The parameters for the second delineation of the Congo basin are summarized in Table 5-4. In the Nile basin, spatially distributed velocities, Muskingum x and loss parameters were used as described in section 5.3.3.

Table 5-4: Parameters for the Congo Basin Delineation

Process	Inputs	Parameter	Value	Outputs
Stream Definition	Flow Accumulation Grid	Stream Definition Threshold (km <sup>2</sup> )	1000	Stream Grid
Stream Linking	Stream Grid	Number of Links	1791	Stream Link Grid
Outlet Definition	Stream Link Grid	Number of Outlets	1791	Outlet Grid
Watershed Definition	Flow Direction Grid, Stream Link Grid	Number of Watersheds	1791	Watershed Grid
Stream Vectorization	Stream Grid	Minimum Stream Length	710	Stream Coverage
Watershed Vectorization	Watershed Grid	Number of Watersheds	1791	Watershed Coverage
Calculating Watershed Attributes	Watershed Coverage, Flow Direction Grid	SCS Unit Hydrograph		Watershed Parameters
		watershed velocity	0.3 m/s	
		initial losses	0	
		constant losses	0	
Calculating Stream Attributes	Stream Coverage, Flow Direction Grid	Muskingum Method:		Stream Routing Parameters
		in-stream velocity	0.3 m/s	
		Muskingum x	0.3	
Basin File Creation	River coverage, watershed coverage	Subbasins	1791	HMS Basin File
		River reaches	943	
		Junctions	894	
		Sinks	1	

### 5.3.1 Longitudinal Decomposability of the HMS Model

Longitudinal decomposability along each flow path linking a source to its sink in the diffusion type STS model was verified in section 5.2.1 of this dissertation. It is imperative that a similar verification be conducted for the HMS model. A model was set up in HMS consisting of a 162 kilometer river reach linked to a subbasin at its upstream end and a sink at its downstream end as shown in Figure 5-17. The watershed served as a source of input for the stream, and input runoff was translated instantaneously through it and without redistribution or losses.

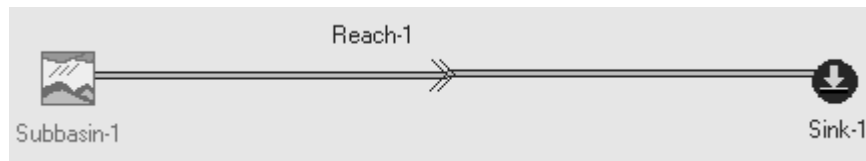


Figure 5-17: HMS Schematic for Longitudinal Decomposability Runs

The Muskingum routing method was used to route flow through the river reach. The routing parameters used include a flow velocity of 0.3 m/s, and a Muskingum  $x$  of 0.3. This resulted in a Muskingum  $K$  of 150 hrs and a Muskingum  $n$  of 4 for the reach. HMS routes flow by applying the Muskingum equation successively to all  $n$  sub-reaches until the flow arrives at the end of the river reach. In built HMS parameter constraints limit the number of sub-reaches into which a river reach can be divided. Hence the task was to determine the extent to which longitudinal decomposability is maintained in a reach when the HMS imposed limitations on the number of subreaches,  $n$ , are adhered to. An

impulse of  $100\text{m}^3/\text{s}$  was applied to the subbasin, and the discharge at the sink was observed for various values of  $n$  between 4 and 8. HMS returned warning messages for values of  $n$  outside this range. These messages indicated that the Muskingum equation was unstable for the routing parameters defined. Muskingum  $n$  values of 4 and 8 correspond to sub-reach lag times of 18.75 hrs and 37.5 hours, respectively. This implies that HMS allows the user to subdivide the 150-hour lag time into four 37.5 hour segments, eight 18.75 hour segments or other whole number of uniform segments between 4 and 8. The problem could be complicated even further by subdividing the single reach into smaller reaches by introducing junctions and then calculating a Muskingum  $n$  for each reach. However, HMS generates error messages when the lag time along the routing reach is less than the routing interval, 24 hours in this case. The largest number of Muskingum routing reaches that could be created from the 150 hour reach is six. A routing reach with a lag time of just over 24 hour would require a Muskingum  $n$  value of 1. Thus the introduction of additional junctions would not lead to a Muskingum  $n$  value outside the 4 to 8 range, assuming a 24-hour routing interval. Figure 5-18 below shows the river reach response for different values of  $n$  with the Muskingum  $K$  and  $x$  values unaltered.

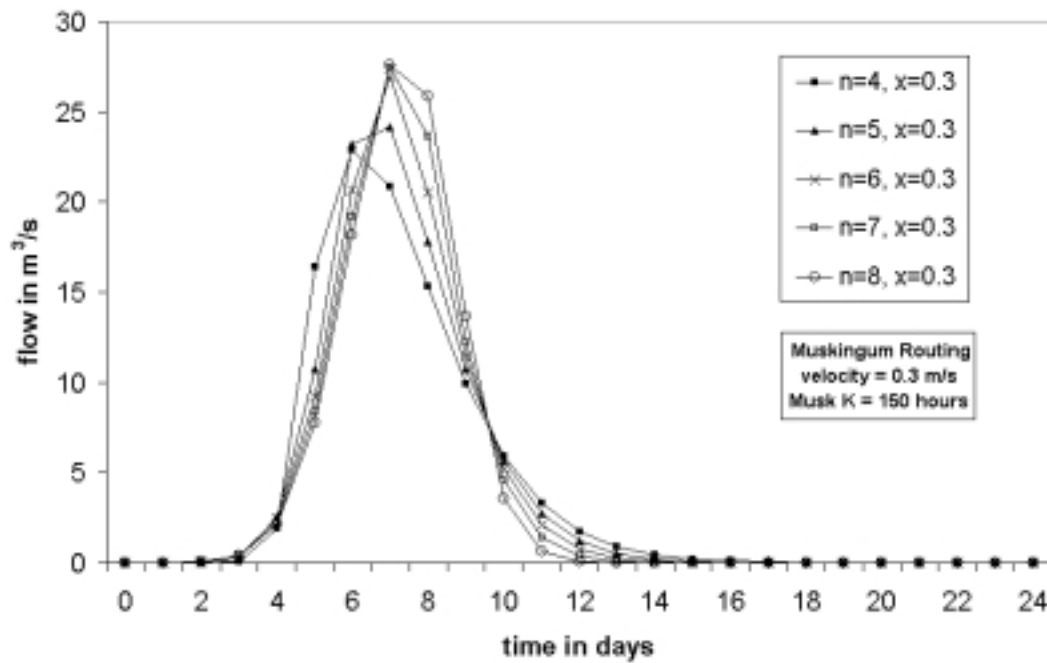


Figure 5-18: Changes in River Reach Response with Muskingum  $n$

The figure indicates that for the same value of Muskingum  $x$  and total reach length, routing flow sequentially over several small distances produces less dispersion than would result from routing the same flow over larger stretches of distance. The Muskingum routing method is consequently not linearly decomposable. The significance of this result is that it provides an indication of the degree of variability permissible in HMS. Table 5-5 provides an analysis the moments of the time series generated for each of the 5 values of Muskingum  $n$  used in the simulations. The equivalent values of dispersion coefficient are determined by equating the second moments of the Muskingum and diffusion wave equations for a routing subreach. The dispersion coefficient can thus be determined from Equation 5-1 (Montes, 1998, pp. 574).

Equation 5-1  $D = Lv(0.5 - x)$

where  $D$  is the equivalent dispersion coefficient in  $\text{m}^2/\text{s}$

$L$  is the length of the reach in  $\text{m}$

$x$  is the dimensionless Muskingum  $x$

$v$  is the velocity of translation through the reach in  $\text{m/s}$

Table 5-5: Effect of Muskingum  $n$  on River Reach Response

Number of Routing Subreaches	First Moment (days)	Second Moment (days <sup>2</sup> )	Equivalent Dispersion Coefficient ( $\text{m}^2/\text{s}$ )	Change in Standard Deviation (hrs)
4	6.250	3.905	2429	BASELINE
5	6.250	3.125	1944	5
6	6.250	2.603	1619	8.7
7	6.250	2.233	1389	11.6
8	6.250	1.953	1215	13.9

Even within the HMS imposed limitations, a 100% increase in dispersion coefficient can be achieved by simply altering the number of subreaches. The result indicates that the response of a routing reach is very sensitive to spatial resolution. If the Muskingum  $x$  parameter is allowed to assume different values, there is a limited range of dispersion coefficients that the reach can assume given the routing interval and velocity.



Table 5-6: Range of Dispersion Coefficients of a Muskingum Routing Reach with 24 hour Routing Interval and Velocity of 0.3m/s

Muskingum	Maximum	Minimum	Maximum	Minimum
x	Routing Reach	Routing Reach	Dispersion	Dispersion
	Lag Time (hrs)	Lag Time (hrs)	Coeff. (m <sup>2</sup> /s)	Coeff. (m <sup>2</sup> /s)
0	150.0	12.2	24300	1976
0.1	120.0	13.4	15552	1737
0.2	60.0	15.0	5832	1458
0.3	40.0	17.2	2592	1389
0.4	30.0	20.0	972	648
0.5	UNSTABLE	UNSTABLE	N/A	N/A

Table 5-6 lists the range of Muskingum K and the corresponding dispersion coefficients that are available to an HMS model with a routing interval of 24 hours and a velocity of 0.3 m/s. For each Muskingum x value, the maximum and minimum values of Muskingum K were determined by repeatedly altering the K value for a single reach with n =1. The respective maximum and minimum Muskingum K values were determined as the values greater and less than which error messages regarding the numerical stability of the Muskingum solution are triggered. Flow velocity for the reach was then determined by dividing the lag time by the actual length of the reach. The significance of this result is that it demonstrates that by choosing a particular value of the Muskingum x, the modeler limits the range of dispersion coefficients. However, the lag time for a particular

reach also plays a role in determining the amount of dispersion the reach experiences. The application of a uniform Muskingum  $x$  coefficient does not therefore result in a model with uniform dispersion properties. To achieve such a model, each river reach would have to be assigned a different value of Muskingum  $x$ . In section 5.3.3, an HMS model of the Nile basin is set up using equivalent Muskingum  $K$  and  $x$  parameters calculated from a spatially distributed field of velocity and dispersion coefficients.

### **5.3.2 Effect of Spatial Resolution of the HMS Model**

To examine the effect of spatial resolution on the basin response, two HMS models of the Congo were created using stream delineation thresholds of 1000 and 10000 km<sup>2</sup>, respectively. These thresholds resulted in HMS models containing 1791 and 214 subbasins, and 943 and 152 river reaches respectively. River reaches with lag times greater than the maximum permissible lag time of 150 hours in HMS were subdivided into shorter reaches using junctions. The basin responses from the respective delineations are shown in Figure 5-19.

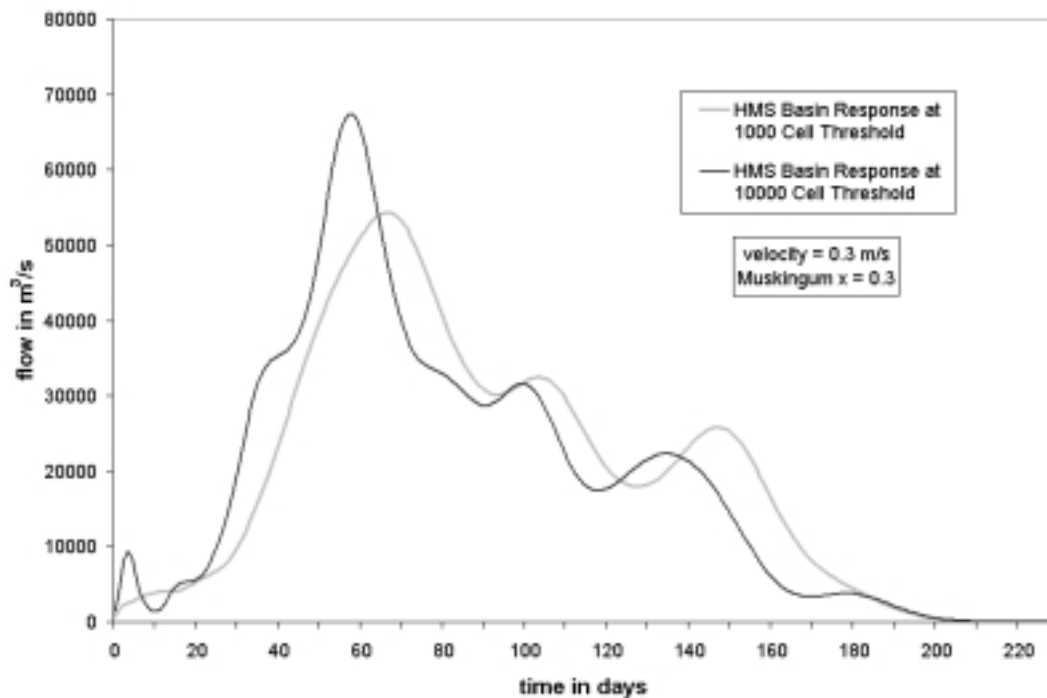


Figure 5-19: Effect of Delineation Threshold on Congo Basin Response for HMS Model with Muskingum Routing

The specification of a higher cell threshold implies that input runoff spends more time on the land surface as opposed to within the river channel. The effect of the approximate unit hydrograph process on the overall basin response thus becomes more pronounced. Conversely, the reduction in time spent in the river channel, results in an overall reduction in the amount of dispersion the flow undergoes for the same set of routing parameters. Consequently, the larger delineation threshold, the less dispersed the resulting hydrographs. Also note that since the Muskingum  $x$  is scale dependent, the value of 0.3 used for the model at the finest resolution is no longer applicable at the coarser scale. A procedure for

predicting the appropriate value of Muskingum  $x$  to use for a change in resolution is described in section 5.3.3.

The HMS basin responses at the respective 1000 and 10000 cell resolutions were also compared with STS basin responses using various values of dispersion coefficient. Figure 5-20 shows a comparison of the finer resolution HMS and STS model response of the Congo basin. For both models, a flow velocity of 0.3m/s was assumed. A dispersion coefficient of 2000  $\text{m}^2/\text{s}$  was assumed for the STS model while a Muskingum  $x$  of 0.3 was assumed for the HMS model. The basin responses from the two models would map almost perfectly on top of each other if the STS model response were shifted 2 days ahead. Possible explanations for this shift are discussed in section 5.2.4.

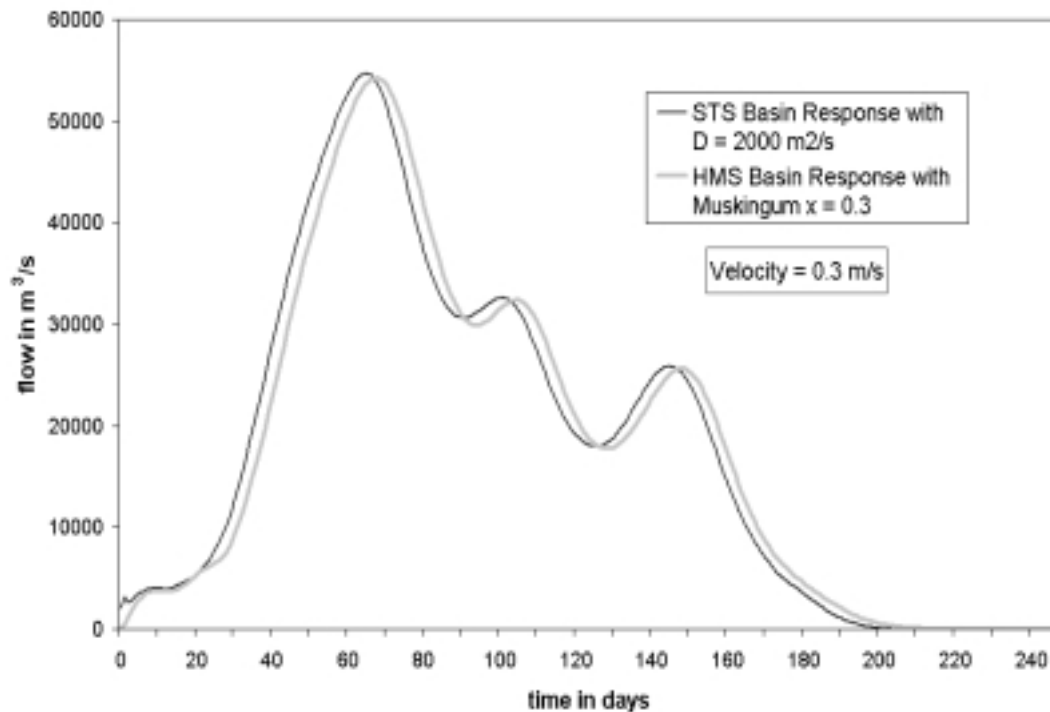


Figure 5-20: Comparison of 1000 Cell Threshold HMS Model Response with the STS Model Responses in the Congo Basin

The Congo basin response for the HMS model delineated at the 10000 cell threshold was similarly compared with an STS model response with a dispersion coefficient of 1500 m<sup>2</sup>/s. This value of dispersion coefficient was selected based on the range of possible values of the coefficient for a Muskingum routing reach with a velocity of 0.3 m/s, a Muskingum x of 0.3 and a routing interval of 24 hours. The results of this comparison are shown in Figure 5-21.

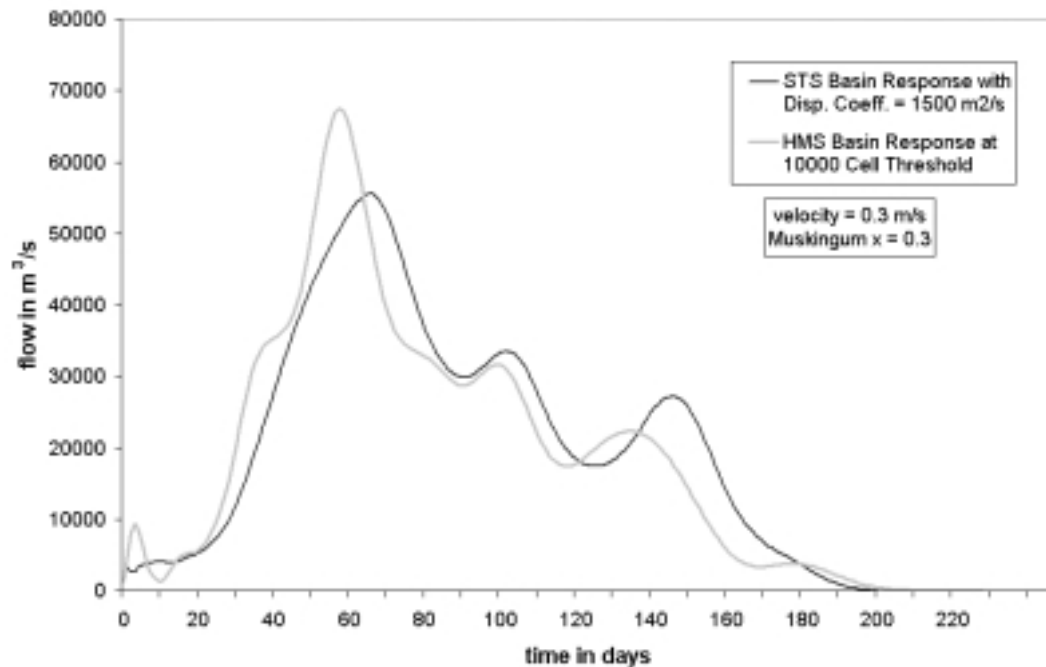


Figure 5-21: Comparison of 1000 Cell Threshold HMS Model Response with the STS Model Responses in the Congo Basin

The match between the two basin responses is not as close as that obtained with the 1000 cell threshold model. The likely explanation for this discrepancy is the increased role of the subbasin response function in the overall basin response.

The SCS synthetic unit hydrograph used for this analysis plays a greater role in the overall basin response at this threshold than it did at the 1000 cell threshold.

In summary, the comparison of responses of two HMS models of the same basin delineated at different thresholds revealed the basin response is very sensitive to spatial scale. When the scale of the model is changed, the basin response changes even if the routing velocity and Muskingum  $x$  parameters remain unchanged. Each HMS model must be parameterized separately making the method unsuitable for establishing scale independent routing parameters. The next logical step is therefore to determine whether routing parameters established using a more scale independent model like the diffusion type source to sink model can be used to parameterize an HMS model. An analysis of this nature is described in section 5.3.3.

### **5.3.3 Effect of Spatial Distribution of HMS Parameters**

The manner in which hydrologic elements are defined in an HMS model allows it to incorporate spatially distributed routing parameters. Hence the task in this section is not to define a procedure for representing spatially distributed parameters as was done for the source to sink model in section 5.2.3. Instead, a procedure is defined for computing equivalent Muskingum  $K$  and  $x$  parameters from a field of spatially distributed dispersion coefficients,  $D$ , and flow velocities,  $v$ . The same dispersion coefficients and velocity fields used in the Nile basin STS model in section 5.2.3 were provided as inputs, thus allowing the basin responses from the respective model runs to be compared.

The first step in determining equivalent Muskingum routing parameters was to extract a flow direction grid containing only in-stream cells by multiplying the stream grid with the flow direction grid. The resulting grid was then multiplied by the outlet grid to insert sinks, in the flow direction grid, at the end of each river reach. As in section 4.1.3, weight grids of  $(1/v)$  and  $(D/v^3)$  were applied for the computation of first and second moment using the weighted flow length function. Equivalent values of Muskingum  $x$  were computed for the longest flow length in each stream reach by equating the second moments of the Muskingum equation with those of the diffusion wave equation using Equation 5.2 which is Equation 5.1 rearranged to make  $x$  the subject. The procedure for performing this computation was written in the Arc Macro Language (AML) of GIS software, Arc Info, and is included in Appendix 4.

$$\text{Equation 5-2} \quad x = 0.5 - \left( \frac{D}{vL} \right)$$

In this first estimate of Muskingum  $x$ , a single routing reach (Muskingum  $n = 1$ ) is assumed. The determination of the number of routing reaches however depends on the value of  $x$ . Hence the two parameters must be estimated by iteration. For the first and second iterations, the respective values of Muskingum  $x$  are computed as

$$\text{Equation 5-3} \quad x_1 = 0.5 - \left( \frac{D}{vL_1} \right)$$

and

Equation 5-4 
$$x_2 = 0.5 - \left( \frac{D}{vL_2} \right)$$

where  $x_1$  and  $x_2$  are the respective values of Muskingum  $x$

$L_1$  and  $L_2$  are the respective values of routing reach length

However, the only parameters that changes between iterations is the number of routing subreaches, the Muskingum  $n$ , and hence,  $L_2 = L_1 / n$

Substituting for  $L_2$  in Equation 5-4 gives

Equation 5-5 
$$x_2 = 0.5 - n \left( \frac{D}{vL_1} \right)$$

which is equivalent to

Equation 5-6 
$$x_2 = 0.5 - n(0.5 - x_1)$$

For the more general case in which  $n$  is not equal to one in the first iteration, the value of the Muskingum  $x$  can similarly be shown to be

Equation 5-7 
$$x_{i+1} = 0.5 - \left( \frac{n_{i+1}}{n_i} \right) (0.5 - x_i)$$

where  $i$  is the number of iterations

Figure 5-22 shows the respective basin responses for first and second iterations of the Muskingum  $x$  and  $n$  parameter computations. HMS basin models of the Nile were created for the Muskingum parameters resulting from the respective first and second moments. Negative Muskingum  $x$  values which



occurred in 14 of the 184 routing reaches were set to zero since HMS does not allow the parameter  $x$  to assume negative values.

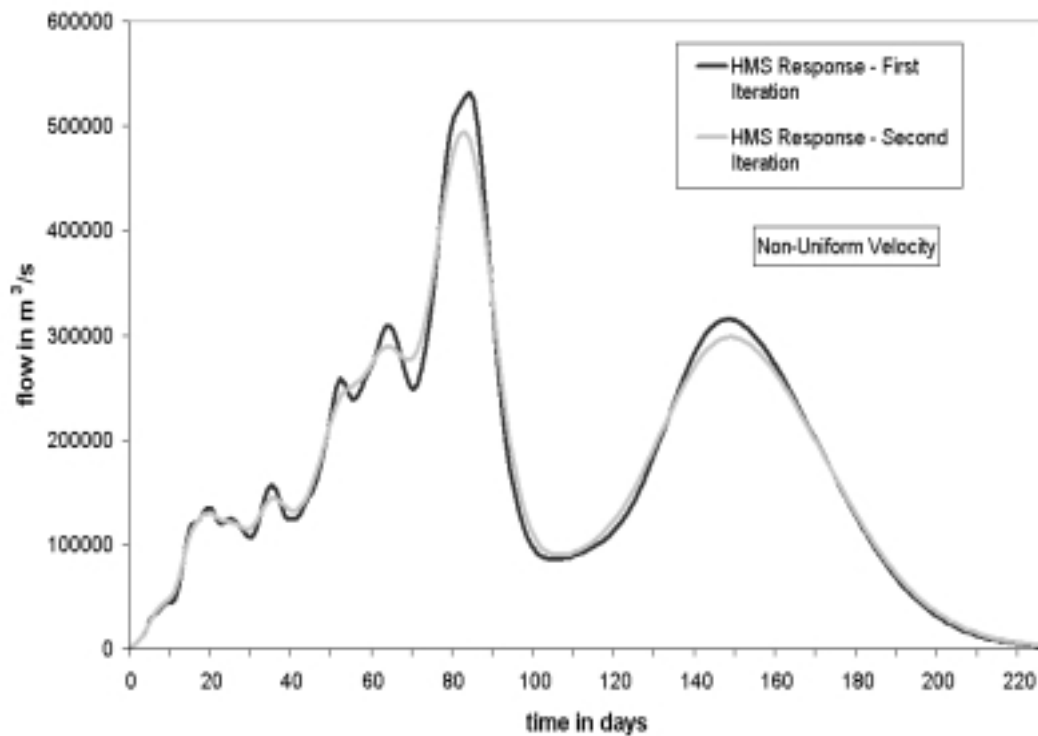


Figure 5-22: Basin Response for Iterations of Muskingum  $x$  and  $n$  Parameters

The second iteration shows an increase in dispersion properties over the first. Local peaks and troughs are consequently less pronounced in the basin response after the second iteration of the Muskingum  $x$  and  $n$  computation. The basin response also exhibits the bimodal nature of observed for the distributed parameter case of the STS model in section 5.2.3. Figure 5-23 shows a comparison of the basin response from the respective Muskingum and dispersion wave routing approaches using the HMS and STS models.

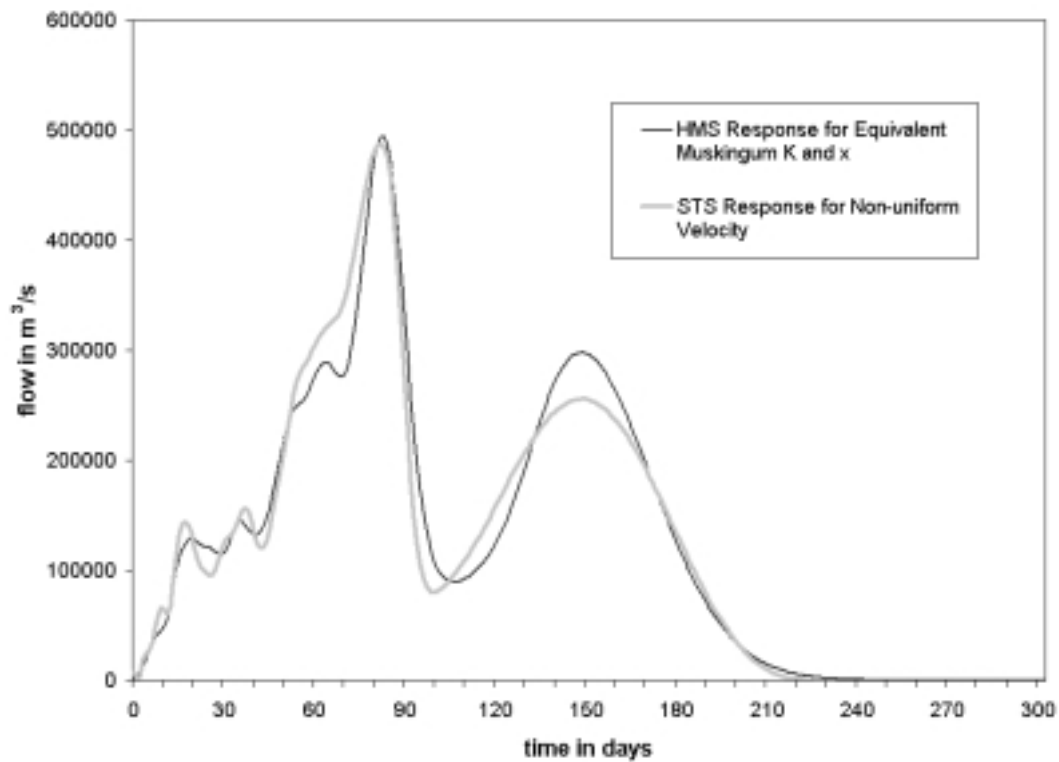


Figure 5-23: Equivalent HMS and STS Basin Response for Distributed Parameters

A comparison of HMS and STS basin responses in Figure 5-23 reveals that while it is able to capture the essential characteristics of the response, the method of moments does not result in an exact duplication of the basin response. The equivalent Muskingum parameters result in a basin response that is more dispersed for the shorter reaches (those associated with the first peak) and less dispersed for the longer reaches. In the Nile basin, the reaches closest to the outlet have lower dispersion coefficients compared to those transmitting inflow from the areas upstream of the Sudd Marshes. Hence the equivalent Muskingum parameters tend to underestimate high dispersion coefficients while

overestimating low coefficients. This result is also significant because it reveals that despite differences in their spatial scale dependence, STS and HMS models parameterized from a common spatially distributed field of velocity and dispersion coefficient yield very similar basin responses. The problems of spatial scale dependence of HMS models can consequently be avoided by determining routing parameters for various hydrologic elements from spatially distributed fields of velocity and dispersion coefficient. An approach for deriving these parameters from observed flow data is demonstrated in section 5.4.1 of this dissertation.

#### **5.3.4 Effect of Temporal Resolution of HMS Model**

The response of a basin in an HMS model is sensitive to the temporal resolution specified for routing. One source of this sensitivity is the subbasin lag time which is computed as a function of the routing interval. If Muskingum method is specified as the routing option within the river reaches, then the number of routing subreaches, Muskingum  $n$ , into which a river reach is divided also varies with temporal resolution as indicated by Equation 4-14 in section 4.2.3. While the lag time within each river reach is independent of temporal resolution, changing the number of routing subreaches results in changes in the dispersion properties of the reach. The magnitude of this change is discussed in section 5.3.3 of this dissertation. An analysis of the relative importance of subbasin lag time and Muskingum  $n$  in influencing basin response is presented in this section.

Additional sources of temporal scale dependence are also studied by performing runs in which the above mentioned factors are kept constant.

Subbasin lag times in HMS are computed as the larger of 0.6 times the length of the longest subbasin flow path divided by the flow path velocity and 3.5 times the routing interval, as described in section 4.2.3. This method of computation ensures that subbasin lag times do not fall below the specified minimum of 3.5 times the routing interval. The smaller the subbasins defined in the study area, the more frequently the minimum lag time rule is enforced. Defining larger subbasins does not solve the problem either since HMS allows a maximum subbasin lag time of 500 hours. Rather than trying to strike a balance between the number of subbasins and the subbasin lag time during delineation, it may be easier to select a routing interval which results in a lower minimum subbasin lag time and hence a lower number of enforced subbasin lag times. The routing interval should consequently be determined not by the desired temporal resolution of the output but rather the number of enforced lag times (and consequently the accuracy of routing).

To quantify the effect of routing interval on overall subbasin response, a spreadsheet was created using the subbasin lag function at different routing intervals. The HMS model of the Congo basin, described in section 5.2, was used in this analysis. For each temporal resolution, a tally was kept of the number of subbasins in which the minimum lag condition was enforced. The overall mean lag time per subbasin was computed and compared with the mean lag time for the case in which no minimum subbasin lag time is enforced. The difference between

the two cases is calculated as the effective enforcement. Table 5-7 shows the effect of enforced lag times at various routing intervals in the Congo basin.

Table 5-7: Effect of HMS Enforced Minimum Subbasin Lag

Routing Interval	Enforced Minimum Lag (hrs)	Number of Enforcements	Mean Lag Time (hrs)	Effective Enforcement (hrs)
24 hours	5040	1550	87.9	33.0
18 hours	3780	1265	71.2	16.3
12 hours	2520	614	59.8	4.9
8 hours	1680	263	56.6	1.7
6 hours	1260	179	55.7	0.8
3 hours	630	58	55.0	0.1
1 hours	210	15	54.9	0.0
0.1 hours	21	0	54.9	0.0

It is evident from the analysis above that it would take a very small routing interval to completely eliminate subbasin lag time enforcements. Such a routing interval would be computationally inefficient for performing long term routing. The resulting flows would also not be reliable given that the temporal resolution of the input runoff is much coarser than that of the output flows. There are at least two approaches to getting around this limitation. The first would be to create a basin file using the actual lag times for all subbasins instead of the HMS enforced minimum lag times. The warning messages issued by HMS would then have to be ignored when the basin file is subsequently used in simulations. The second approach would be to accept a few of lag time enforcements in exchange for improved computational efficiency. An objective approach to determining a

suitable routing interval would be to perform an analysis like the one shown in Table 5-7. The routing interval could be chosen such that the difference between the resulting subbasin lag time and that of the zero enforcements case is much less than the temporal resolution of the input data. This difference is labeled as the effective enforcement in Table 5-7 above. For the example of the Congo basin, an HMS model with a routing interval of 12 hours would be suitable because it results in an effective enforcement of 4 hours which is much less than the resolution of the daily input available for running the model. No significant delay is expected when a model of this resolution is used. To verify this hypothesis, HMS basin files of the Congo were created, at different temporal resolutions, for the respective enforced minimum and unbounded lag time cases. Routing intervals 12 hourly and 24 hourly were specified for the models. For the first set of runs, pure lag routing was specified for river reach routing while the Muskingum method was specified for the second set of runs to allow the scale dependence of the methods to be studied. Following is an analysis of the results of the temporal resolution runs. The hydrographs resulting from the run are described in terms of their respective first moment and second moments. Figures 5-24 (a) and (b) show the results of the pure lag routing runs at 12 and 24 hour intervals respectively. The figures show that the minimum subbasin rule has the effect of shifting the whole basin response forward by an almost uniform amount.

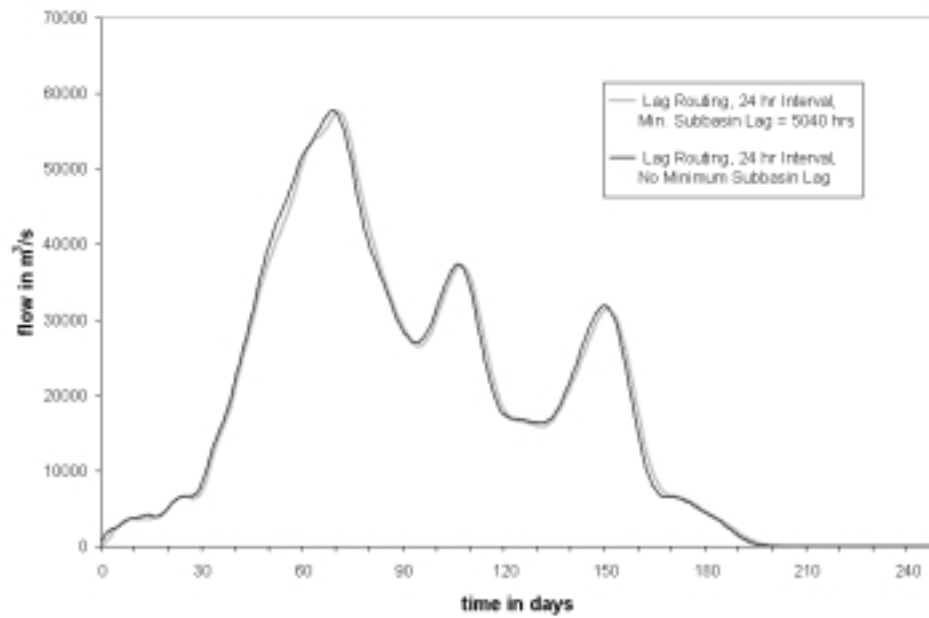


Figure 5-24(a): Effect of Minimum Subbasin Lag for 24hr-Interval Lag Routing

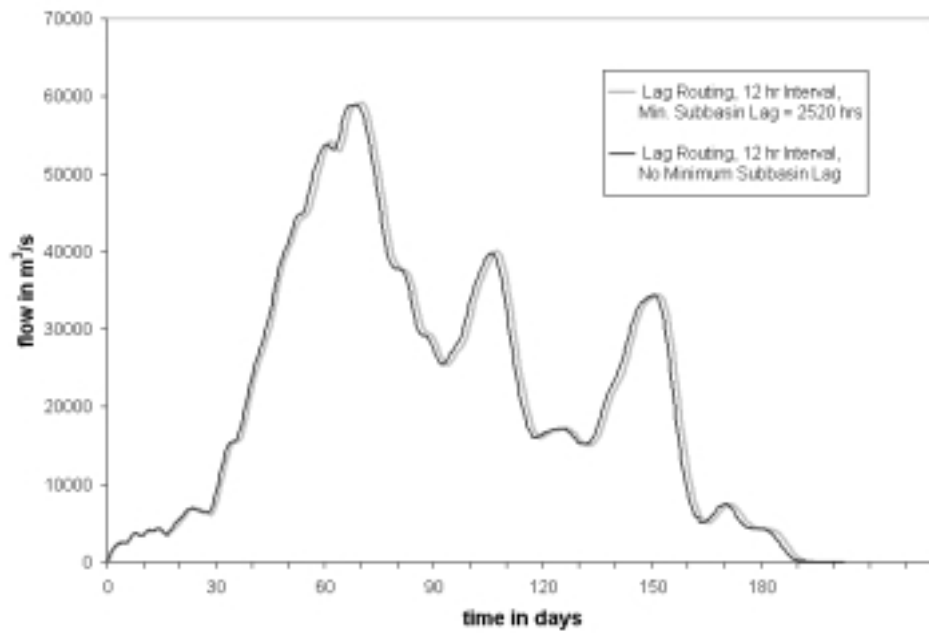


Figure 5-24(b): Effect of Min. Subbasin Lag for 12hr-Interval Lag Routing

From Table 5-8, the difference in first moments between the basin response with and without minimum subbasin lag enforcement is 0.47 days at a 12-hour routing interval and 0.99 days at the 24-hour interval. A much larger difference of about 23 days is observed between the basin response at the respective 12 and 24 hour intervals. The results in Table 5-8 also show a slight change in dispersion characteristics between runs with minimum subbasin lag enforcements and runs without it. However, a much larger increase in second moment, approximately 200%, occurs with the change in routing interval, from 12 to 24 hours.

Table 5-8: Effect of Min. Subbasin Lag Rule on Basin response, Lag Routing

Routing Interval (hrs)	Min. Subbasin Lag Enforced	First Moment (days)	Second Moment (days <sup>2</sup> )
12	Yes	68.71	494.17
12	No	68.24	505.57
24	Yes	91.25	1546.90
24	No	90.26	1538.11

In the second set of runs, the Pure Lag routing was replaced with the Muskingum method in river reach elements in order to determine whether the features observed in the first set of runs were specific to the routing method. As with the Lag routing runs, routing was performed at 12 and 24 hour intervals with and without enforcing the minimum subbasin lag rule. Figure 5-25(a) and (b) show the effect of the minimum subbasin lag rule on basin response with Muskingum routing in the river reaches.



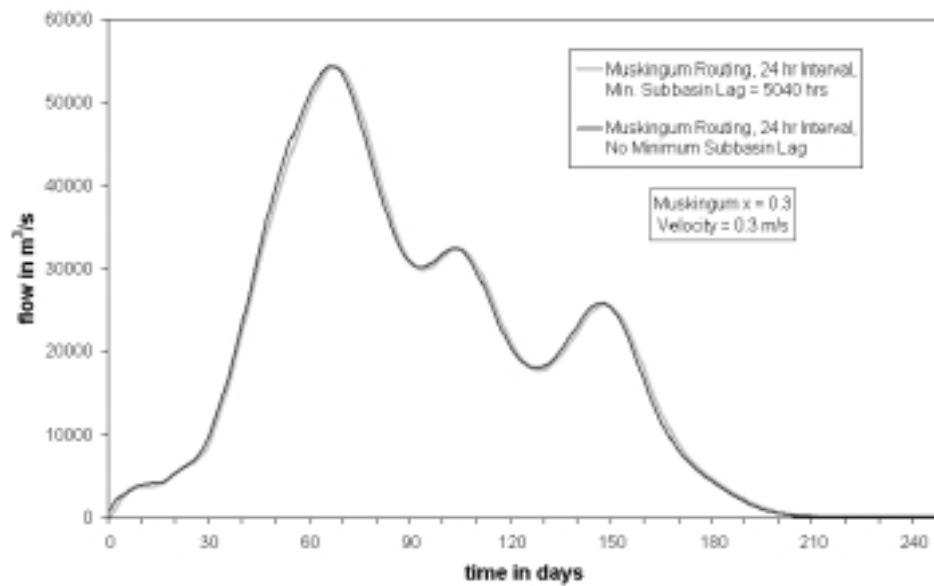


Figure 5-25(a): Effect of Min. Subbasin Lag for 24hr-Interval Muskingum Routing

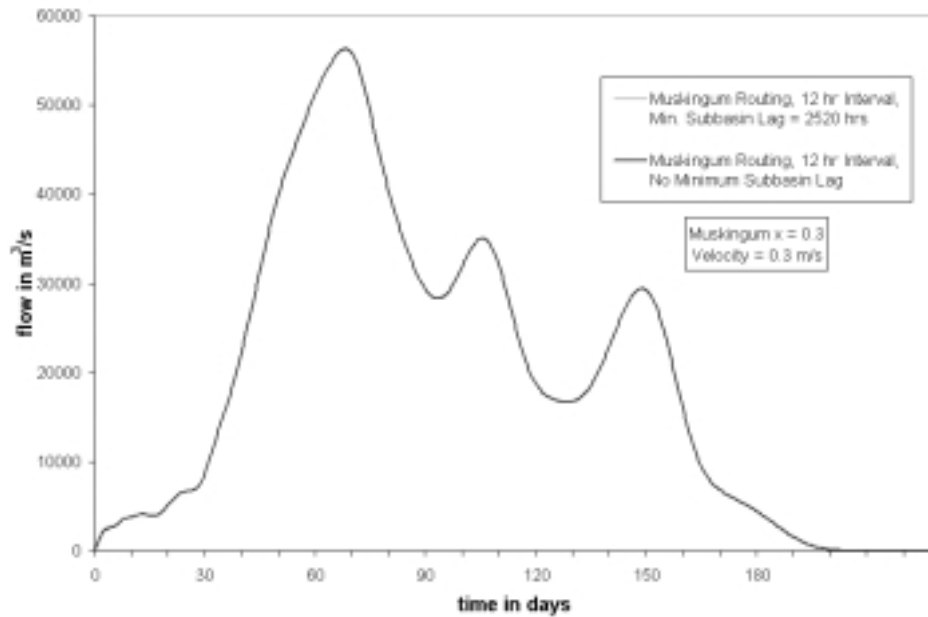


Figure 5-25(b): Effect of Min. Subbasin Lag for 12hr-Interval Muskingum Routing

The basin responses for the Muskingum runs, Figure 5-25(a) and (b), display similar characteristics to those observed for the Lag routing runs. As the routing interval is increased, there is increased dispersion and the effect of the subbasin lag rule becomes more pronounced. From Table 5-9, the lag times in the Muskingum runs are approximately equal to those in the Lag runs and the second moments are generally higher in the former.

Table 5-9: Effect of Subbasin Lag Rule on Basin response, Muskingum Routing

Routing Interval (hrs)	Minimum Subbasin Lag Enforced	First Moment (days)	Second Moment (days <sup>2</sup> )
12	Yes	68.45	493.68
12	No	68.43	494.31
24	Yes	91.25	1580.71
24	No	90.26	1572.00

However, the difference between lag first and second moments at the 12 and 24 hour routing intervals remains the most significant feature of the runs. Figures 5-26(a) and (b) show the effects of routing interval on the basin response for the respective Lag and Muskingum runs.

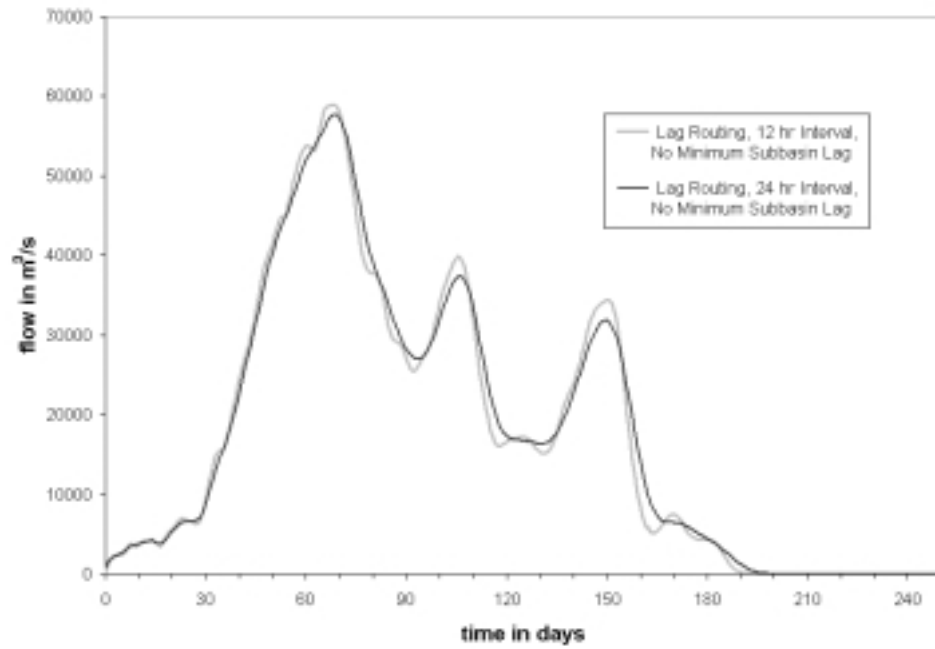


Figure 5-26(a): Effect of Routing Interval on Response with Lag Routing

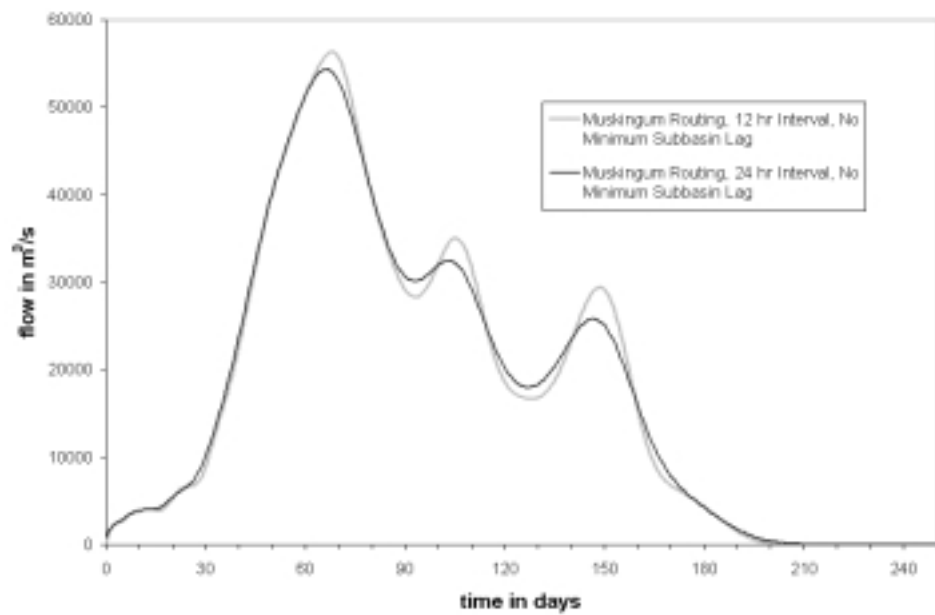


Figure 5-26(b): Effect of Routing Interval on Response with Muskingum Routing

For both the Muskingum and Lag routing runs, an increase in routing interval leads to increased dispersion. This increased dispersion can be attributed to the stretching of flow at junctions where one flow element transfers flows to the next downstream element. The discretization of time into routing intervals ensures that flow is stretched at such intersections. For example, a flow time of 3.4 days could be interpreted in one of three ways when routing flow at a daily time interval. The flow time could be converted to a whole number of routing intervals by rounding off to the nearest whole number, 3 days in this example. The flow time could also be rounded off to the next higher whole number, 4 days in this example, with the implicit assumption that flows arriving after the third day can only contribute to the fourth day. The third approach, which is adopted by HMS, involves resolving the uncertainty in definition of arrival interval by dividing the flow between the two adjacent intervals, the 3<sup>rd</sup> or the 4<sup>th</sup> days in this example. For the 3.4-day flow time assumed in the example above, 60% of the flow is assumed to arrive within the 3<sup>rd</sup> day while the remaining 40% arrives within the 4<sup>th</sup> day. This subdivision results in the stretching out of flow, and the magnitude of the stretching out is proportional to the magnitude of the routing interval over which the flow is split. Larger routing intervals therefore lead to more dispersed flows.

There is a secondary mechanism that acts to increase dispersion with increasing routing interval when the Muskingum method is applied. The number of routing subreaches, the Muskingum  $n$ , in each river reach decreases with increasing routing interval. Consequently, keeping all other factors constant, the

amount of dispersion experienced by flow within each routing subreach also increases. This increase must however be balanced with the decrease in dispersion due to the reduction in the number of points at which flow is rerouted within each river reach. (Dispersion at change over points occurs within a river reach every time flow is passed from one routing subreach to the next). The change in dispersion with change in routing interval is slightly higher for the Muskingum runs than pure lag runs in Table 5-9. This indicates that the length of the routing sub-reaches is a more important factor in determining routing reach dispersion characteristics than the number of internal change points within the reach.

#### **5.4 COMPARISON WITH OBSERVED FLOWS**

The concept of a basin response, used in sections 5.2 and 5.3 of this dissertation, allows the effect of modeling parameters to be studied. Changes in the basin response provide an indication of how changes in a given model parameter influence flow characteristics. However, a basin response is not a realistic representation of the flow transformation process in a continental scale basin because it incorporates an assumption of uniformly distributed input. In large basins, the occurrence of rainfall is non-uniform both in space and in time. The validation of the transformation process of a continental scale routing model must consequently be done by comparison with observed flow data. Simulation runs to compare routed flows with observed flows are described in sections 5.4.1 and 5.4.2 for the respective STS and HMS models.

#### **5.4.1 Comparing STS Simulated Flows with Observed Flows**

The distributed nature of sources in the STS model makes it more suited for routing spatially distributed input. This would in turn require the use of a land-atmosphere interaction or other water balance model for input runoff generation. The use of such a runoff model would result introduce an additional source of errors making it difficult to determine which set of errors to attribute solely to the routing model. A single source, whose location was designated by a river gauging station, was defined for the comparison in this study. Mongalla, a gauging station located just upstream of the Sudd marshes in the Nile basin, was defined as the source. Lake Nyong, located about 409 km downstream of Mongalla, was defined as the sink location. In-stream flows recorded at Mongalla were routed using the diffusion wave equation to Lake Nyong. Observed flows at Lake Nyong were then compared with simulated flows at the same station. Because of the presence of the Bahr el Zeraf and other braided channels between the two stations, the magnitude of the routed and simulated flows at the station were not compared. However, the translatory characteristics of flow including velocity and dispersion coefficient can be deduced from the intercomparison.

Appropriate values of velocity and dispersion coefficient were determined using the method of moments previously mentioned in section 4.1.4 of this dissertation. 10 day observed flows for the period 1953 to 1957 (Hurst and Phillips, 1931-) were used in this analysis. The flow values used in this analysis are also given in Appendix 5 of this dissertation. As shown in Figure 5-27, both the inflow hydrograph at Mongalla and the discharge at Lake Nyong were broken

into 3 periods each representing a full hydrograph cycle with a duration of one year.

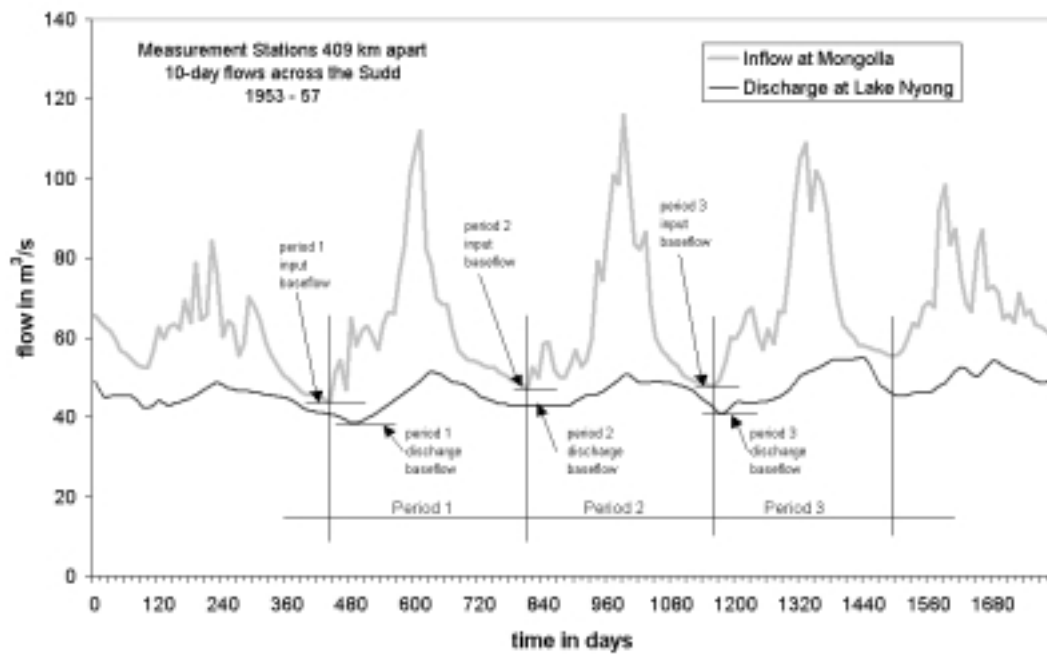


Figure 5-27: Inflow and Discharge Hydrographs in the Sudd Marshes

Within each of these periods, a constant discharge baseflow separation was performed to allow for better isolation of the input flow signal. The lowest flow recorded during the period was defined as the baseflow, and all flows above this baseflow were defined as runoff for the source at Mongalla. Likewise, a baseflow for each period was defined for the discharge at Lake Nyong, and flows in excess of this were defined as sink discharges. Figures 5-28 (a), (b) and (c) show the excess inflows and discharges for periods 1, 2 and 3, respectively.

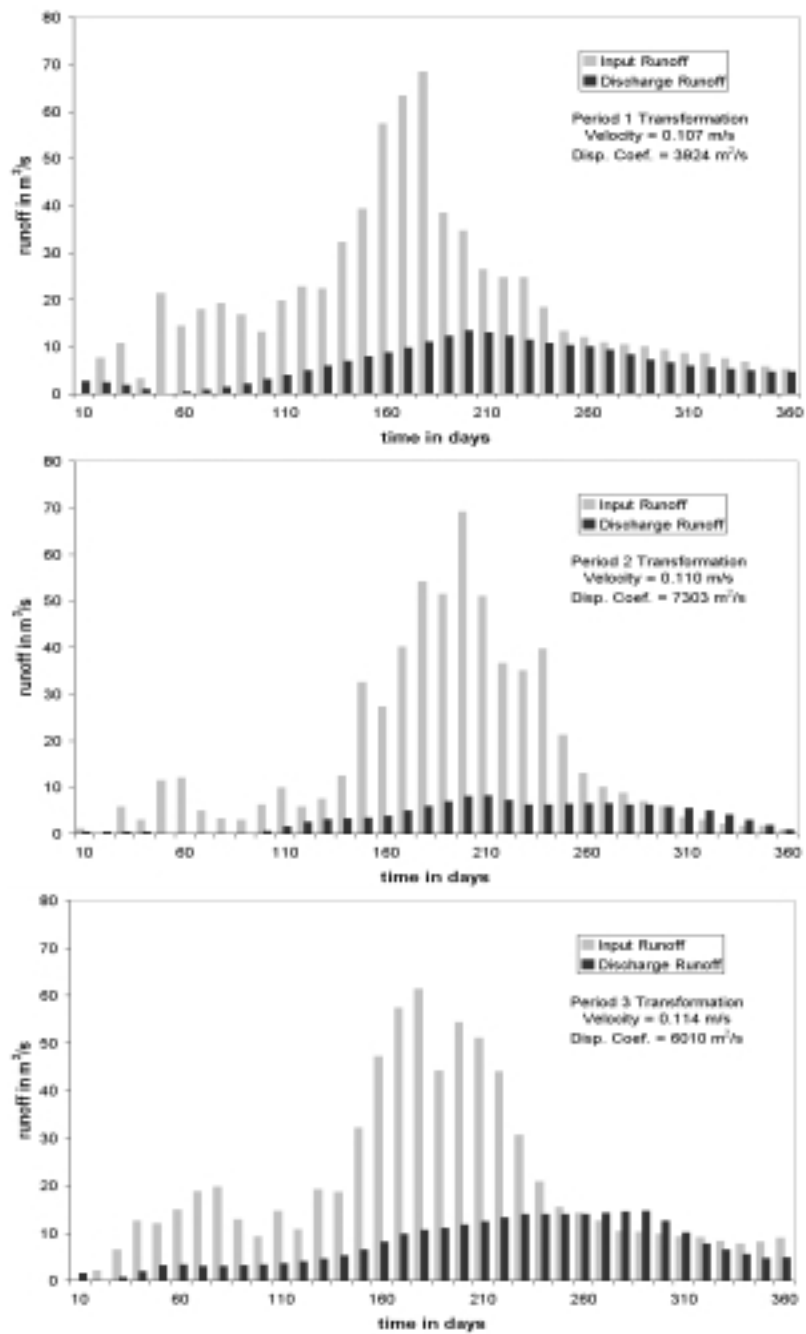


Figure 5-28: Excess Input and Discharge Runoff after Baseflow Separation for (a) Period 1, (b) Period 2 and (c) Period 3



Table 5-10 below shows the duration of the periods, the 1<sup>st</sup> and 2<sup>nd</sup> moments of the excess flows and the velocity and dispersion coefficients resulting from the moments. Velocity is computed by dividing the difference in 1<sup>st</sup> moments of the input and discharge by the distance between the source and the sink (409 km). Variance along the flow path is computed as the difference between the 2<sup>nd</sup> moments of the input and discharge about their respective means. Dispersion coefficient is then computed from the variance using Equation 4-12 in section 4.1.4.

Table 5-10: Routing Parameters Computed by Method of Moments

<b>Period</b>	<b>Period 1</b>	<b>Period 2</b>	<b>Period 3</b>
<b>Start</b>	440	800	1160
<b>End</b>	790	1150	1510
<b>Input Baseflow</b>	43.9	47.2	47
<b>Discharge Baseflow</b>	38.5	42.7	40.8
<b>Input 1st Moment about origin</b>	173.5046	191.4872	185.4032
<b>Discharge 1st Moment about origin</b>	217.6234	234.3801	227.1073
<b>Input 2nd Moment about mean</b>	5184.534	3208.575	5134.602
<b>Discharge 2nd Moment about mean</b>	5532.649	3803.898	5584.91
<b>Velocity (m/s)</b>	<b>0.107297</b>	<b>0.110363</b>	<b>0.113509</b>
<b>Dispersion Coefficient (m<sup>2</sup>/s)</b>	<b>3924.246</b>	<b>7302.953</b>	<b>6010.043</b>

Figures 5-29 (a), (b) and (c) show a comparison of observed excess discharge at Lake Nyong (shown as black bars) with the simulated discharge (shown as gray bars) using the velocity and dispersion parameters computed for the respective periods in Table 5-10. The input at Mongalla for each period is represented by a continuous gray line.

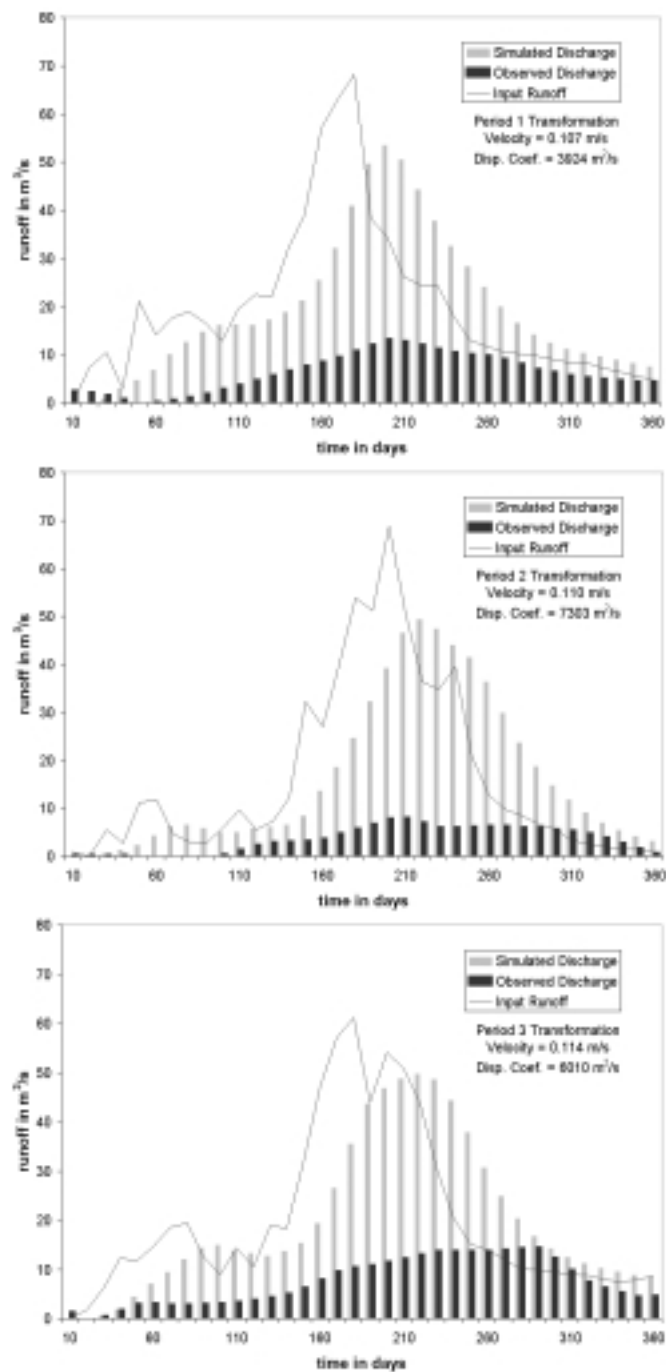


Figure 5-29: Routing Excess Runoff using Computed Velocities and Dispersion Coefficients for (a) Period 1, (b) Period 2 and (c) Period 3

The mean values of the velocity and dispersion coefficient were computed from the three period values as 0.11 m/s and 5746 m<sup>2</sup>/s, respectively. Figure 5-30 shows the effect of routing the entire input at Mongalla to Lake Nyong using the diffusion wave equation with the computed mean velocity and dispersion coefficient. In the figure, the light gray line represents the input at Mongalla while the thicker gray line is the simulated discharge at Lake Nyong. The black line represents the observed flows at Lake Nyong.

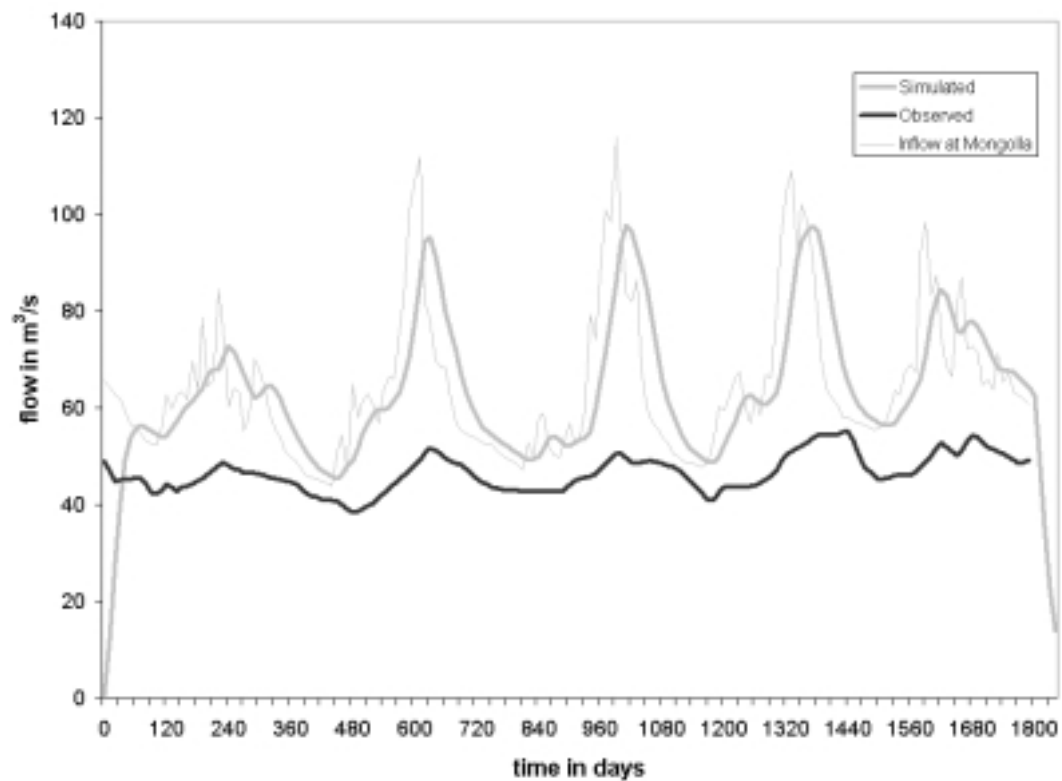


Figure 5-30: Effect of Routing Input Flow using Mean Velocity and Dispersion Coefficients

From the diagram, it can be seen that despite differences in magnitude, the transformation with mean parameters is able to capture key features of the observed flow at Lake Nyong. The simulated and observed hydrographs peak at about the same time indicating that the mean velocity is representative of the translation velocity in the field. The width of the hydrograph cycles of the simulated and observed cases are also approximately the same indicating that the dispersion coefficient results in the right amount of spread. It can therefore be concluded that the method of moments results in parameters that ensure a representative transformation of inputs at a source to discharges at a sink. Hence a STS model for which velocity and dispersion coefficient are estimated by the method of moments results in a good representation of the flow process in a real hydrologic system.

#### **5.4.2 Comparing HMS Simulated Flows with Observed Flows**

Having compared performance of the respective STS and HMS models under various parametric conditions, a set of runs was required to compare simulated flows from the model with observed data. For these comparisons, the routing process had to be isolated from the soil water balance process which is typically used to generate input runoff for routing models. Without such isolation of the two processes, it would be impossible to determine from the resulting flows which errors to attribute to the routing process and which to attribute to the water balance process. Hence model verification in this study was done by routing

observed flows at an upstream gauging location to a downstream location using an HMS model and comparing the results with observed flows at the downstream location. The quantity of simulated flow in this test is not expected to equal the observed flow exactly since flow entering the river system between the two gauging locations is not taken into account. However, the flows simulated by the model should duplicate the major features of the observed hydrograph at the downstream gauge if upstream stations with comparatively high flows as chosen as the input sources. Comparisons of this nature were performed for the HMS model and the results are described in this section. The simulations were conducted in the Nile basin because of the availability of flow data at various locations throughout the basin. Upstream source stations were located at Mongalla and Roseires in the White and Blue Nile respectively. Downstream observation points were located at Malakal, Khartoum and Aswan. Figure 31 (a) shows a map of the Nile Basin with the gauge and source locations indicated. Part (b) of the figure shows the HMS representation of the basin.

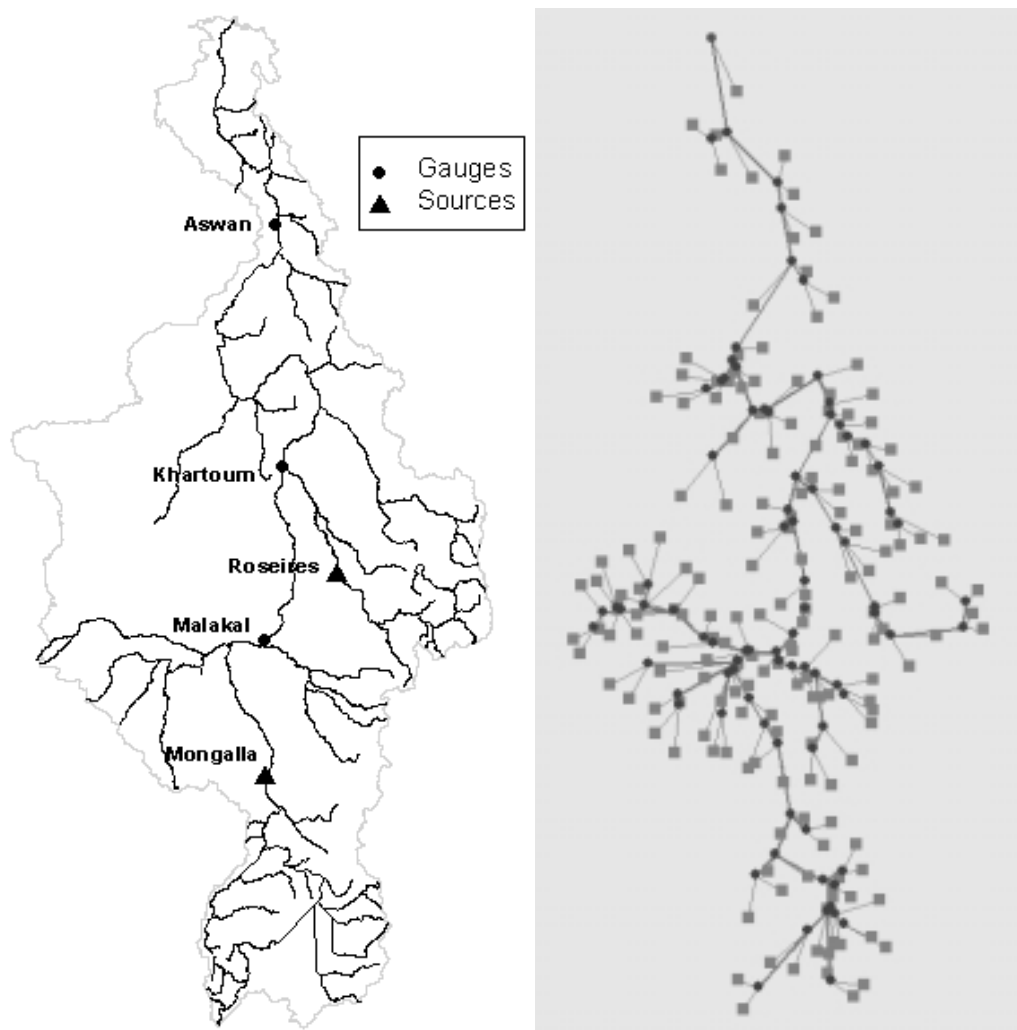


Figure 5-31: Nile Basin (a) Gauge Locations and (b) HMS Model Components

Malakal is the first major gauging station that captures the flows coming out of the Sudd Marshes in Southern Sudan. The high dispersion coefficients and low velocities encountered in the region ensure that flow undergoes significant redistribution between Mongalla and Malakal. In addition, flows from the small Bahr el Ghazel and Sobat tributaries of the White Nile are neglect in this analysis.

Nevertheless, the simulated hydrograph at Malakal generally arrives at the same time and has similar flow distribution as the observed flows at the same station. Figure 5-32 shows the match between the simulated and observed flows at Malakal.

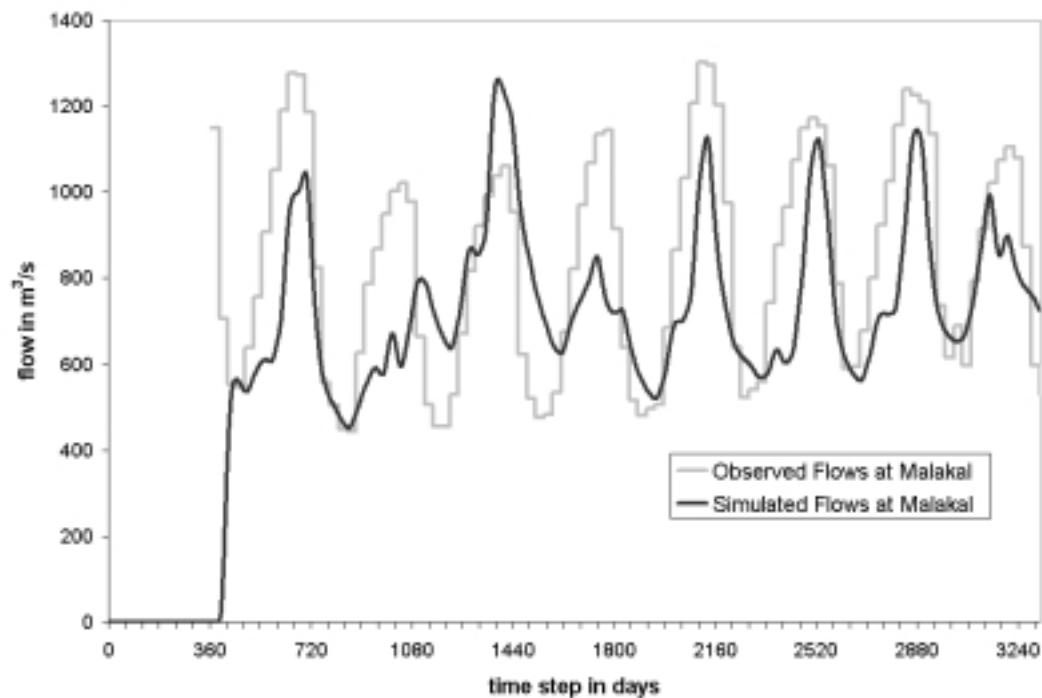


Figure 5-32: Observed and HMS Simulated Flows at Malakal

Simulated flows match observed flows almost exactly at Khartoum because of the relatively short time of translation for flow between Roseires and Khartoum. Steep slopes in the region result in high flow velocities with low in-stream dispersion rates. The routing model was consequently able to simulate

flow between the two stations almost exactly. Figure 5-33 shows the match between observed and HMS simulated flows at Khartoum.

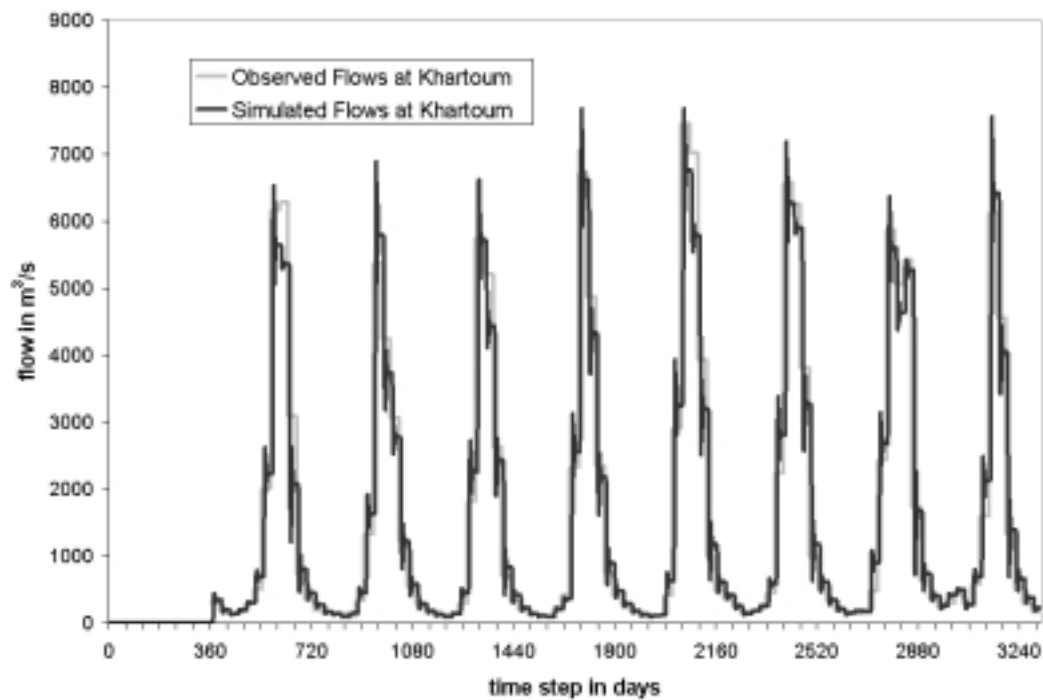


Figure 5-33: Observed and HMS Simulated Flows at Khartoum

Aswan is located downstream of the intersection between the White and Blue Nile tributaries. Routed flows from the two tributaries are superimposed at the station. Figure 5-34 shows a comparison between the simulated and observed flows at Aswan. The simulated hydrographs capture the rise and fall of the observed flow hydrographs well though the simulated flows are generally smaller in magnitude.



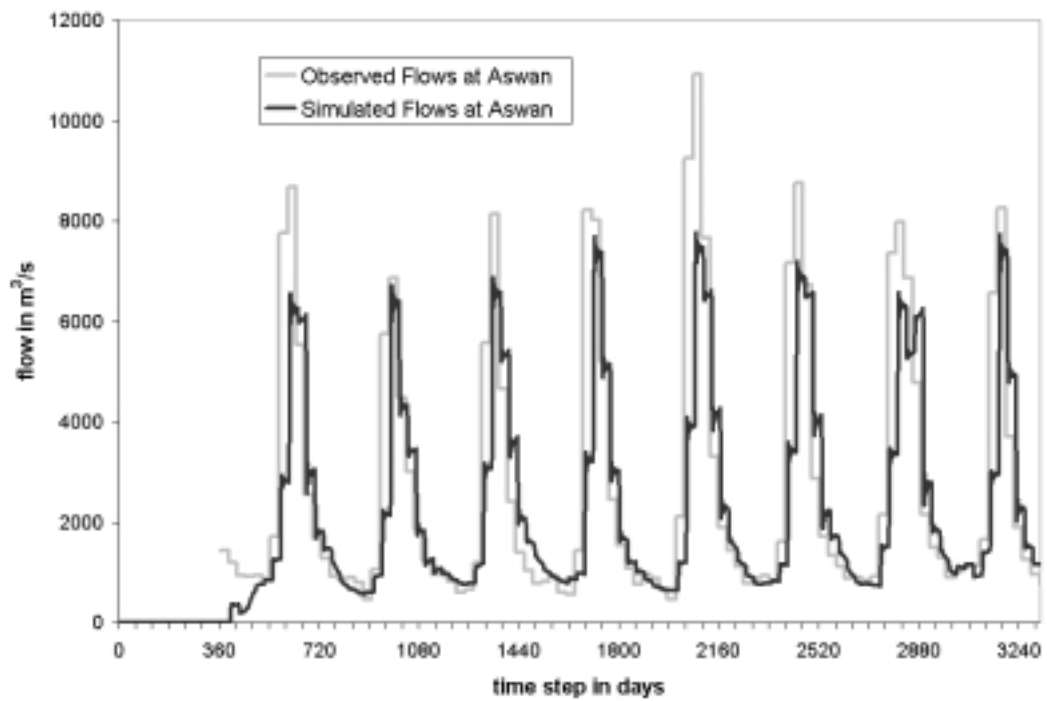


Figure 5-34: Observed and HMS Simulated Flows at Aswan

The results of these simulations indicate that an HMS model can be used to route flow in a continental scale basin like the Nile. It allows flows to be routed over long distances through various types of topographic conditions, and routed flows from various upstream sources can be superimposed at location further downstream. The use of HMS as a baseline model for comparisons with the STS model is consequently justifiable.

## CHAPTER 6

### Conclusions and Recommendations

#### 6.1 CONCLUSIONS

The measure of the success in any study is the extent to which the research objectives have been met. In this section, the objective of the study as laid out in section 1.2 of this dissertation are revisited to determine the extent to which they have been met. The lessons learnt in meeting each objective are subsequently summarized in sections 6.1.1 to 6.1.3.

The first research objective was stated as follows:

*“to develop a GIS database to support large-scale surface water routing globally”*

The global terrain analysis performed with 1 kilometer Digital Elevation Models of the earth resulted in corrected terrain grids, flow direction grids, flow accumulation grids, flow length grids and drainage basins of the whole world. These data were subsequently used to parameterize two surface water models for continental scale.

The second research objective was stated as follows:

*“to implement a modeling framework which incorporates basin boundaries in a grid based model while maintaining computational efficiency by only performing routing at desired locations”*

A routing model which subdivided the earth into a series of 0.5 by 0.5 degree boxes was implemented globally. The modeling framework allowed for the incorporation of drainage basin boundaries and modeling unit boundaries defined in water balance model by intersecting vector representations of the respective boundaries to define new modeling units called sources. The modeling framework was implemented in the routing of runoff generated by a Global Circulation Model (GCM) to terminal points (also called sinks) at the continental margin and in internally draining catchments. Computational efficiency was ensured by routing flows from directly from the sources to their respective sinks.

The third objective was stated as follows:

*“to examine of the robustness of the source to sink approach as compared to the watershed based approach in continental scale applications”*

The Source to Sink (STS) routing model was compared with the watershed modeling approach of the Hydrologic Modeling System (HMS) in the Congo and Nile basins, two of the largest river basins in Africa. The basin responses computed by the two modeling approaches were compared for various spatial and temporal resolutions, and for uniform and non-uniformly distributed routing parameters.

The three objectives of the study have therefore been met. The key inferences made during each phase of the research are described in sections 6.1.1 to 6.1.3 below.

### **6.1.1 Inferences from Global Terrain Analysis**

Due to the high number and varied characteristics of pits in DEMs, the differentiation of inland catchments from erroneously created pits is best done by referring to other secondary sources of information such as cartographic maps and databases of lakes. Inland catchments identified from such secondary sources can subsequently be preserved in the DEM.

In creating DEMs which correctly represent flow direction, the insertion of a single null value cell at the lowest elevation of an inland catchment is sufficient to preserve the boundaries of the inland catchment as well as the flow direction of all cells that drain towards it. Large inland water bodies such as the Caspian Sea can also be preserved in the DEM using a single null value cell.

Flow direction grids can be checked for the presence of pits by computing a histogram of the cell values. The presence of cell values other than powers of 2 from 0 to 8 implies that there are pits in the DEM.

The eight direction pour point model used to determine flow direction in this study is biased in favor of the four cardinal directions. However, this bias does not adversely impact the location of river networks and basin boundaries delineated from the resulting flow direction grid.

The definition of the study area in a large scale terrain analysis must take into account the location of major drainage basin boundaries as well as the computer processing resources available for the study. In this study for example, the inclusion of the drainage basin of the Caspian Sea in Asia would result in a

DEM with well over 50 million grid cells. A DEM of this size would be too large to be processed using the computer resources available for the study.

After eliminating erroneously created pits, delineations performed using the 30 arc-second DEM resulted in river networks and drainage basins that corrected represented the actual locations of the respective features. While there were some minor deviations between delineated and actual drainage features, no blunders which would severely impact the results of hydrologic modeling applications developed using these derived datasets were identified. The 30 arc-second DEMs are therefore suitable for continental scale hydrologic delineation and parameter derivation.

#### **6.1.2 Inferences from Global STS Model Implementation**

If the modeling units of a source to sink model are defined in a vector environment (as opposed to a raster environment) then they can assume any shape. Hence a source defined on a rectangular mesh (in geographic coordinates) can be split up into smaller sources if the drainage basin boundary passes through it. Thus a source to sink model constructed in a vector environment can retain the rectangular land surface subdivision used in other grid-based models while incorporating the exact location of basin boundaries delineated from the DEM.

After the processing of underlying DEMs, source to sink models of any resolution can be developed with relative ease. The process involves dividing the continental margin into desired segments, delineating drainage basins from these segments and subdividing the basins into sources whose parameters are then

determined from the processed DEM using zonal averaging and summation functions. This is a much less involved process than that required to change the resolution of a cell to cell model or a watershed based model.

The use of the diffusion wave equation instead of the linear reservoir equation in continental scale cell to cell routing models could significantly reduce the scale dependence of these models.

Links between routing models and atmospheric or soil water balance models which provide input runoff for the routing process can be established by spatially intersecting the respective modeling units. Such an intersection results in modeling units that are uniquely linked to both the input and routing models by key fields.

Links between routing models and ocean models which receive routed flows can be established by using ocean modeling units located at the continental margin as outlets in the drainage basin delineation. All modeling units defined within each drainage basin can subsequently be linked to the single receiving ocean model unit used to delineate the basin.

The use of non-uniform velocity and dispersion parameters in continental scale routing applications can significantly alter the response of a river basin. It may expose important hydrograph features that cannot be depicted with a uniform parameter model. The STS model implemented in this study is an improvement over other STS models because it can account for spatially distributed velocity and dispersion parameters.

### **6.1.3 Inferences from HMS Model Development**

The preprocessor used in the delineation of HMS hydrologic elements, CRWR Prepro, was able to accurately classify and derive the connectivity among 3150 hydrologic elements at the continental scale. The preprocessor was also able to determine hydrologic routing parameters for each of the elements based on the DEM and additional parameters supplied.

While the preprocessor ensures that subbasin routing parameters are within the ranges permitted by HMS, it does not perform a similar check for river reach routing parameters. River reach parameters that are outside the constraints set by HMS can result from the preprocessing and may require manual editing to correct.

The process of deriving HMS basin files from DEMs at the continental scale is memory intensive and time consuming. Consequently, care must be taken in defining the modeling parameters such as delineation threshold, flow velocity and other routing parameters to be used in creating the model.

In working with HMS at the continental scale, it was determined that some of its imposed constraints on routing parameters, particularly those relating to the maximum river reach lag time and the maximum number of routing subreaches for a Muskingum reach, could be removed without affecting the accuracy of the routed flows.

Given a field of spatially distributed flow velocities and dispersion coefficients, the weighted flow length function can be used in conjunction with

and the method of moments to determine routing parameters for hydrologic elements in an HMS model.

An HMS model is sufficient to represent the processes observed in flow at the continental scale. It is able to perform flow routing over long distances, through various topographic conditions and aggregate flow from various sources. It is therefore a suitable model to use for model intercomparisons at the continental scale.

#### **6.1.4 Inferences from Comparing STS and HMS Models**

The hydrologic processes exhibited by an HMS model were successfully duplicated using a STS model. A better match was obtained when a finer delineation threshold was specified for the HMS model. At the finer threshold input runoff spends more time within the flow channels than on the land surface, making it similar to the single flow path approach of the STS model.

Any model that involves subdividing the earth into a series of linked segments as in the watershed based and cell to cell models, will result in numerical dispersion. This is because at the end of each segment, an essentially continuous response must be discretized into time steps. The discretization results in the redistribution of flow between two or more adjacent time steps at the end of each segment. The larger the number of segments, the larger the net dispersion experienced by flow arriving at the discharge outlet.

The discretization of continuous flow at the end of a segment occurs only once in a source to sink model irrespective of the resolution of the model. In a



watershed based model, discretization occurs every time flow is passed from one flow element to another. The choice of spatial resolution of a watershed based model greatly influences the dispersion properties of the model while the dispersion properties of a source to sink model are relatively unaffected by the choice of spatial scale.

Redistribution of flow due to discretization is also influenced by the choice of routing interval. A large routing interval results in greater redistribution every time flow is discretized. The dispersion characteristics of a watershed based model are consequently impacted more by the choice of temporal resolution than those of a source to sink model in which redistribution only occurs once.

Velocity and dispersion parameters in a river basin can be derived from observed flow data by equating the difference between the moments of flow at two gauging stations to the moments of the flow routing method used in the model. The method of moments is consequently a good approach for deriving spatially distributed velocity and dispersion parameters.

Grids of spatially distributed velocity and dispersion coefficients can be used to parameterize both a watershed based model using the Muskingum equation for in-stream routing and a dispersion type source to sink model, irrespective of resolution. The resulting basin responses for the STS and HMS models are very similar. Hence, parameterizing watershed based models from spatially distributed grids of velocity and dispersion coefficient can reduce their spatial scale dependence.

## **6.2 RECOMMENDATIONS**

The development of a global grid of flow velocity and dispersion coefficients would greatly advance the development of continental scale routing models. The derivation of these parameters from observed flow data using the method of moments offers a promising avenue to proceed with this development. The approach lends itself to automated implementation using network algorithms since distances and hierarchy along a river network can be determined automatically. Further research could be conducted to investigate the possibility of implementing this approach globally using a river network model with flow gauges and associated flow time series along it.

In testing the longitudinal decomposability of the diffusion type source to sink model in this study, a diffusion type cell to cell routing model was developed. The model offers all the advantages of a conventional cell to cell model while simultaneously affording many of the advantages of diffusion wave routing such as longitudinal decomposability as well as spatial and temporal scale independence. The implementation of the diffusion type cell to cell routing and its comparison with the linear reservoir type cell to cell model would provide valuable insight into its viability at the continental scale.

The assumption of time invariant flow velocities and dispersion coefficients may be insufficient to represent the flow regime in some regions. Further research is required to study the effect of temporally varying routing parameters on the basin response. In regions where time invariant parameters are shown to be insufficient, alternate flow paths between a source and a sink could

be defined to allow flow to be routed using different response functions at different flow stages. Further research is required to develop ways of partitioning flow into different flow paths to allow the continued application of the source to sink method in such regions.

Flow regimes in nature are often interrupted by the presence of reservoirs and other control structures with non-linear release schedules which cannot be included in the linear source to sink model. A secondary source to sink model could be used to route upstream flow into the reservoir, followed by the application of the reservoir regulation rules to determine reservoir discharges. Such a nested source to sink approach would allow the reservoir and the sources located upstream of it can be treated a single source whose input could subsequently be routed in the primary source to sink model as before. Research towards the implementation of such an approach and its testing in a large basin would further enhance the ability of the source to sink model to represent flow regimes encountered at the continental scale.

The use of the diffusion wave equation for routing was found to result in significantly less scale dependent models. Its inclusion as a routing option in a watershed based model like HMS would result in a much more versatile model. Further research should be conducted to determine the scale dependence of a watershed based model employing the diffusion wave equation for in-stream routing.

## **APPENDICES**

### **Contents**

**Appendix 1:** AML Code for Source to Sink Model Preprocessing

**Appendix 2:** Parameters of the T42 mesh

**Appendix 3:** FORTRAN Code for Source to Sink Routing Model

**Appendix 4:** AML Code for Computing Equivalent Muskingum Parameters from  
a Field of Velocities and Dispersion Coefficients

**Appendix 5:** 10 day flows in the Nile basin, 1953-57

## Appendix 1: AML Code for Source to Sink Model Preprocessing

```
/* -----
/*                               STSPREPRO.AML
/* ARC MACRO LANGUAGE (AML) CODE FOR PREPROCESSING STS MODELING UNITS
/* -----
/* BY FRANCISCO OLIVERA AND KWABENA ASANTE
/* CRWR, UNIV. OF TEXAS AT AUSTIN
/* WITH EXTRACTS FROM CODE BY FERDINAND HELLWEGER
/* -----
/* THIS PROGRAM TAKES USGS FLOW DIRECTION GRIDS (HYDRO1K DATASET) AND
/* USES THEM TO DEFINE SINKS, DELINEATE RIVER BASINS, DEFINE AND
/* PARAMETERIZE SOURCES FOR THE STS MODEL.
/* -----
/* INPUTS INCLUDE:
/*      USGS FLOW DIRECTION GRID              -> AF_FD
/*      OCEAN 5-DEGREE MESH COVERAGE          -> SEALAMB
/*      LAND SURFACE MESH (0.5-DEGREE) COVERAGE -> MESHAFRLAM
/*      SOIL WATER BALANCE UNITS MESH COVERAGE -> T42AFR
/* -----
/* *****

/* INITIAL SETTINGS
SETWINDOW AF_FD AF_FD
SETCELL AF_FD

/* ASSIGNING NODATA TO THE SINK CELLS (INTERNAL AND EXTERNAL)
FDR0 = CON(AF_FD <> 55537, AF_FD)
SINKS = SINK(FDR0)
SINKSZERO = ISNULL(SINKS)
FDR = FDR0 / SINKSZERO

/* CREATING THE CONTINENT BORDER (VECTOR AND RASTER)
BORDER = GRIDPOLY(CON(FDR,1))
QUIT
CLEAN BORDER BORDERLN # # LINE
GRID
/* INITIAL SETTINGS
SETWINDOW AF_FD AF_FD
SETCELL AF_FD

SEASHORE1 = CON(LINEGRID(BORDERLN),1)
SEASHORE_SW = CON(SEASHORE1(0,-1) == 1 AND SEASHORE1(1,0) == 1,1)
SEASHORE_SE = CON(SEASHORE1(0,-1) == 1 AND SEASHORE1(-1,0) == 1,1)
SEASHORE_NE = CON(SEASHORE1(0,1) == 1 AND SEASHORE1(-1,0) == 1,1)
SEASHORE_NW = CON(SEASHORE1(0,1) == 1 AND SEASHORE1(1,0) == 1,1)
```

```

SEASHORE2 =
MERGE( SEASHORE1, SEASHORE_SW, SEASHORE_SE, SEASHORE_NE, SEASHORE_NW)

SEAMESH = POLYGRID( SEALAMB, SEALAMB-ID)
SEASHORE = SEASHORE2 * SEAMESH
SEA_WSH = WATERSHED( FDR, SEASHORE)
SEA_WSH_PC = GRIDPOLY( SEA_WSH)
QUIT
/* WHAT ABOUT BUILDING THE TOPOLOGY OF SEA_WSH
TABLES
SELECT SEALAM.PAT
ALTER AREA
AREACOARSE
~
~
~
~
SELECT MESHAFRLAM.PAT
ALTER AREA
AREAFINE
~
~
~
~
QUIT
INTERSECT MESHAFRLAM SEA_WSH_PC MESHFINEWSH
QUIT
TABLES
SELECT MESHFINEWSH.PAT
RESELECT GRID-CODE < 0
PURGE
Y
QUIT

/* CREATE THE ZONE GRID FOR THE ZONALSTATS COMMAND
/* USE 500 INSTEAD OF 1000 FOR BETTER POLYGON DEFINITION

POLYGRID MESHFINEWSH FINEWSHGRID MESHFINEWSH-ID
500
Y

GRID

/* INITIAL SETTINGS
SETWINDOW AF_FD AF_FD
SETCELL AF_FD

/* COMPUTE MEAN FLOWLENGTH FROM FLDS USING FINEWSHGRID TO DEFINE ZONES

```

```

MEANLENGRID = ZONALMEAN ( FINEWSHGRID , FLDS , DATA )

/* CONVERT TO AN INTEGER GRID
MEANLEN = INT ( MEANLENGRID )
BUILDVAT MEANLEN

/* ASSIGN 999999999999 TO NODATA CELLS
MEANLEN2 = CON ( ISNULL(MEANLEN), 999999999999, MEANLEN)
BUILDVAT MEANLEN2
QUIT

/* MOVE POLYGON LABELS TO CENTROID BUT ENSURE ALL LABELS WITHIN POLYGON
CENTROIDLABELS MESHFINEWSH INSIDE

/* ADD X AND Y COORDINATES TO PAT AND CREAT FIELD SPOT
ADDXY MESHFINEWSH

DROPITEM MESHFINEWSH.PAT MESHFINEWSH.PAT SPOT
ADDITEM MESHFINEWSH.PAT MESHFINEWSH.PAT SPOT 16 16 B 3

/* GO INTO ARC PLOT TO READ VALUES FROM GRID TO POLYGON
/* DISPLAY 1040 DOES NOT REQUIRE A VISUAL DISPLAY, ONLY AN OUTPUT FILE
(DISTORE)
/* USEFUL FOR REMOTE EXECUTION
AP
DISPLAY 1040
DISTORE
MAPE MESHFINEWSH

/* RESEL MESHFINEWSH POLY OVERLAP BORDER POLYGON WITHIN
/* THIS LINE IS NOT REQUIRED WHEN USING MEANLEN2
/* DECLARE AND OPEN A CURSOR TO READ AND WRITE TO THE PAT

CURSOR PTCUR DECLARE MESHFINEWSH POLY RW
CURSOR PTCUR OPEN
CURSOR PTCUR FIRST

&S OLD$ECHO [SHOW &ECHO]

/*START A LOOP TO GO THROUGH THE PAT, FIND THE CELL VALUE AT EACH
/*POINT LOCATION, AND WRITE IT TO THE SPOT ITEM IN THE PAT.

&DO &WHILE %:PTCUR.AML$NEXT%
&S :PTCUR.SPOT := [SHOW CELLVALUE MEANLEN2 [SHOW SELECT MESHFINEWSH POLY
1 XY]]
CURSOR PTCUR NEXT
&END

CURSOR PTCUR CLOSE

```

```
Q      /*QUIT FROM ARC PLOT

&DATA ARC INFO; ARC
SEL MESHFINEWSH.PAT
ALTER SPOT
FLOWLENGTH,,,,,,,,,
Q STOP
&END
&RETURN /*TO CALLING AML
```



## Appendix 2: Parameters of the T42 mesh

(SUPPLIED BY WILLIAM G. LARGE, CLIMATE SYSTEM MODEL GROUP,  
NATIONAL CENTER FOR ATMOSPHERIC RESEARCH)

THE FOLLOWING ARE THE PARAMETERS OF THE T42 MESH ON WHICH THE COMMUNITY CLIMATE MODEL (CCM3) GENERATES INPUT RUNOFF.

**I AND J** ARE COORDINATE INDICES FROM INDICATING THE LOCATION OF THE RUNOFF GENERATING UNIT

**XEDGE AND YEDGE** ARE THE LONGITUDE AND LATITUDE OF THE LOWER LEFT CORNER OF EACH RUNOFF GENERATING UNIT (VALUES OF -1 ARE DUMMY VALUES)

**XMID AND YMID** ARE THE LONGITUDE AND LATITUDE OF THE CENTROID OF EACH RUNOFF GENERATING UNIT (VALUES OF -1 ARE DUMMY VALUES)

I/J	XEDGE	XMID	YEDGE	YMID
1	-1.406	0	-90	-87.864
2	1.406	2.813	-86.48	-85.097
3	4.219	5.625	-83.705	-82.313
4	7.031	8.438	-80.919	-79.526
5	9.844	11.25	-78.131	-76.737
6	12.656	14.063	-75.342	-73.948
7	15.469	16.875	-72.553	-71.158
8	18.281	19.688	-69.763	-68.368
9	21.094	22.5	-66.973	-65.578
10	23.906	25.313	-64.182	-62.787
11	26.719	28.125	-61.392	-59.997
12	29.531	30.938	-58.602	-57.207
13	32.344	33.75	-55.811	-54.416
14	35.156	36.563	-53.021	-51.626
15	37.969	39.375	-50.23	-48.835
16	40.781	42.188	-47.44	-46.045
17	43.594	45	-44.649	-43.254
18	46.406	47.813	-41.859	-40.464
19	49.219	50.625	-39.068	-37.673
20	52.031	53.438	-36.278	-34.883
21	54.844	56.25	-33.487	-32.092
22	57.656	59.063	-30.697	-29.301
23	60.469	61.875	-27.906	-26.511
24	63.281	64.688	-25.115	-23.72

25	66.094	67.5	-22.325	-20.93
26	68.906	70.313	-19.534	-18.139
27	71.719	73.125	-16.744	-15.348
28	74.531	75.938	-13.953	-12.558
29	77.344	78.75	-11.162	-9.767
30	80.156	81.563	-8.372	-6.977
31	82.969	84.375	-5.581	-4.186
32	85.781	87.188	-2.791	-1.395
33	88.594	90	0	1.395
34	91.406	92.813	2.791	4.186
35	94.219	95.625	5.581	6.977
36	97.031	98.438	8.372	9.767
37	99.844	101.25	11.162	12.558
38	102.656	104.063	13.953	15.348
39	105.469	106.875	16.744	18.139
40	108.281	109.688	19.534	20.93
41	111.094	112.5	22.325	23.72
42	113.906	115.313	25.115	26.511
43	116.719	118.125	27.906	29.301
44	119.531	120.938	30.697	32.092
45	122.344	123.75	33.487	34.883
46	125.156	126.563	36.278	37.673
47	127.969	129.375	39.068	40.464
48	130.781	132.188	41.859	43.254
49	133.594	135	44.649	46.045
50	136.406	137.813	47.44	48.835
51	139.219	140.625	50.23	51.626
52	142.031	143.438	53.021	54.416
53	144.844	146.25	55.811	57.207
54	147.656	149.063	58.602	59.997
55	150.469	151.875	61.392	62.787
56	153.281	154.688	64.182	65.578
57	156.094	157.5	66.973	68.368
58	158.906	160.313	69.763	71.158
59	161.719	163.125	72.553	73.948
60	164.531	165.938	75.342	76.737
61	167.344	168.75	78.131	79.526
62	170.156	171.563	80.919	82.313
63	172.969	174.375	83.705	85.097
64	175.781	177.188	86.48	87.864
65	178.594	180	90	-1
66	181.406	182.813	-1	-1

67	184.219	185.625	-1	-1
68	187.031	188.438	-1	-1
69	189.844	191.25	-1	-1
70	192.656	194.063	-1	-1
71	195.469	196.875	-1	-1
72	198.281	199.688	-1	-1
73	201.094	202.5	-1	-1
74	203.906	205.313	-1	-1
75	206.719	208.125	-1	-1
76	209.531	210.938	-1	-1
77	212.344	213.75	-1	-1
78	215.156	216.563	-1	-1
79	217.969	219.375	-1	-1
80	220.781	222.188	-1	-1
81	223.594	225	-1	-1
82	226.406	227.813	-1	-1
83	229.219	230.625	-1	-1
84	232.031	233.438	-1	-1
85	234.844	236.25	-1	-1
86	237.656	239.063	-1	-1
87	240.469	241.875	-1	-1
88	243.281	244.688	-1	-1
89	246.094	247.5	-1	-1
90	248.906	250.313	-1	-1
91	251.719	253.125	-1	-1
92	254.531	255.938	-1	-1
93	257.344	258.75	-1	-1
94	260.156	261.563	-1	-1
95	262.969	264.375	-1	-1
96	265.781	267.188	-1	-1
97	268.594	270	-1	-1
98	271.406	272.813	-1	-1
99	274.219	275.625	-1	-1
100	277.031	278.438	-1	-1
101	279.844	281.25	-1	-1
102	282.656	284.063	-1	-1
103	285.469	286.875	-1	-1
104	288.281	289.688	-1	-1
105	291.094	292.5	-1	-1
106	293.906	295.313	-1	-1
107	296.719	298.125	-1	-1
108	299.531	300.938	-1	-1

109	302.344	303.75	-1	-1
110	305.156	306.563	-1	-1
111	307.969	309.375	-1	-1
112	310.781	312.188	-1	-1
113	313.594	315	-1	-1
114	316.406	317.813	-1	-1
115	319.219	320.625	-1	-1
116	322.031	323.438	-1	-1
117	324.844	326.25	-1	-1
118	327.656	329.063	-1	-1
119	330.469	331.875	-1	-1
120	333.281	334.688	-1	-1
121	336.094	337.5	-1	-1
122	338.906	340.313	-1	-1
123	341.719	343.125	-1	-1
124	344.531	345.938	-1	-1
125	347.344	348.75	-1	-1
126	350.156	351.563	-1	-1
127	352.969	354.375	-1	-1
128	355.781	357.188	-1	-1
129	358.594	-1	-1	-1

### Appendix 3: FORTRAN Code for Source to Sink Routing Model

```
!
!                                ROUTDISP VERSION 1.0
!                                *****
!THIS PROGRAM TAKES RUNOFF GENERATED BY A VERTICAL BALANCE AND ROUTES
!IT TO THE CONTINENTAL MARGIN. THIS VERSION OF THE PROGRAM ACCOUNTS FOR
!BOTH GEOMORPHOLOGICAL AND HYDRODYNAMIC DISPERSION. THIS VERSION ALLOWS
!FOR THE USE OF SPATIALLY VARIABLE FLOW VELOCITY, DISPERSION COEFFICIENT
!AND LOSS COEFFICIENT
!
!INPUTS :
!    SINKCELL.TXT - LIST OF GRID CODES OF THE OUTLET CELLS
!
!    PARAMETER.TXT - LIST OF PARAMETERS (COMMA DELIMITED, NO HEADER)
!        PARAMETER(1) = NUMBER OF TIME STEPS TO BE SIMULATED
!        PARAMETER(2) = INTERVAL FOR RUNOFF GENERATION IN SECONDS
!        PARAMETER(3) = NUMBER OF OUTLETS OR SINK CELLS
!        PARAMETER(4) = NUMBER OF DRAINAGE POLYGONS OR SOURCES
!
!    LANDCELL.TXT - LIST OF ATTRIBUTES OF SOURCES (COMMA DELIMITED)
!        WITH A SINGLE LINE ASSIGNED FOR EACH SOURCE.
!        ATTRIBUTES INCLUDE
!            SOURCE-ID DEFINED BY THE SOURCE COVERAGE POLYGON ID
!            AREA OF THE SOURCE IN METERS SQUARED
!            SINK-ID DEFINED BY GRID-CODE OF DRAINAGE BASINS
!            FLOW LENGTH FROM SOURCE TO SINK IN METERS
!            VELOCITY ALONG THE FLOW PATH IN METERS PER SECOND
!        DISPERSION COEFFICIENT IN METERS SQUARED PER SECOND
!        LOSS COEFFICIENT IN FRACTION OF FLOW LOST PER SECOND
!        KEY FIELD LINKING SOURCES TO INPUT RUNOFF UNITS
!
!    INPUT RUNOFF FILES - H0001.TXT TO H3700.TXT
!        ONE FILE FOR EACH SIMULATION TIME STEP CONTAINING
!            AN X-COORDINATE INDEX FROM 1 TO 128
!            A Y-COORDINATE INDEX FROM 1 TO 64
!            INPUT RUNOFF IN MILLIMETERS PER SECOND
!
!    INFILES.TXT - LISTS NAMES OF INPUT RUNOFF FILES
!
!OUTPUTS :
!
!    INFLOW.TXT - RUNOFF VOLUME (M3) ENTERING EACH BASIN PER TIME STEP
!
!    SINKFLOW.TXT - DISCHARGE (M3/S) TO EACH SINK PER TIME STEP
!
!
```



```

ALLOCATE (RUNOFFIN(8192, STEPS), STAT = ALLOCATESTATUS)
IF (ALLOCATESTATUS /= 0) STOP "***NOT ENOUGH MEMORY: RUNOFFIN()***"

ALLOCATE (T42RUN(SOURCES), STAT = ALLOCATESTATUS)
IF (ALLOCATESTATUS /= 0) STOP "***NOT ENOUGH MEMORY: T42RUN() ***"

ALLOCATE (FILENAME(STEPS), STAT = ALLOCATESTATUS)
IF (ALLOCATESTATUS /= 0) STOP "***NOT ENOUGH MEMORY: FILENAME()***"

ALLOCATE (ADESUM(SOURCES), STAT = ALLOCATESTATUS)
IF (ALLOCATESTATUS /= 0) STOP "***NOT ENOUGH MEMORY: ADESUM()***"

ALLOCATE (LOSSFACTOR(SOURCES), STAT = ALLOCATESTATUS)
IF (ALLOCATESTATUS /= 0) STOP "***NOT ENOUGH MEMORY: LOSSFACTOR()***"

ALLOCATE (LOSSES(SINKCELLS, STEPS), STAT = ALLOCATESTATUS)
IF (ALLOCATESTATUS /= 0) STOP "***NOT ENOUGH MEMORY: LOSSES()***"

ALLOCATE (LANDCELL(SOURCES, 8), STAT = ALLOCATESTATUS)
IF (ALLOCATESTATUS /= 0) STOP "***NOT ENOUGH MEMORY: LANDCELL()***"

! LANDCELL(SOURCES, 1) = POLYGON IDENTIFICATION NUMBER
! LANDCELL(SOURCES, 2) = POLYGON AREA
! LANDCELL(SOURCES, 3) = SINK WHERE FLOW IS DISCHARGED(GRID CODE)
! LANDCELL(SOURCES, 4) = FLOW LENGTH FROM SOURCE TO SINK
! LANDCELL(SOURCES, 5) = VELOCITY FROM SOURCE TO SINK
! LANDCELL(SOURCES, 6) = DISPERSION COEFFICIENT ALONG THE FLOWPATH
! LANDCELL(SOURCES, 7) = LOSS COEFFICIENT ALONG THE FLOWPATH
! LANDCELL(SOURCES, 8) = SOIL WATER BALANCE UNIT FOR INPUT RUNOFF

ALLOCATE (FLOWTIME(SOURCES), STAT = ALLOCATESTATUS)
IF (ALLOCATESTATUS /= 0) STOP "***NOT ENOUGH MEMORY: FLOWTIME()***"

PRINT *, "OPENING INPUT FILE SINKCELL.TXT....."
OPEN (UNIT = 11 , FILE = "SINKCELL.TXT" , STATUS ="OLD" , ACTION
     . = "READ" , POSITION = "REWIND" , IOSTAT = OPENSTATUS )
IF (OPENSTATUS > 0) STOP "***CANNOT OPEN SINKCELL.TXT FILE***"

READ (11, *, IOSTAT = INPUTSTATUS) SINKCELL
IF (INPUTSTATUS > 0) STOP "*****INPUT ERROR IN SINKCELL*****"
IF (INPUTSTATUS < 0) STOP "*****NOT ENOUGH SINK CELLS*****"

PRINT *, "OPENING INPUT FILE LANDCELL.TXT....."
OPEN (UNIT = 12 , FILE = "LANDCELL.TXT" , STATUS ="OLD" , ACTION =
     . "READ" , POSITION = "REWIND" , IOSTAT = OPENSTATUS )
IF (OPENSTATUS > 0) STOP "*****CANNOT OPEN LANDCELL.TXT FILE*****"

DO Z = 1, SOURCES, 1
  READ (12, *, IOSTAT = INPUTSTATUS) LANDCELL(Z, 1),
  .   LANDCELL(Z, 2), LANDCELL(Z, 3), LANDCELL(Z, 4),
  .   LANDCELL(Z, 5), LANDCELL(Z, 6), LANDCELL(Z, 7), LANDCELL(Z, 8)

```

```

END DO

IF (INPUTSTATUS > 0) STOP "****INPUT ERROR IN LANDCELL****"
IF (INPUTSTATUS < 0) STOP "****NOT ENOUGH LAND CELLS****"

!      OPEN FILES AND READ DATA INTO ARRAYS

PRINT *, "OPENING INPUT FILE INFILES.TXT....."
OPEN (UNIT = 41, FILE = "INFILES.TXT", STATUS = "OLD", ACTION =
.READ", POSITION = "REWIND", IOSTAT = OPENSTATUS)
IF (OPENSTATUS > 0) STOP "****CANNOT OPEN FILES4.TXT****"

PRINT *, "OPENING INPUT FILE AFRUNOFF.TXT....."
OPEN (UNIT = 43, FILE = "AFRUNOFF.TXT", STATUS = "OLD", ACTION =
.READ", POSITION = "REWIND", IOSTAT = OPENSTATUS)
IF (OPENSTATUS > 0) STOP "****CANNOT OPEN AFRUNOFF.TXT****"

READ (43, *, IOSTAT = INPUTSTATUS) (T42RUN(X), X = 1, SOURCES, 1)
IF (INPUTSTATUS > 0) STOP "****INPUT ERROR IN T42NUMS****"
IF (INPUTSTATUS < 0) STOP "****NOT ENOUGH T42NUMS****"

!      DETERMINE THE MAXIMUM FLOW LENGTH, TIME AND DISPERSED FLOW WIDTH

MAXLENGTH = 0
MAXDISPCOEFF = 0

DO X = 1, SOURCES, 1
    FLOWTIME(X) = INT(LANDCELL(X,4) / (LANDCELL(X, 5)*INTERVAL))
    LOSSFACTOR(X) = EXP(-LANDCELL(X,7)*FLOWTIME(X)*INTERVAL)

    IF (FLOWTIME(X) .GT. MAXFLOWTIME) THEN
        MAXLENGTH = LANDCELL(X, 4)
        MAXFLOWTIME = MAXLENGTH / (LANDCELL(X, 5)*INTERVAL)
        MAXVELOCITY = LANDCELL(X, 5)
        MAXDISPCOEFF = LANDCELL(X, 6)
    ENDIF
END DO

END DO

!      THIS GIVES THE WIDTH OF THE DISPERSED FLOW IN METERS
!      (FISCHER ET AL, 1979, MIXING IN INLAND LAKES AND RESERVOIRS)

MAXWIDTH = INT((SQRT(32*MAXDISPCOEFF*MAXFLOWTIME*INTERVAL))/
.      (MAXVELOCITY*INTERVAL))

ALLOCATE (COEFFICIENTS(SOURCES,MAXWIDTH), STAT = ALLOCATESTATUS)
IF (ALLOCATESTATUS /= 0) STOP "****NOT ENOUGH MEMORY: COEFFS.( )****"

ALLOCATE (ADECOEFF(SOURCES, MAXWIDTH), STAT = ALLOCATESTATUS)
IF (ALLOCATESTATUS /= 0) STOP "****NOT ENOUGH MEMORY: ADECOEFF.( )****"

```



! CREATE AN OUTPUT FILE FOR STORING ROUTED FLOWS TO SINK (OUTLET) CELLS

```
PRINT *, "CREATING OUTPUT FILE DISPCOEF.TXT....."
OPEN (UNIT = 44 , FILE = "DISPCOEF.TXT" , STATUS = "UNKNOWN" ,
.ACTION = "READWRITE" , POSITION = "REWIND" , IOSTAT = OPENSTATUS)
IF (OPENSTATUS > 0) STOP "***CANNOT CREATE DISPCOEF.TXT FILE***"
```

PRINT \*, "COMPUTING DISPERSION COEFFICIENTS....."

DO X = 1, SOURCES, 1

ADESUM(X) = 0

IF (LANDCELL(X, 4) .GT. 0) THEN

DO Y = 1, MAXWIDTH, 1

FLOWTIMEB = (INT(FLOWTIME(X)) - INT(MAXWIDTH/2)+ Y)\* INTERVAL  
IF (FLOWTIMEB .GT. 0) THEN

TEMPCALC = 4 \* PI \* LANDCELL(X, 6) \* FLOWTIMEB \*\* 3  
ADEPARTA = LANDCELL(X, 4)/( TEMPCALC \*\* 0.5)  
EXPPARTA=-(LANDCELL(X,5)\*FLOWTIMEB)-LANDCELL(X, 4))\*\*2  
ADEPARTB = EXP(EXPPARTA/(4\*LANDCELL(X,6)\* FLOWTIMEB))

ADECOEFF(X,Y) = ADEPARTA \* ADEPARTB

ELSE ! IF (FLOWTIMEB .LE. 0)

ADECOEFF(X,Y) = 0

ENDIF ! (FLOWTIMEB .GT. 0)

ADESUM(X) = ADESUM(X) + ADECOEFF(X, Y)

ENDDO ! Y = 1, MAXWIDTH, 1

DO Z = 1, MAXWIDTH, 1

COEFFICIENTS(X, Z) = ADECOEFF(X, Z) / ADESUM(X)

ENDDO

ELSE ! IF (LANDCELL(X, 4) .LE. 0)

COEFFICIENTS(X,(INT(MAXWIDTH\*0.5)+1)) = 1

! DO Z = 2, MAXWIDTH, 1  
! COEFFICIENTS(X,Z) = 0  
! ENDDO

ENDIF ! IF (LANDCELL(X, 4) .GT. 0)

```

END DO      !      DO X = 1, SOURCES, 1

! LANDCELL(X,4) IS THE FLOWLENGTH FROM THE UNIT TO THE OUTLET IN M
! COMPUTE FIRST PASSAGE TIMES COEFFICIENTS FOR EACH INTERVAL IN MAXWIDTH
! START AND END AT HALF A MAXWIDTH ON EITHER SIDE OF THE ELEMENT FLOWTIME
! MAKE ALLOWANCE FOR CASE WHERE THIS RANGE GOES PAST THE TIME OF INPUT

PRINT *, "WRITING OUTPUT FILE DISPCOEF.TXT....."

DO Y = 1, SOURCES, 1

    WRITE (44, 200) (LANDCELL(Y, 1)), (COEFFICIENTS(Y, X), X = 1,
. MAXWIDTH)

END DO

DO X = 1, STEPS, 1
    READ (41, *, IOSTAT = INPUTSTATUS) FILENAME(X)
    IF (INPUTSTATUS > 0) STOP "***INPUT ERROR IN FILENAMES***"
    IF (INPUTSTATUS < 0) STOP "*****NOT ENOUGH FILENAMES*****"

    !PRINT *, FILENAME(X)
    OPEN (UNIT = 42, FILE = FILENAME(X), STATUS = "OLD", ACTION =
.      "READ", POSITION = "REWIND", IOSTAT = OPENSTATUS)
    IF (OPENSTATUS > 0) STOP "***CANNOT OPEN INPUT FILES***"

    DO Y = 1, 8192, 1
        READ (42, *, IOSTAT = INPUTSTATUS) XCOORD(Y) , YCOORD(Y),
.      RUNOFFIN(Y, X)
        IF (INPUTSTATUS > 0) STOP "***INPUT ERROR IN PARAMETERS***"
        IF (INPUTSTATUS < 0) STOP "*****NOT ENOUGH PARAMETERS*****"

        T42NUM(Y) = ((YCOORD(Y)*1000) + (129-XCOORD(Y)))

    END DO      ! Y = 1, 8192, 1

END DO      ! X = 1, STEPS, 1

DO X = 1, SOURCES, 1

    DO Y = 1, 8192, 1
        IF (T42RUN(X).EQ.T42NUM(Y)) THEN

            ! PRINT *, "MATCH FOUND"
            DO Z = 1, STEPS, 1

                RUNOFF(X,Z) = RUNOFFIN(Y,Z)*86.4

```

```

                                END DO          ! Z = 1, STEPS, 1

                                END IF

                                END DO          ! Y = 1, 8192, 1

                                END DO          ! X = 1, SOURCES, 1

! CREATE AN OUTPUT FILE FOR STORING ROUTED FLOWS TO SINK (OUTLET) CELLS

PRINT *, "CREATING OUTPUT FILE SINKFLOW.TXT....."
OPEN (UNIT = 15 , FILE = "SINKFLOW.TXT" , STATUS ="UNKNOWN" ,
.ACTION = "READWRITE" , POSITION = "REWIND" , IOSTAT = OPENSTATUS)
IF (OPENSTATUS > 0) STOP "***CANNOT CREATE SINKFLOW.TXT FILE***"

! CREATE OUTPUT FILE FOR SOIL WATER BALANCE RUNOFF PER BASIN PER INTERVAL

PRINT *, "CREATING OUTPUT FILE INFLOW.TXT....."
OPEN (UNIT = 16 , FILE = "INFLOW.TXT" , STATUS ="UNKNOWN" , ACTION
.= "READWRITE" , POSITION = "REWIND" , IOSTAT = OPENSTATUS )
IF (OPENSTATUS > 0) STOP "***CANNOT CREATE INFLOW.TXT FILE***"

! CREATE AN OUTPUT FILE FOR STORING LOSSES FOR BASINS
PRINT *, "CREATING OUTPUT FILE LOSSES.TXT....."
OPEN (UNIT = 17 , FILE = "LOSSES.TXT" , STATUS ="UNKNOWN" , ACTION
.= "READWRITE" , POSITION = "REWIND" , IOSTAT = OPENSTATUS )
IF (OPENSTATUS > 0) STOP "***CANNOT CREATE LOSSES.TXT FILE***"

PRINT *, "ROUTING FLOWS TO SINK....."

DO X = 1, SOURCES, 1

    DO Y = 1, STEPS, 1

        ! LANDCELL(X,2) IS THE AREA OF THE POLYGON IN M2
        ! COMPUTE FLOW FROM RUNOFF, AND CONVERT FROM M/DAY TO M3/S
        ! COMPUTE LOSSES FROM FLOW TIME AND LOSS COEFFICIENT
        ! UPDATE FLOW AVAILABLE FOR ROUTING

        RUNOFF(X,Y) = ((RUNOFF(X,Y) * LANDCELL(X,2))/86400)

        DO M = 1, SINKCELLS, 1
            IF (SINKCELL(M) .EQ. LANDCELL(X,3)) THEN
                INFLOW(M, Y) = RUNOFF(X,Y)*86400 + INFLOW(M, Y)

                LOSSES(M,Y)= RUNOFF(X,Y)*86400*(1 - LOSSFACTOR(X))
                + LOSSES(M,Y)
            .
        
```

```

        GOTO 100

    END IF
END DO          ! M = 1, SINKCELLS, 1

100 IF (FLOWTIME(X) .GT. 0) THEN

    RUNOFF(X,Y)=RUNOFF(X,Y)*LOSSFACTOR(X)

    ELSE

        RUNOFF(X,Y) = RUNOFF(X,Y)*1

    END IF

END DO          ! Y = 1, STEPS, 1

    ! PRINT *, "WRITING FLOWS TO LANDFLOW.TXT....."

    ! WRITE (14,70) LANDCELL(X,1), (LANDFLOW(X,Y), Y = 1, STEPS)

END DO          ! X = 1, SOURCES, 1

PRINT *, "WRITING TOTAL RUNOFF TO INFLOW.TXT....."

WRITE (16, 90) (0.0), (SINKCELL(Z), Z = 1, SINKCELLS)
WRITE (17, 90) (0.0), (SINKCELL(Z), Z = 1, SINKCELLS)

DO M = 1, STEPS, 1
    WRITE (16, 80) (M-1), (INFLOW(Z, M), Z = 1, SINKCELLS)
    WRITE (17, 110) (M-1), (LOSSES(Z, M), Z = 1, SINKCELLS)
END DO

OUTSTEPS = (STEPS + INT(MAXFLOWTIME) + INT(MAXWIDTH/2))

ALLOCATE (SINKFLOW(SINKCELLS, OUTSTEPS), STAT = ALLOCATESTATUS)
IF (ALLOCATESTATUS /= 0) STOP "****NOT ENOUGH MEMORY****"

! INITIALIZE SINKFLOW()

DO R = 1, OUTSTEPS, 1

    DO S = 1, SINKCELLS, 1

        SINKFLOW(S, R) = 0

    END DO          ! S = 1, SINKCELLS, 1

```

```

END DO          ! R = 1, OUTSTEPS, 1

PRINT *, "AGGREGATING FLOWS AT OUTLET....."

DO X = 1, SOURCES, 1
  DO Y = 1, STEPS, 1
    DO Z = 1, SINKCELLS, 1
      IF (SINKCELL(Z) .EQ. LANDCELL(X,3)) THEN
        LTIME=INT(FLOWTIME(X) )
        DO M = 1, MAXWIDTH, 1
          CTIME = Y + LTIME + M - INT(MAXWIDTH/2) - 1
          IF (CTIME .GT. 0) THEN
            SINKFLOW(Z,CTIME)= SINKFLOW(Z,CTIME) +
              (RUNOFF(X,Y)*COEFFICIENTS(X, M))
          .
          ELSEIF (CTIME .LE. 0) THEN
            CTIME = Y + LTIME
            SINKFLOW(Z,CTIME)= SINKFLOW(Z,CTIME) +
              (RUNOFF(X,Y)*COEFFICIENTS(X, M))
          .
          END IF  !      IF (COEFFICIENTS(X, M) .GT. 0) THEN
        END DO      !      M = 1, MAXWIDTH, 1
      END IF ! IF (SINKCELL(Z) .EQ. LANDCELL(X,3)) THEN
    END DO      !      Z = 1, SINKCELLS, 1
  END DO      !      Y = 1, SOURCES, 1
END DO      !      X = 1, SOURCES, 1

PRINT *, "WRITING OUTPUT FILE SINKFLOW.TXT....."

WRITE (15, 90) 0.0, (SINKCELL(Z), Z = 1, SINKCELLS)

DO Y = 1, OUTSTEPS, 1
  WRITE (15, 90) (Y-1), (SINKFLOW(Z, Y), Z = 1, SINKCELLS)
END DO

```

```
80 FORMAT(I5, 1000F15.1)
90 FORMAT(F7.2, 1000F15.5)
110 FORMAT(I5, 1000F20.1)
200 FORMAT(F10.1, X, 1000F12.10)

PRINT *, "PROCESSING COMPLETE"
END
```

## Appendix 4: AML Code for Computing Equivalent Muskingum Parameters from a Field of Velocities and Dispersion Coefficients

```
/* AML FOR COMPUTING MUSKINGUM RIVER REACH PARAMETERS FROM FIELDS OF
/*   FLOW VELOCITIES AND DISPERSION COEFFICIENTS
/* INPUTS INCLUDE GRIDS INCLUDE THE FOLLOWING
/* FLOWDIR: A FLOW DIRECTION GRID
/* STREAMGRID: A STREAM GRID
/* OUTLETGRID: AN OUTLET GRID
/* LINKGRID: A STREAM LINK GRID
/* VELOCITY: A GRID OF LOCAL VELOCITY
/* DISPCOEF: A GRID OF LOCAL DISPERSION COEFFICIENT

GRID
SETWINDOW FLOWDIR FLOWDIR
SETCELL FLOWDIR

/* COMPUTE RIVER FLOWDIR FROM STREAM GRID AND BASIN FLOWDIR
RIVERFDR = FLOWDIR * STREAMGRID

/* INSERT NODATA CELLS AT STREAM JUNCTIONS BY MULTIPLYING BY OUTLET GRID
LINKFDR = CON(ISNULL(OUTLETGRID), RIVERFDR)

/* COMPUTE LINK FLOW LENGTH
LINKLENGTH = FLOWLENGTH ( LINKFDR )

/* COMPUTE MAXIMUM LINK FLOW LENGTH
LINKLENMAX = ZONALRANGE (LINKGRID, LINKLENGTH)

/* COMPUTE THE INVERSE OF VELOCITY
INVVEL = 1 / VELOCITY

/* COMPUTE WEIGHTED FLOW LENGTH GRID USING THE INVERSE OF VELOCITY AS
WEIGHT
LINKTIME = FLOWLENGTH ( LINKFDR, INVVEL )

/* COMPUTE THE FLOW TIME FOR EACH STREAM LINK
LINKTIMEMAX = ZONALRANGE (LINKGRID, LINKTIME)

/* COMPUTE THE FLOW VELOCITY FOR EACH STREAM LINK
LINKVELOCITY = LINKLENMAX / LINKTIMEMAX

/* COMPUTE THE DISPERSION WEIGHT, (D/V3)
DISPWEIGHT = DISPCOEF * POW (INVVEL, 3)

/* COMPUTE WEIGHTED FLOW LENGTH GRID USING (D/V3) AS WEIGHT
LINKVARIANCE = FLOWLENGTH ( LINKFDR, DISPWEIGHT )
```

```

/* COMPUTE LINK VARIANCE
LINKVARMAX = ZONALRANGE (LINKGRID, LINKVARIANCE)

/* COMPUTE LINK MUSKINGUM X
LINKDISP = LINKVARMAX * (POW (LINKVELOCITY, 3)) / LINKLENMAX

/* COMPUTE LINK MUSKINGUM X
LINKMUSKX = 0.5 - (LINKDISP / (LINKVELOCITY * LINKLENMAX))

/* CONDITIONAL STATEMENT TO REMOVE NEGATIVE MUSKINGUM X VALUES
LINKMUSKX1 = CON ( LINKMUSKX < 0 , 0 , LINKMUSKX )

/* COMPUTE LINK MUSKINGUM N, 86400 SECONDS ASSUMING DAILY ROUTING
INTERVAL
LINKMUSKN = ( INT (2 * LINKMUSKX1 * LINKTIMEMAX / 86400 ) + 1)

/* RECOMPUTE MUSKINGUM X BASED ON MUSKINGUM N
LINKMUSKX2 = 0.5 - LINKMUSKN * ( 0.5 - LINKMUSKX1 )

/* CONDITIONAL STATEMENT TO REMOVE NEGATIVE MUSKINGUM X VALUES
LINKMUSKX3 = CON ( LINKMUSKX2 < 0 , 0 , LINKMUSKX2 )

/* COMBINE LINKGRID AND LINKLAG
JOINGRID = COMBINE ( LINKGRID, LINKTIMEMAX, LINKVELOCITY, LINKMUSKX3 )

&RETURN

```



## Appendix 5: 10 day flows in the Nile basin, 1953-57

OBSERVED FLOWS AT MONGALLA, 1953-57,  
(REPORTED IN HURST AND PHILLIP, 1931-)

PERIOD	FLOWS	PERIOD	FLOWS	PERIOD	FLOWS	PERIOD	FLOWS	PERIOD	FLOWS
0	65.7	360	49.9	720	53.6	1080	53.9	1440	57.9
10	64.3	370	48.9	730	53	1090	52.9	1450	57.4
20	62.7	380	47.4	740	52.3	1100	50.5	1460	56.8
30	61.8	390	46.1	750	52.3	1110	49.9	1470	56.7
40	59.4	400	45.7	760	51.1	1120	49.1	1480	55.9
50	56.7	410	45.5	770	50.4	1130	48.6	1490	55.4
60	55.9	420	45	780	49.4	1140	48.6	1500	55.7
70	54.6	430	44.5	790	48.9	1150	47.9	1510	56.6
80	53.2	440	43.9	800	48.1	1160	47.9	1520	59.5
90	52.6	450	51.2	810	47.2	1170	49.7	1530	63.6
100	52.4	460	54.4	820	52.7	1180	54.1	1540	62.6
110	56.2	470	46.8	830	49.9	1190	60.2	1550	67.6
120	62.6	480	64.9	840	58.3	1200	59.6	1560	68.9
130	59.8	490	58	850	58.9	1210	62.5	1570	67.4
140	62.8	500	61.6	860	51.8	1220	66.4	1580	92.1
150	63.4	510	62.9	870	50.2	1230	67.4	1590	98.5
160	61.9	520	60.5	880	49.9	1240	60.4	1600	83.3
170	69.6	530	56.8	890	53.1	1250	56.9	1610	87.4
180	63.8	540	63.4	900	56.8	1260	62.2	1620	74.8
190	78.7	550	66.4	910	52.7	1270	58.4	1630	68.6
200	64.5	560	66	920	54.4	1280	66.8	1640	66.5
210	65.6	570	75.9	930	59.3	1290	66.2	1650	82.1
220	84.4	580	82.9	940	79.4	1300	79.8	1660	87
230	76.4	590	101	950	74.2	1310	94.8	1670	72.1
240	60.3	600	107	960	87.1	1320	105	1680	72.9
250	64.1	610	112	970	101	1330	109	1690	71.2
260	63.2	620	82.1	980	98.4	1340	91.8	1700	64.8
270	55.3	630	78.2	990	116	1350	102	1710	65.9
280	58.5	640	70	1000	98	1360	98.7	1720	63.8
290	70.2	650	68.3	1010	83.5	1370	91.6	1730	71.3
300	67.5	660	68.3	1020	82	1380	78.3	1740	65.5
310	64.4	670	62	1030	86.6	1390	68.4	1750	67
320	58.6	680	56.9	1040	68.1	1400	63.1	1760	63.1
330	55.6	690	55.6	1050	59.9	1410	61.8	1770	62.6
340	53.6	700	54.5	1060	57	1420	60.2	1780	61.7
350	51.1	710	54.1	1070	55.7	1430	58	1790	60.7

OBSERVED FLOWS AT LAKE NYONG, 1953-57  
(REPORTED IN HURST AND PHILLIP, 1931-)

PERIOD	FLOWS	PERIOD	FLOWS	PERIOD	FLOWS	PERIOD	FLOWS	PERIOD	FLOWS
0	49.1	360	44.8	720	45.4	1080	48.6	1440	55.1
10	46.9	370	44.3	730	44.8	1090	48.2	1450	53.1
20	44.8	380	43.4	740	44.2	1100	47.9	1460	50.6
30	45.2	390	42.4	750	43.7	1110	47.3	1470	48.2
40	45.2	400	41.8	760	43.4	1120	46.5	1480	47
50	45.2	410	41.5	770	43.2	1130	45.4	1490	46
60	45.6	420	41.1	780	42.9	1140	44.3	1500	45.2
70	45.4	430	41	790	42.9	1150	43.2	1510	45.3
80	44.4	440	40.9	800	42.9	1160	42	1520	45.6
90	42.5	450	40.6	810	42.8	1170	40.8	1530	46
100	42.2	460	40	820	42.8	1180	41.2	1540	46
110	42.9	470	39.2	830	42.8	1190	42.5	1550	46
120	44.2	480	38.5	840	42.7	1200	43.7	1560	46
130	43.5	490	38.6	850	42.7	1210	43.8	1570	46.8
140	42.7	500	39.1	860	42.7	1220	43.6	1580	47.8
150	43.6	510	39.7	870	42.7	1230	43.5	1590	48.7
160	43.9	520	40.3	880	42.7	1240	43.7	1600	50.1
170	44.2	530	41.3	890	43	1250	43.9	1610	51.6
180	44.9	540	42.2	900	44	1260	44.1	1620	52.7
190	45.5	550	43.1	910	44.9	1270	44.5	1630	52
200	46.3	560	44.2	920	45.5	1280	45.1	1640	50.9
210	47.3	570	45.1	930	45.7	1290	45.8	1650	50.1
220	48.2	580	46.1	940	45.8	1300	47	1660	51.3
230	48.8	590	47	950	46.3	1310	48.7	1670	53
240	48	600	48	960	47.3	1320	50.3	1680	54.4
250	47.4	610	49.2	970	48.4	1330	51.1	1690	53.9
260	47.1	620	50.5	980	49.4	1340	51.6	1700	52.9
270	46.6	630	51.6	990	50.5	1350	52.2	1710	52
280	46.5	640	51.2	1000	50.6	1360	52.9	1720	51.5
290	46.5	650	50.5	1010	49.6	1370	53.7	1730	51
300	46.2	660	49.7	1020	48.7	1380	54.4	1740	50.5
310	46	670	48.9	1030	48.6	1390	54.5	1750	49.9
320	45.6	680	48.6	1040	48.8	1400	54.4	1760	49.2
330	45.5	690	48.3	1050	48.9	1410	54.4	1770	48.6
340	45.2	700	47.5	1060	48.9	1420	54.7	1780	48.8
350	45	710	46.5	1070	48.7	1430	55	1790	49.2

## REFERENCES

- Barkstrom, B., E. Harrison, R. Lee, (1990), Earth Radiation Budget Experiment, Preliminary Seasonal Results, Transactions - American Geophysical Union, vol. 71, pp. 279, 299, 304-305
- Bartholomew (John) and Sons, ltd., (1975), The Times Atlas of the World, Quadrangle/The New York Times Book Company, NY, NY
- Birkett, C.M. and I.M. Mason, (1995), A new Global Lakes Database for a remote sensing programme studying climatically sensitive large lakes, Journal of Great Lakes Research, Vol. 21, no. 3, pp. 307-318
- Bonan, G.B., (1996), The NCAR land surface model (LSM version 1.0) coupled to the NCAR Community Climate Model, NCAR Technical Note NCAR/TN-429+STR, National Center for Atmospheric Research, Boulder, Colorado
- Branstetter, M. L., and J. S. Famiglietti, (1998), An Investigation of the Effects of Continental Runoff on Climate Dynamics Using a Parallel Earth System Model, Proceedings of the American Geophysical Union Spring Meeting, Boston, MA
- Carlston, C.W., (1969), Downstream variations in the hydraulic geometry of streams: Special emphasis on mean velocity, American Journal of Science, vol. 267, pp. 499-509
- Chow, V.T., D.R. Maidment, L.W. Mays, (1988), Applied Hydrology, McGraw-Hill, Inc., NY, NY
- Clark, C.O., (1945), Storage and the Unit Hydrograph, Transactions, American Society of Civil Engineers, vol. 110, pp. 1419-1488
- Coe, M., (1994) Simulating Continental Surface Waters: An Application to Holocene Northern Africa, Journal of Climate, v10, pp. 1680 -1689
- Cunge, J.A., (1969), On the subject of a flood propagation computation method (Muskingum Method), Journal of Hydraulic Research, 7, no. 2, pp. 205-230
- Dooge, J.C., (1973), Linear Theory of Hydrologic Systems, USDA Technical Bulletin no. 1468, USDA, Washington, DC

- Easterling, D. R., T. Peterson, and R. K. Thomas, (1996), On the development and use of homogenized climate data sets, *Journal of Climate*, 9, 1429-1434, “<http://www.ncdc.noaa.gov/wdcamet.html#GPCP>”
- Environmental Systems Research Institute Inc. (ESRI), (1992), *ArcWorld 1:3M, User's Guide & Data Reference*, ESRI, Redlands, CA
- Environmental Systems Research Institute Inc. (ESRI), (1993), *Data Dictionary: The Digital Chart of the World*, ESRI, Redlands, CA
- Food and Agriculture Organization (FAO) of the United Nations, (1970-78), *Soil map of the world, scale 1:5,000,000, volumes I- X: United Nations Educational, Scientific, and Cultural Organization, Paris*, “[http://daac.gsfc.nasa.gov/CAMPAIGN\\_DOCS/FTP\\_SITE/INT\\_DIS/readmes/soils.html](http://daac.gsfc.nasa.gov/CAMPAIGN_DOCS/FTP_SITE/INT_DIS/readmes/soils.html)”
- Fischer, H.B., E.J. List, R.C.Y. Koh, J. Imberger and N.H. Brooks, (1979), *Mixing in Inland and Coastal Waters*, Academic Press, New York
- Fischer, H.B., (1967) The Mechanics of Dispersion in Natural Streams, *Journal of the Hydraulic Division, ASCE*, v.93, 187 - 216
- Gupta, V.K., I. Rodriguez-Iturbe, and E.F. Wood. (eds.), (1986), *Scale Problem in Hydrology : runoff generation and basin response*, Dordrecht, Holland
- Gupta, V.K., O.J. Mesa, D.R. Dawdy, (1994), Multiscaling theory of flood peaks: Region quantile analysis, *Water Resources research*, vol. 30, no. 12, pp. 3405-3421
- Hagemann, S. and L. Dumenil, (1998), A parameterization of the lateral waterflow for the global scale, *Climate Dynamics* 14: 17 – 31
- Hellweger, F., and D.R.Maidment (1996), *A GIS Preprocessor for Lumped Parameter Hydrologic Modeling Programs*, CRWR Online Report 97-8, The University of Texas at Austin
- Hortal, M., and A.J. Simmons, 1991: Use of reduced Gaussian grids in spectral models, *Monthly Weather Review*, 119, pp. 1057-1074.
- Huffman, G.A., R.F. Adler, P.A. Arkin, A. Chang, R. Ferraro, A. Gruber, J. Janowiak, R.J. Joyce, A. McNab, B. Rudolf, U. Schneider, and P. Xie, (1997), *The Global Precipitation Climatology Project (GPCP) Combined*

- Precipitation Data Set, Bulletin of American Meteorological Society, 78, pp. 5-20, "<ftp://ftp.ncdc.noaa.gov/pub/data/gpcp/version1/>"
- Hurst, H.E. and Phillips, (1931-), The Nile Basin, Volumes I – V, Nile Control Department
- Kiehl, J.K., J.J. Hack, G.B. Bonan, B.A. Boville, B.P. Briegleb, D.L. Williamson, P.J. Rasch, (1996), Description of the NCAR Community Climate Model (CCM3), Tn-420+STR, NCAR, Boulder, Colorado
- Kite, G.W., A. Dalton, K. Dion, (1994), Simulation of streamflow in a macroscale watershed using general circulation model data, Water Resources Research, vol. 30, No. 5, pp. 1547-1559
- Korzoun, V.I., A.A. Sokolov, M.I. Budyko, K.P. Voskresensky, G.P. Kalinin, E.S. Konoplyantsev and M.I. Lvovich (edited by), (1977), Atlas of World Water Balance, The UNESCO Press, Paris
- Kull, D.W., Feldman, (1998), Evolution of Clark's Unit Graph Method to Spatially Distributed Runoff, Journal of Hydrologic Engineering, v3, no.1, pp. 9-19
- Lasdon, L. and A.D. Waren, (1978), Generalized Reduced Gradient Software for Linearly and Nonlinearly Constrained Problems, in Design and Implementation of Optimization Software, H. Greenberg, ed., Sijthoff and Noordhoff, Pubs., 1978, pp. 363-397
- Legates, D.R., and C.J. Willmott (1990), "Mean Seasonal and Spatial Variability in Gauge-Corrected Global Precipitation", International Journal of Climatology, v.10, pp. 111-127  
["http://www.scd.ucar.edu/dss/datasets/ds236.0.html"](http://www.scd.ucar.edu/dss/datasets/ds236.0.html)
- Leopold, L.B., (1953), Downstream Change of Velocity in rivers, American Journal of Science, vol.251, pp. 606-624
- Liston, G.E., Y.C. Sud, E.F. Wood (1994), Evaluating GCM land surface hydrology parameterizations by computing river discharges using a runoff routing model: Application to the Mississippi Basin, Journal of Applied Meteorology, v33, n3, pp.394 - 406
- Loaiciga, H.A., (1997), Runoff scaling in large rivers of the world, Professional Geographer, vol.49, n3, pp.356-365

- Lohmann, D., E. Raschke, B. Nijssen, D. P. Lettenmaier, (1998), Regional Scale Hydrology: 1. Formulation of VIC-2L Model Coupled to a Routing Model, *Hydrological Sciences Journal*, vol.43, n. 1, pp.131-141
- Lohmann, D., R. Nolte-Holube, E. Raschke, (1996), A Large-Scale Horizontal Routing Model to be Coupled to Land Surface Parameterization Schemes, *Tellus*, vol. 48A, pp.708-721
- Kazadi, S., F. Kaoru, (1996), Interannual and long-term climate variability over the Zaire River Basin during the last 30 years, *Journal of Geophysical Research*, v.101, no. D16, 21,351 - 360
- Maidment, D.R. (*ed.*) (1993), *Handbook of Hydrology*, McGraw-Hill, Inc., NY, NY
- Maidment, D.R., F. Olivera, A. Calver, A. Eatherall, W. Fraczek, (1996), Unit Hydrograph Derived from a Spatially Distributed Velocity Field, *Hydrological Processes*, vol. 10, 831-844
- Meyer, O.H., (1941), Simplified Flood Routing, *Civil Engineering*, v.11, no. 5, pp. 306 - 307
- McCuen, R.H. (1998), *Hydrologic Analysis and Design*, Prentice-Hall Inc., Upper Saddle River, New Jersey
- Miller, J.R., G.L. Russell, G. Caliri (1994) Continental-Scale River Flow in Climate Models, *Journal of Climate*, v7, pp. 914 - 928
- Montes, S., (1998), *Hydraulics of Open Channel Flow*, ASCE Press, Reston, VA
- Naden, P.S., (1993), A routing model for continental-scale hydrology, Macroscale modeling of the the Hydrosphere, *Proceedings of Yokohama Symposium*, July 1993, International Association of Scientific Hydrology (IASH) Publ., 214, 67-79
- Naden, P.S., (1992), Spatial variability in flood estimation for large catchments: the exploitation of channel network structure, *Hydrological Science Journal*, v37, pp.53-71
- Nash, J.E., (1959), A note on the Muskingum Flood-Routing Method, *Journal of Geophysical Research*, vol. 64, pp. 1053 – 1056

- Olivera, F., (1996), Spatially Distributed Modeling of Storm Runoff and Non-Point Source Pollution Using Geographic Information Systems, Doctoral Dissertation, Submitted to the Graduate School, The University of Texas at Austin
- Olivera, F., and D.R.Maidment (1999), GIS Tools for HMS Modeling Support, Proceedings of the 19<sup>th</sup> ESRI Users Conference-CDROM, San Diego, California
- Olivera, F., and D.R.Maidment (1999), Geographic Information Systems (GIS) Based Spatially Distributed Model for Runoff Routing, Water Resources Research, vol. 35, no. 4, pp. 1155-1164
- Olivera, F., J.S.Famiglietti and K.O.Asante (2000), Global-Scale Flow Routing Using a Source-To-Sink Algorithm, Submitted to Water Resources Research
- Perry, G.D., P.B. Duffy, and N.L. Miller, (1996), An extended data set of river discharges for validation of general circulation models, Journal of Geophysical Research, v.101, no. D16, pp. 21,339-349  
“ftp://kosmos.agu.org/” in the directory “/apend/96Jd00932”
- Peters, J.C., (1998), HEC-HMS, Hydrologic Modeling System, US Army Corps of Engineers Hydrologic Engineering Center, Davis, CA
- Pilgrim, D.H., (1981), Effects of catchment size on runoff relationships, J. Hydrology, 58: 205-221
- Pilgrim, D.H., (1977), Isochrones of Travel Time and Distribution of Flood Storage from a Tracer Study on a Small Watershed, Water Resources Research, vol. 13, no. 3, pp. 587-595
- Ponce, V.M., R.M.Li, D.B.Simons, (1978), Applicability of Kinematic and Diffusion Models, J.Hydraulic Engineering, vol.104, no.hy3, pp. 353-360,1978
- Reed, S.M., J. Patoux, D.R. Maidment (1997), CRWR Online Report 97-1: Spatial Water Balance of Texas, CRWR, The University of Texas at Austin
- Reed, S.M., D.R. Maidment (1997), CRWR Online Report 95-3: A GIS Procedure for Merging NEXRAD Precipitation Data and Digital Elevation

Models to Determine Rainfall-Runoff Modeling Parameters, CRWR, The University of Texas at Austin

Revenga, C., S. Murray, J. Abramovitz, A. Hammond, (1998), Watersheds of the World, A joint publication of the Water Resources Institute and WorldWatch Institute, Washington, D.C.

Rodriguez-Iturbe, I. and J.B. Valdes, (1979), The geomorphological structure of hydrologic response, Water Resources Research, vol. 15, no. 6, pp. 1409-1420

Sherman, L.K. (1932), Streamflow from rainfall by unit-graph method, Engineering News record, Vol. 108, 501-505

Snyder, F.F. (1938), Synthetic Unit-Graphs, Trans. Am. Geophysical Union, Vol. 19, 447-454

Sausen, R., S.Schubert, L.Dumenil, (1994), A model of river runoff for use in coupled atmosphere-ocean models, Journal of Hydrology, 155 (1994), pp. 337 - 352

Seo, I.W., T.S. Cheong, (1998), Predicting Longitudinal Dispersion Coefficient in Natural Streams, Journal of Hydraulic engineering, vol. 124, no.1, pp. 25 - 32

Shahin, M., (1985), Hydrology of the Nile Basin, Developments in Water Science No.21, Elsevier, Amsterdam, Netherlands

Simmons, A.J., and D.M. Burridge, (1981), An energy and angular-momentum conserving vertical finite difference scheme and hybrid vertical coordinates, Monthly Weather Review, 109, pp.758-766.

Sposito, G, (1998), Scale Dependence and Scale Invariance in Hydrology, Cambridge University Press, Cambridge, UK

Storm, B. and J. Kjelds, (1999), Integrated River Basin Management Modeling Water Use and Water Quality Simulation, Proceedings of the ASCE Water Resource Conference, Seattle, WA

USGS, (1996), GTOPO30 Documentation, Sioux Falls, South Dakota

USGS, (1997), HYDRO1K Documentation, Sioux Falls, South Dakota



- Vörösmarty, C.J., B.Fekete, and BA Tucker (1996), River Discharge Database, Version1.0 (RivDIS v1.0) Volumes 0-6, A contribution to IHP-V Theme 1, Technical Documents in Hydrology Series, UNESCO, Paris  
[“http://www.rivdis.sr.unh.edu/”](http://www.rivdis.sr.unh.edu/)
- Vörösmarty, C.J., B.Moore III, A.L. Grace, M.P. Gildea, M.Melillo, B.J. Peterson, E.B. Rastetter, P.A. Steudler, (1989), Continental Scale Models of Water Balance and Fluvial Transport: An Application to South America, *Global Biogeochemical Cycles*, v3, no.3, pp. 241 - 265
- Vose, R.S., R.L. Schmoyer, P.M. Steurer, T.C. Peterson, R.Heim, T.R. Karl, and J. Eischeid, (1992), The Global Historical Climatology Network: long-term monthly temperature, precipitation, sea level pressure, and station pressure data. ORNL/CDIAC-53, NDP-041, Carbon Dioxide Information Analysis Center, Oak Ridge National Laboratory, Oak Ridge, Tennessee
- Zoch, R.T., (1934), On the relation between rainfall and stream flow, *Monthly Weather Review*, vol. 62

## **Vita**

Kwabena Oduro Asante was born in Kintampo, Ghana, on November 23, 1971, the son of Beatrice Oduro Asante and Kofi Oduro Asante. After completing his work at Starehe Boys Centre and School, Nairobi, Kenya, in 1989, he studied computer programming at the Kestrel College, Nairobi. He entered the University of Nairobi in August of 1990 and received the degree of Bachelor of Science in Civil Engineering in December, 1994. He served as an Engineering Trainee at the Water Resources Research Institute in Accra, Ghana, before entering the Graduate School of The University of Texas in August, 1995. He was awarded the degree of Master of Science in Civil Engineering in December, 1997. During his tenure at the university, he served as a teaching assistant in the Department of Civil Engineering and as a graduate research assistant at the Center for Research in Water Resources.

Permanent address: P.O.Box 3188, Accra, Ghana

This dissertation was typed by the author.